A MASS SPECTRAL STUDY OF HALOGENATED N-t-BUTYLACETAMIDES

Gerald Foder

A THESIS

in

The Department of

Chemistry

Presented in Partial Fulfillment of the Requirements for
the Degree of Master of Science at
Sir George Williams University
Montreal, Canada

August, 1972

Abstract

Gerald Foder

A Mass Spectral Study of Halogenated N-t-butylacetamides

A number of different N-t-butyl-α-chloroacetamides and N-t-butyl-α-fluoroacetamides were prepared. These compounds were prepared in order to study the effect upon the fragmentation pattern by an increasing number of halogen atoms in the acyl portion of the molecule.

After identification of the ions that produced peaks in the mass spectrum, the observed results were analyzed from a number of different viewpoints. Peaks that were common to each spectra, or analogous to each spectra were reviewed and significant trends were identified and commented upon. Also the peaks in each spectrum were examined as to the pathway that led to their formation. The data were further analyzed by comparing peak intensities of daughter and parent ions, selected rearrangement ions, and selected fragment ions.

Mass spectral data are given in the Appendix in both figure and table form.

Acknowledgements

I wish to express my thanks to the Department of Chemistry for the use of equipment and facilities that made this study possible. Also I am grateful to the Department of Chemistry for providing a teaching assistantship during the course of my full time study.

Dr. R. Rye, my research director, deserves a special note of thanks for his extreme patience and encouragement. I also wish to express my gratitude to fellow students, with whom I have had many interesting discussions.

Table of Contents

Table of Contents

Table of Contents

List of Tables

List of Tables

List of Tables

List of Tables

List of Illustrations

Statement of the Problem

The aim of this investigation was to gain a fuller understanding of the electron impact induced fragmentation of halogenated amides. A series of N-t-butyl-α-chloroacetamides and N-t-butyl-α-fluoroacetamides were chosen for study. The halogen atoms were incorporated into the acetyl portion of the amides so as to give an increasingly strong electronegative centre, which would affect the fragmentation pathway.

Historical Review

In an early mass spectral study, Gilpin [1] reported two major pathways of decomposition in secondary and tertiary amides.

Process I

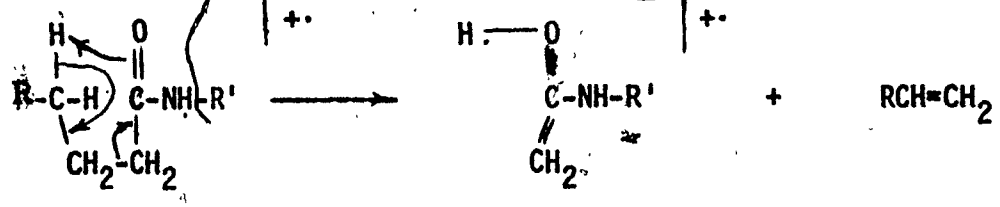

Process II

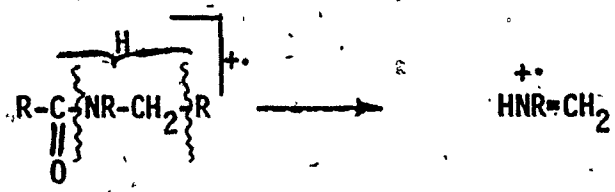

Process I occurs when the acyl group contains a hydrogen atom γ to the carbonyl group. A rearrangement that proceeds via the same mechanism has been observed in esters, [2] and has been confirmed by labelling experiments.

Processes of fragmentation analogous to Process II have been observed in the mass spectra of amines [3] and ethers [4]. Pelah [5] clarified Process II, previously suggested by Gilpin. N-t-butyl-d_3-acetamide gave a mass spectrum that showed the peak at m/e 30 (observed in N-n-butyl-acetamide) changing to m/e 31 in the spectrum of N-n-butyl-d_3-acetamide. This suggests that the migrating hydrogen originates from the acetyl function. Two possible processes then could be proposed.

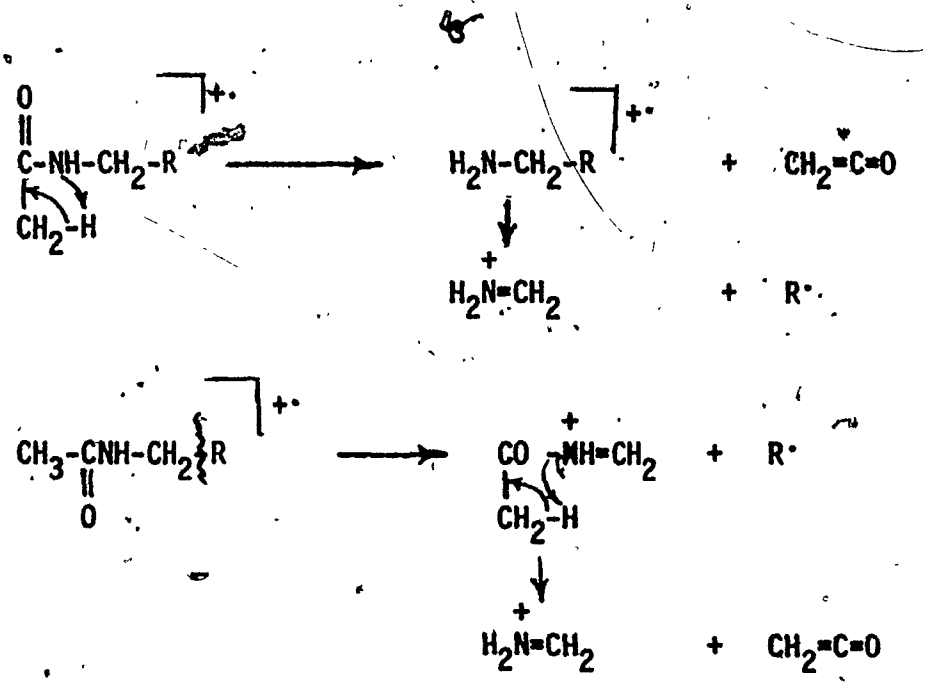

Additional work on tertiary amides has helped to confirm Process II. For N,N-diethylacetamide the base peak was at m/e 58, and changed to m/e 59 in N,N-diethyl-d_3-acetamide, and is split almost equally between m/e 58 and m/e 61 in the mass spectra of N-ethyl-N-β,β,β-d_3-ethylacetamide; these observations are compatible with Process II.

Recent investigations into the fragmentation pattern of N-substituted-α,α,α-trifluoroacetamide have been reported by Saxby [6,7]. These secondary amides were characterized by peaks appearing at m/e 69 and $[M-69]^+$, corresponding to the $[CF_3]^+$ ion and the loss of $\cdot CF_3$ from the molecular ion, respectively. Ions resulting from the loss of HF followed by rearrangement are quite common. The base peak in the straight chain derivatives occurs at m/e 126 due to alkyl radical loss from the molecular ion.

Prox and Schmid [8] studied a series of N-trifluoroacetyl-α-amino acids and their derivatives and found that these compounds fragment by the elimination of a neutral molecule; this breakdown is influenced by the structure of the substituents in the molecule. Skeletal rearrangements

are observed in some of the compounds. In a second study on some substituted N-methylbenzylamides, Prox and Schmid [9] noted a cleavage that leads to the formation of N-methyl-α-acylamine carbonium ions indicating skeletal rearrangement; intensity of the rearrangement ions depended upon the nature of the N-acyl group. Migration of the methyl group in the mass spectrum of N-acetyl and N-p-chlorobenzoyl-N-methyl-α-phenylethylamide was also observed.

Zeman and Wirotama [10] reported the mass spectra of a series of aliphatic and aromatic trifluoroacetyl derivatives of amines. Characteristic peaks in the mass spectra of the amides were; m/e 126, m/e 114, m/e 78, $[M-CF_3]^+$, and $[CF_3]^+$. A base peak in the spectra for many of the prepared amides, resulted from alpha alkyl splitting to give the peak at m/e 126; or from α-alkyl splitting and transfer of a hydrogen atom to give the peak at m/e 127.

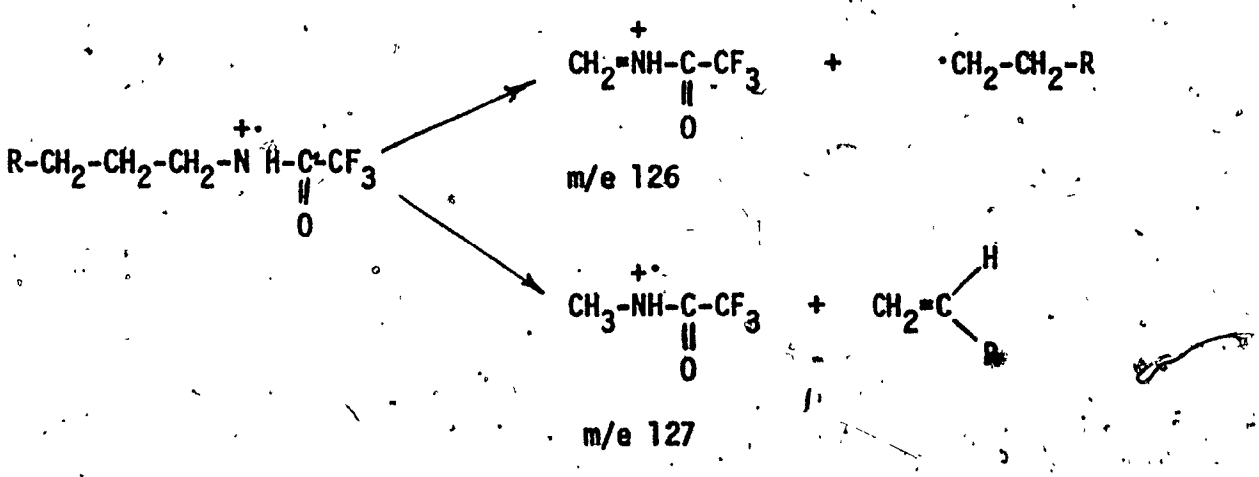

Theory

The process of ionization

A mass spectrum will only result if the molecule under study ionizes. Ionization may occur through the following processes.

$$M + e^- = M^- \qquad (1)$$

$$M + e^- = M^+ + 2e^- \qquad (2)$$

$$M + e^- = M^{n+} + (n+1)e^- \qquad (3)$$

Equations (1) to (3) show the formation of negative, positive and multiple positive molecular ions. For the mass spectra of organic compounds, the formation of a unipositively charged molecular ion is an important case, because of its frequent occurrence.

The removal of an electron from a molecule occurs when the impinging electron has an energy equal to or higher than the ionization potential of the molecule in question. For the case of bombarding electrons having an energy equal to the ionization potential, a complete transfer of energy must occur before ionization results. An increase in the energy of bombarding electrons will increase the probability of ionization occurring. With a greater probability of ionization occurring, a more intense peak is observed. A plot of peak intensity of the molecular ion *versus* increasing electron energy gives an "ionization efficiency curve" [1].

With increasing electron energy, the excess energy of the molecular ion will reach a value equal to, or higher than the energy required to break a certain bond within the molecule; when this occurs fragmentation results.

A theory put forth by Eyring[12], tries to explain possible fragmentation patterns on the basis of a "statistical theory of mass spectra". Eyring uses the working assumptions that: (1) it is possible to remove any one of the valence electrons; (2) free and rapid "travel" of excess energy throughout the molecule; (3) fragmentation of a bond will occur when sufficient energy is located at a given bond. Simple molecules have been tested using the statistical theory of mass spectra. The mass spectra of propane, propane-2,2-d_2 and n-butane have been calculated and found to agree well with experimental results. However complex molecules have calculated and experimental results that agreed only in a qualitative fashion.

There are various pathways by which fragmentation may occur. The probability of a particular fragmentation mode occurring will be dependent upon the energy of the electron beam. Most spectra however, are run under conditions in which the bombarding electron beam has considerably more energy than required to rupture one bond. Thus a more complex spectrum consisting of many peaks results.

Fragmentation patterns

The intensity of a peak, corresponding to a positively charged fragment, represents the number of ions arriving at the ion collector and not the original number of ions produced. The intensity of a peak is found to depend upon the ion's stability *versus* its tendency to undergo further fragmentation. Structural features will determine the stability of fragments. Elements of structure, that tend to stabilize a positively charged fragment, will aid in the production of an intense peak. Stabilization of a positively charged fragment is aided by the production of a stable radical or a neutral molecule.

In general it has been found that the following cleavages or rearrangements are responsible for the most intense peaks in the mass spectra of organic molecules. [1]

A. Simple Cleavage

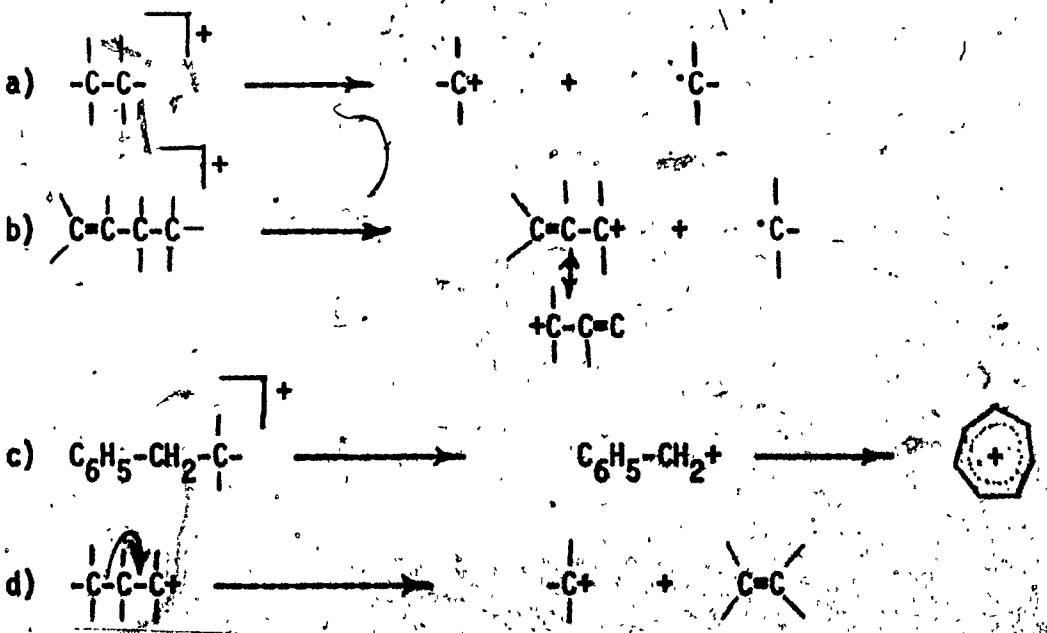

e) 

X = halogen, OR, SR, NR_2 with R=H or alkyl

f) 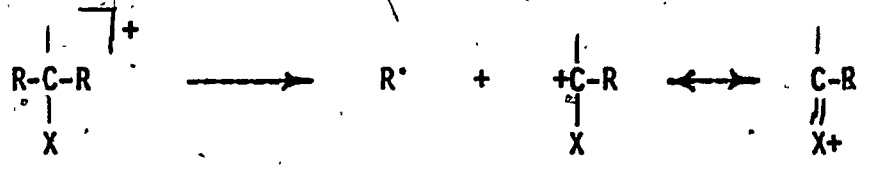

g) 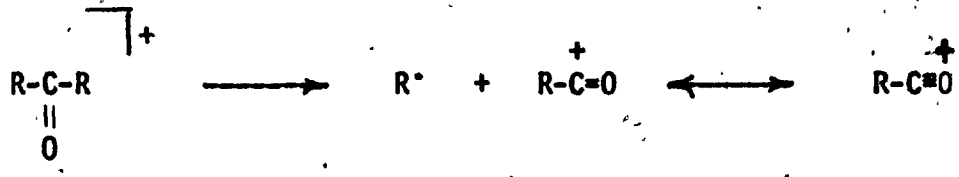

h) 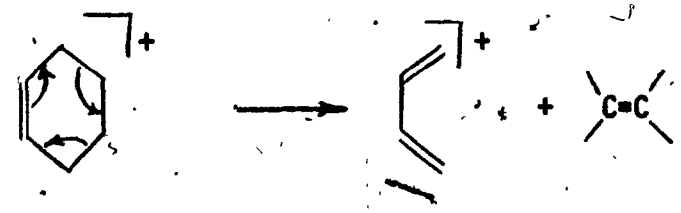

B. Rearrangements

a) 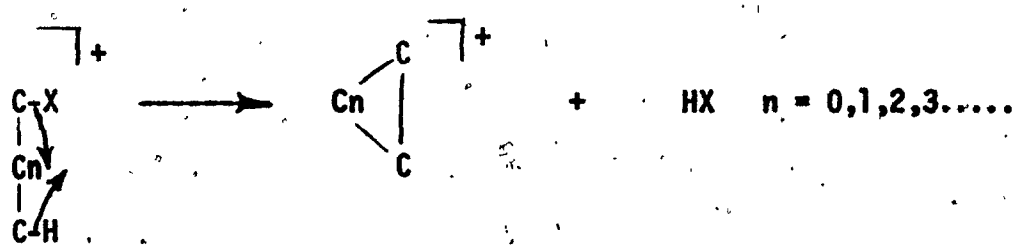

b) 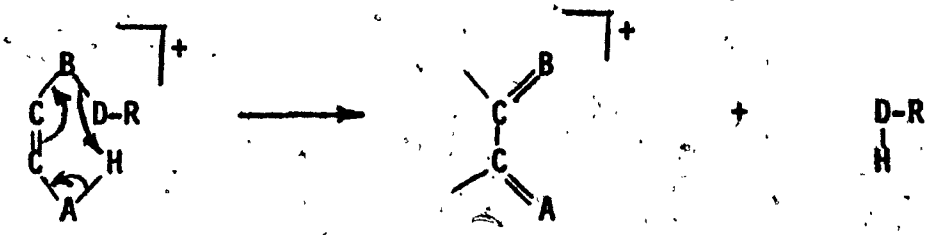

c) 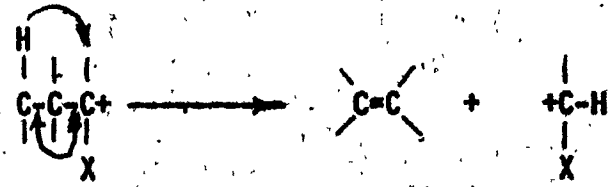

X = O, S, N, R, H

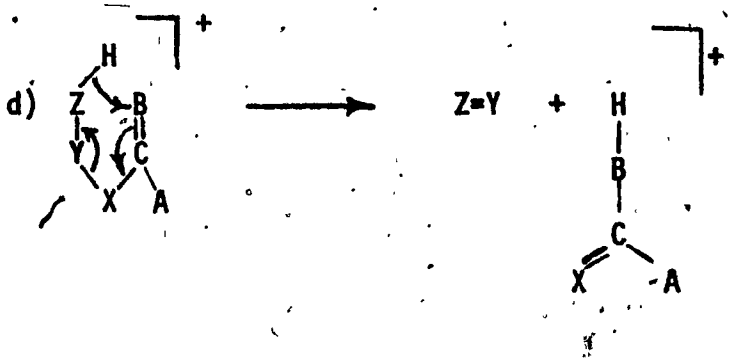

It must be noted that there are major factors which tend to militate against a certain pathway for fragmentation. These factors may be summarized as (1) the localization of a positive charge on a certain atom rather than having the charge dissipated throughout the molecule by electronic effects; (2) a distribution of the atoms in the molecule that overrides the possibility of a rearrangement process; (3) formation of a neutral fragment of high energy content.

Effects of Isotopes

i) Chlorination

Chlorine has two naturally occurring isotopes, ^{35}Cl and ^{37}Cl. The relative abundance of these isotopes can aid in the interpretation of a mass spectrum. If a number of chlorine atoms are incorporated into a molecule, the relative intensity of the isotope peaks can be predicted by the binomial expansion. A binomial expansion can be expressed as $(a+b)^n$, where a = relative abundance of the light isotope, and b = relative abundance of the heavy isotope, and n = the number of chlorine atoms present.

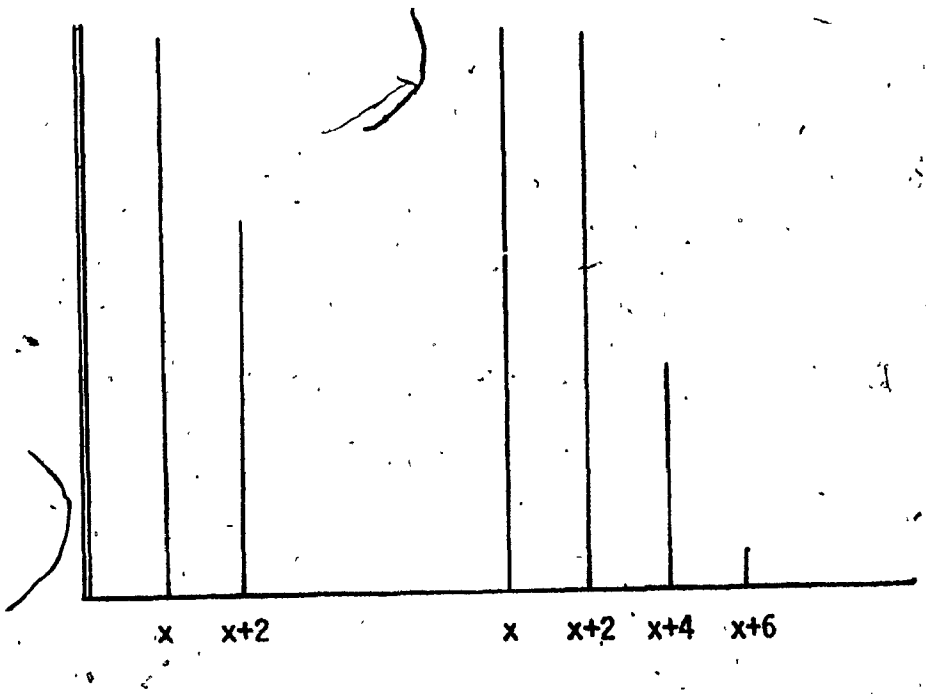

For two Cl atoms For three Cl atoms

The characteristic isotope pattern of chlorine containing fragments make them readily identifiable.

One must keep in mind the possibility of errors in interpretation when looking at isotopic systems, as coincidental overlap of fragment ions will destroy the characteristic pattern being sought after.

ii) Isotopic labelling

Planned isotopic labelling can aid in determining the mechanism of fragmentation. By specific deuteration of functional groups within a molecule it often becomes possible to determine the relative importance of competing fragmentation pathways. As an example, a peak appearing at m/e 43 has two common possibilities, $[CH_3-\overset{\overset{O}{\|}}{C}]^+$ or $[C_3H_7]^+$. A molecule with both of these functional groups is $CH_3-\overset{\overset{O}{\|}}{C}-(CH_2)_2CH_3$. By specific deuteration of the methyl group attached to the carbonyl, the mass spectrum of $CD_3-\overset{\overset{O}{\|}}{C}-(CH_2)_2CH_3$ would now show a peak at m/e 46 for $[CD_3-\overset{\overset{O}{\|}}{C}]^+$ and a peak at m/e 43 for $[C_3H_7]^+$. It now becomes possible to distinguish the formation of each fragment. The conclusion reached is based upon the premise that complete deuteration has occurred at the desired position and that no isotope scrambling has occurred.

With the technique of specific deuteration, it then becomes possible to describe where a particular hydrogen abstraction occurs in a rearrangement process. As an example the general process,

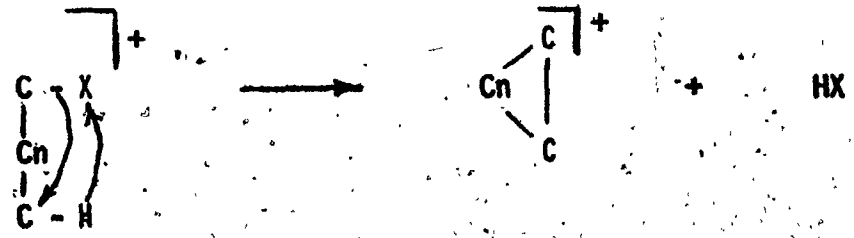

can be better understood by reviewing specifically deuterated positions within the alkyl chain. To further illustrate this point, the elimination of water from ethanol upon electron impact was thought to be a 1,2 elimination. The mass spectrum of ethanol-1-d_2 showed an elimination of H_2O has occurred rather than HDO.

Metastable ions

If an ion is accelerated from near rest through a potential drop of V and undergoes decomposition after acceleration, but before analysis, a metastable transition may be observed. For example, if an ion of mass m_1 and charge q_1 is accelerated through a potential drop and then decomposes into an ion of mass m_2 and charge q_2, and a neutral species n, one then has the equation:

$$m_1 q_1 \longrightarrow m_2 q_2 + n \qquad (4)$$

The apparent mass, m^*, of the daughter ion is given by:

$$m^* = \frac{(m_2)^2 q_1 e}{m_1 (q_2)^2} \qquad (5)$$

where e is the charge of one electron. The most commonly observed cases are where; (I) $q_1 = q_2 = e$ and therefore

$m^* = \frac{(m_2)^2}{m_1}$, (II) $q_1 = q_2 = 2e$ and therefore $m^* = \frac{(m_2)^2}{2m_1}$,

(III) $q_1 = 2e$, $q_2 = e$, then $m^* = \frac{2(m_2)^2}{m_1}$. These equations can be applied when mass spectrometers of the sector, or semi circular magnetic deflection type are used.

In a normal double focussing mass spectrometer the metastable transitions that are observed are those that occur between the electric and the magnetic sector. Those decompositions that occur between the ion source and the electrostatic sector are normally observed. Metastable transitions occurring between the ion source and the electric sector may however, be observed if appropriate variations are made in the electronics of the electric sector. Struck and Major [13] have developed a technique to observe metastable transitions that occur between the ion source and the electric sector.

Metastable transitions occurring between the ion source and the electric sector may be observed by increasing the ratio of the accelerating voltage to the electric sector voltage, V/E, by the factor m_1/m_2. The main ion beam will be defocussed, and only the daughter ion m_2 from the decomposition shown in equation (4) will be observed. The ratio of V/E may be changed by varying the voltage of the electric sector in a continuous fashion from its normal value of E_0. The ratio E_1/E_0 for a particular metastable ion gives the ratio m_2/m_1, since $E_1/E_0 = m_2/m_1$. Then if the electric sector voltage is set at the ratio of E_1/E_0, where a metastable ion occurred, and then a magnetic scan is taken, a peak will be observed for the transition $m_1 \longrightarrow m_2 + n$. This peak will be found at the same m/e position on the spectrum, as the metastable peak for this transition in the normal spectrum. From the following relationship $E_1/E_0 = m_2/m_1 = m^*/m_1$ where $m^* = (m_2)^2/m_1$, one can calculate m_2 and m_1.

This technique focusses the metastable daughter ion so that the peak is more intense. The normal ion beam will not be transmitted to the magnetic sector. Since there are few peaks in such a spectrum it is necessary to calibrate the mass scale, either by using a mass marker or by running part of the normal spectrum so that it can be overlaid to obtain the mass of the peak resulting from the decomposition of the metastable species.

High resolution

Perhaps the most powerful technique in mass spectral work, is that of high resolution. High resolution offers the possibility of separating peaks of relatively small mass difference. An operational definition of resolution that is often used, is that two peaks are fully resolved if the depth of the valley between the peaks is less than 10% of the height of either peak. The resolution required to separate peaks is the difference in the masses of the two peaks being considered. High resolution may be considered to be resolution above the level, R = 5000.

Resolution that can be attained by a particular mass spectrometer is dependent upon whether the instrument is a single focussing or a double focussing instrument. Variable parameters of the instrument, such as the slit widths of the source and collector slit, as well as the position of the magnet can be adjusted to give maximum resolution.

High resolution can be attained with a double focussing mass spectrometer, the term double focussing means that the ion beam is focussed in two ways, electrostatically, and magnetically.

Electrostatic focussing of the ion beam involves the elimination of an energy spread in the ion beam. Ions are passed through a radial

electrostatic field and undergo velocity focussing, so that ions of a particular kinetic energy can then be selected by the use of a variable slit between the electrostatic analyzer and the magnetic field. Selected ions then pass from electrostatic sector to the magnetic sector.

Direction focussing is accomplished in a magnetic field. Ions are accelerated from the ion source by a high voltage, the potential energy (eV) that an ion fragment had the instant before acceleration will be equal to its kinetic energy after it has fully accelerated.

$$eV = \frac{Mv^2}{2} \qquad (6)$$

The magnetic field will act upon the accelerated particle with a centripetal force HeV. This will be counterbalanced by a centrifugal force Mv^2/r where r is the radius of the semicircular path of the magnetic field.

$$He\mathbf{v} = \frac{Mv^2}{r} \qquad (7)$$

The mass to charge ratio for the particle upon eliminating v will then be;

$$\frac{M}{e} = \frac{H^2r^2}{2V} \qquad (8)$$

To observe the complete spectrum of mass fragments either the magnetic field or the accelerating voltage is varied.

Using high resolution to determine the exact mass of particular peaks, in addition to specific deuteration studies, one can elucidate a very complex problem.

Experimental

The preparation of the N-t-butyl-α-chloroacetamides was accomplished without taking any special precautions in the synthetic methods used. However the preparation of the N-t-butyl-α-fluoroacetamides was a more difficult task, as they evaporate easily. Crystallization of the crude product from the reaction mixture could only be managed if the solvent for the reaction was evaporated in a refrigerator, otherwise both the solvent and the prepared amide evaporated. Purification of the N-t-butyl-α-fluoroacetamides was by sublimation alone, this provided a sample pure enough for mass spectral studies.

The N-t-butyl-d_9 used in the preparation of the N-t-butyl-α-fluoroacetamides was most generously provided by T. Schulz.

All melting points of the prepared compounds were taken on a Mettler melting point apparatus. Melting points are uncorrected.

The mass spectra that were studied in this work were obtained using a double focussing Hitachi RMU6E mass spectrometer. All of the compounds studied were admitted into the mass spectrometer through the solid sample inlet. Since the compounds were of such a volatile nature, they were enclosed in a specially prepared sample tube. The sample tube was produced by sealing a glass tube at one end, admitting approximately five milligrams of sample, and then partially sealing the other end of the tube to form a pin hole. While the process of partially sealing the sample was carried out, the sample tube was partly immersed in liquid nitrogen to prevent vaporization of the sample. Approximate dimensions of the sample tubes are; length: 2 cm, inside diameter 1.5 mm, outside

diameter: 2.5 mm. Using sample tubes prepared in this manner, a controlled amount of sample was admitted into the ionization chamber of the mass spectrometer.

All of the spectra were run under conditions that were as uniform as possible. The ionization energy was maintained at 70 eV for each mass spectrum. Care was taken so that sample vapour pressure within the mass spectrometer remained at a constant level. A recording of the mass spectrum was accomplished by simultaneously running the mass spectrometer (speed 5), and a Bell and Howell visirecorder (at 2.5 x 10 mm/sec) connected to the mass spectrometer. The resulting photographic copy of the mass spectrum was then developed in the light, and finally sprayed with a yellow Kodak spray, to retard further light developing. The determination of the m/e values in each spectrum was by reference to the peaks for nitrogen (m/e 28), and oxygen (m/e 32).

Presentation of spectral data throughout this thesis is in terms of $\%\Sigma_{36}$. This simply means that all of the peak heights starting at m/e 36 were totaled up to, and including the parent peak. This total is then referred to as the total ion current measured from m/e 36. Individual peak intensities are calculated by dividing the height of the peak, by the total ion current measured from m/e 36; this then is multiplied by 100% to give the $\%\Sigma_{36}$ for that particular peak. The choice of m/e 36 as a starting point was based upon a number of factors; one factor was that interfering peaks which do not result from the fragmentation process such as nitrogen and oxygen are eliminated; another factor is that the first major peak in a number of spectra is at m/e 36; and finally the work in this thesis could easily be compared with that of T. Schulz's, who also used $\%\Sigma_{36}$.

Experiments

N-t-butylacetamide

This compound was prepared by the method of Speziale and Hamm [15]. The white crystals obtained were recrystalized from ligroin (40-60°) and sublimed twice; m.p. 98.6°, (lit. [16] 98-99°). (Found: C, 62.4: H, 11.4; N, 12.1%. Calcd. for $C_6H_{13}NO$: C, 62.6; H, 11.4, 12.6%).

N-t-butyl-α-chloroacetamide

N-t-butyl-α-chloroacetamide was prepared by the general procedure described by Speziale and Hamm [15]. The white crystals obtained were recrystallized from ligroin (40-60°) and sublimed twice; m.p. 83.6°, (lit. [15] (82-83°). (Found: C, 48.2; H, 8.1; N, 9.4%. Calcd. for $C_6H_{12}NOCl$: C, 48.6; H, 8.7; N, 9.4%.)

N-t-butyl-α,α-dichloroacetamide

N-t-butyl-α,α-dichloroacetamide was prepared by the general method of Speziale and Hamm [15]. The white crystals obtained were recrystalized from a ligroin-acetone mixture and sublimed twice to give the amide, m.p. 156.4°. (Found: C, 39.9; H, 6.0; N, 7.8%. Calcd. for $C_6H_{11}NOCl_2$: C, 39.2; H, 6.0; N, 7.6%.)

N-t-butyl-α,α,α-trichloroacetamide

This compound was prepared by the general method of Speziale and Hamm [15]. The white crystals obtained were recrystalized from a ligroin-carbon tetrachloride mixture and sublimed twice; m.p. 112.4°, (lit. [17]

110-111°.) Found: C, 32.6; H, 4.3; N, 6.5%. Calcd. for $C_6H_{10}NOCl_3$: C, 32.9; H, 4.61; N, 6.41%.)

N-t-butyl-d_9-acetamide

Acetylchloride (0.156 g, 0.002 mole) in 30 ml of dichloromethane, and t-butylamine-d_9 (0.164 g, 0.002 mole) in 30 ml of dichloromethane, were each added dropwise to a previously cooled (-10°) solution of triethylamine (0.202 g, 0.002 mole), in 15 ml of dichloromethane. The temperature of the reaction mixture was then allowed to rise to 25°. The solution was then washed twice with 30 ml of water. After separating and drying (Na_2SO_4), the dichloromethane was evaporated, and the remaining crystalline amide was sublimed three times; m.p. 98.3° (0.16 g, 72%).

N-t-butyl-d_9-α-chloroacetamide

Chloroacetylchloride (0.224 g, 0.002 mole) in 30 ml of dichloromethane and t-butylamine d_9 (0.164 g, 0.002 mole) in 30 ml of dichloromethane, were each added dropwise to a previously cooled (-10°) solution of triethylamine (0.202 g, 0.002 mole), in 15 ml of dichloromethane. The temperature of the reaction mixture was then allowed to rise to 25°. The solution was then washed twice with 30 ml of 5% sodium bicarbonate solution and once with 30 ml water. After separating and drying (Na_2SO_4), the dichloromethane was evaporated, and the remaining crystalline amide was sublimed twice; m.p. 82.7° (0.13 g, 45%).

N-t-butyl-d_9-α,α-dichloroacetamide

Dichloroacetylchloride (0.292 g, 0.002 mole) in 30 ml of

dichloromethane, and t-butylamine d_9 (0.164 g, 0.002 mole) in 30 ml of dichloromethane, were each added dropwise to a previously cooled (-10°) solution of triethylamine (0.202 g, 0.002 mole), in 15 ml of dichloromethane. The temperature of the reaction mixture was then allowed to rise to 25°. The solution was then washed twice with 30 ml of sodium bicarbonate solution and once with 30 ml of water. After separating and drying (Na_2SO_4), the dichloromethane was evaporated, and the remaining crystalline amide was sublimed twice; m.p. 155.8° (0.28 g, >73%).

N-t-butyl-d_9-α,α,α-trichloroacetamide

Trichloroacetylchloride (0.360 g, 0.002 mole) in 30 ml of dichloromethane, and t-butylamine d_9 (0.164 g, 0.002 mole) in 30 ml of dichloromethane were each added dropwise to a previously cooled (-10°) solution of triethylamine (0.202 g, 0.002 mole), in 15 ml of dichloromethane. The temperature of the reaction mixture was then allowed to rise to 25°. The solution was then washed twice with 30 ml of 5% sodium bicarbonate solution and once with 30 ml of water. After separating and drying (Na_2SO_4), the dichloromethane was evaporated, and the remaining crystalline amide was sublimed twice; m.p. 111.6° (0.30 g, 68%).

N-t-butyl-α-fluoroacetamide

Fluoroacetylchloride (0.96 g, 0.01 mole) in 30 ml of dichloromethane, and t-butylamine (0.73 g, 0.01 mole) in 30 ml of dichloromethane, were each added dropwise, to a previously cooled (-70°) solution of triethylamine (1.01 g, 0.01 mole) in 15 ml of dichloromethane. The temperature of the reaction mixture was then allowed to rise to 25°. The solution was then washed twice with 30 ml of saturated sodium bicarbonate

solution and once with 30 ml of water. After separating and drying over anhydrous sodium sulphate, the dichloromethane was evaporated at -5°, and the remaining crystalline amide was sublimed twice m.p. 38° (0.93 g, 70%).

Fluoroacetylchloride

Fluoroacetic acid (0.78 g, 0.01 mole) was added over a period of fifteen minutes to previously cooled (-25°) phosphorous pentachloride (2.06 g, 0.01 mole). After the addition of fluoroacetic acid was complete, the reaction mixture was refluxed for thirty minutes. Distillation of the fluoroacetylchloride occurred at 78° (0.43 g, 45%).

Difluoroacetic anhydride

Difluoroacetic anhydride was prepared by the method of Sawicki [18]. The liquid had a boiling point of 125-127° and gave a yield of 65%.

N-t-α,α-difluoroacetamide

Difluoroacetic anhydride (1.74 g, 0.01 mole) in 30 ml of dichloromethane, and t-butylamine (0.73 g, 0.01 mole) in 30 ml of dichloromethane, were each added dropwise to a previously cooled (-70°) solution of triethylamine (1.01 g, 0.01 mole), in 15 ml of dichloromethane. The temperature of the reaction mixture was then allowed to rise to 25°. The solution was then washed twice with 30 ml of saturated sodium bicarbonate solution and once with 30 ml of water. After separating and drying over anhydrous sodium sulphate the dichloromethane was evaporated at -5°, and the remaining crystalline amide was sublimed twice; m.p. 50.5° (0.92 g, 61%).

N-t-butyl-α,α,α-trifluoroacetamide

Trifluoroacetic anhydride (2.10 g, 0.01 mole) in 30 ml of dichloromethane, and t-butylamine (0.73 g, 0.01 mole) in 30 ml of dichloromethane, were each added dropwise to a previously cooled (-70°) solution of triethylamine (1.01 g, 0.01 mole) in 15 ml of dichloromethane. The temperature of the reaction mixture was then allowed to rise to 25°. The solution was then washed twice with 30 ml of saturated sodium bicarbonate solution and once with 30 ml of water. After separating and drying over anhydrous sodium sulphate, the dichloromethane was evaporated at -5°, the remaining crystalline amide was sublimed twice m.p. 45.6° (1.32 g, 78%).

N-t-butyl-d_9-α-fluoroacetamide

Fluoroacetylchloride (0.19 g, 0.002 mole) in 30 ml of dichloromethane and t-butylamine d_9 (0.16 g, 0.002 mole) in 30 ml of dichloromethane, were each added dropwise to a previously cooled (-70°) solution of triethylamine (0.20 g, 0.002 mole), in 15 ml of dichloromethane. The temperature of the reaction mixture was then allowed to rise to 25°. The solution was then washed twice with 30 ml of saturated sodium bicarbonate solution and once with 30 ml of water. After separating and drying over anhydrous sodium sulphate, the dichloromethane was evaporated at -5°, the remaining crystalline amide was sublimed twice m.p. 37.8° (0.20 g, 70%).

N-t-butyl-d_9-α,α-difluoroacetamide

Difluoroacetic anhydride (0.35 g, 0.002 mole) in 30 ml of dichloromethane, and t-butylamine d_9 (0.16 g, 0.002 mole) in 30 ml of

dichloromethane, were each added dropwise to a previously cooled (-70°) solution of triethylamine (0.202 g, 0.002 mole) in 15 ml of dichloromethane. The temperature of the reaction mixture was then allowed to rise to 25°. The solution was then washed twice with 30 ml of saturated sodium bicarbonate solution and once with 30 ml of water. After separating and drying over anhydrous sodium sulphate, the dichloromethane was evaporated at -5°, the remaining crystalline amide was sublimed twice m.p. 50.2° (0.18 g, 58%).

N-t-butyl-d_9-α,α,α-trifluoroacetamide

Trifluoroacetic anhydride (0.42 g, 0.002 mole) in 30 ml of dichloromethane, and t-butylamine d_9 (0.16 g, 0.002 mole) in 30 ml of dichloromethane, were each added dropwise to a previously cooled (-70°) solution of triethylamine (0.20 g, 0.002 mole) in 15 ml of dichloromethane. The temperature of the reaction mixture was then allowed to rise to 25°. The solution was then washed twice with 30 ml of saturated sodium bicarbonate solution and once with 30 ml of water. After separating and drying over anhydrous sodium sulphate, the dichloromethane was evaporated at -5°, the crystalline amide was sublimed twice m.p. 44.8° (0.27 g, 80%).

Results and Discussion

Part I Identification of peaks

Tables 1,3,5,7,9,11, and 13 list all of the mass spectral peaks that were observed to be above 0.8% Σ_{36} for the compounds studied; the tables also contain the proposed elemental formula of the fragment peak and the assumed structural formula of that fragment. Some of the fragment peaks listed in these tables gave distinct doublets, in such cases the percentage of the prominent peak at the nominal mass of this fragment peak is included in the table. The structural formula of prominent ^{13}C isotopes, or ^{37}Cl isotopes of ion fragments is not given.

Fragmentation peaks which were not accounted for in the proposed fragmentation patterns are underlined in the tables. There is little evidence as to the origin of these species. Isotopic labelling was used as a tool to identify particular fragment peaks. Tables 2,4,6,8,10,12 and 14 list fragment peaks, and the elemental formula of these fragments; also contained within the tables are the analogous nominal mass for the analogous d_9-deuterated compound, as well as the corresponding assumed elemental formula of the deuterated fragment.

In cases where labelling was not complete in the deuterated compound, high resolution measurements were used to confirm the particular peak's identity. Any peaks that were identified in this manner are in Tables 9, 11 and 13, and are marked with an asterisk.

A) N-t-butylacetamide

Table 1

A compilation of m/e, $\%\Sigma_{36}$, proposed elemental formula and proposed structural formula for peaks in the mass spectrum of N-t-butylacetamide

m/e	$\%\Sigma_{36}$	Proposed elemental formula	Proposed structural formula
39	1.4	C_3H_3	
41	4.1	C_3H_5	$CH_3-\overset{+}{C}=CH_2$
42	3.9	C_2H_4N	$CH_3-C\equiv\overset{+}{N}-H$
43	8.2	C_2H_3O	$CH_3-\underset{\|\|}{C}-\overset{+}{}$ (O)
55	1.0	C_4H_7	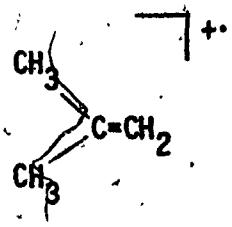
56	3.7	C_4H_8	
57	3.8	C_4H_9	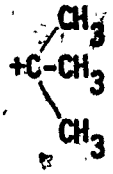
58	36.1	C_3H_8N (94%) C_2H_4NO (6%)	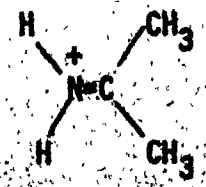

Table 1 Continued

m/e	$\%\Sigma_{36}$	Proposed elemental formula	Proposed structural formula
59	2.1	C_3H_7O (42%)	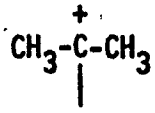
		C_3H_7DN (58%)	
		an isotope of m/e 58	
60	13.8	C_3H_6NO	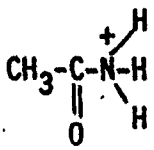
100	3.4	$C_5H_{10}NO$	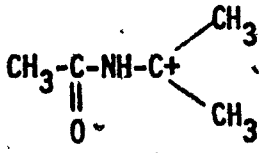
115	12.7	$C_6H_{13}NO$	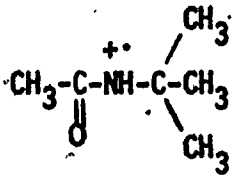

The peaks tabulated account for 95.9% of the ion current from m/e 36.

Table 2

A comparison of the mass spectra of N-t-butylacetamide and N-t-butyl-d_9-acetamide for peak identification purposes

m/e N-t-B.A.	Proposed elemental formula of fragment peaks in the N-t-B.A. mass spectrum	Proposed analogous nominal mass in the N-t-B.A. d_9 mass spectrum	Proposed analogous elemental formula of fragment peaks in the N-t-B.A. d_9 mass spectrum
39	C_3H_3	42	C_3D_3
41	C_3H_5	46	C_3D_5
43	C_2H_3O	43	C_2H_3O
55	C_4H_7	62	C_4D_7
56	C_4H_8	64	C_4D_8
57	C_4H_9	66	C_4D_9
58	C_2H_4NO	58	C_2H_4NO
59	C_3H_7O	65	C_3HD_6O
59	C_3H_8N (a ^{13}C isotope of m/e 58)	65	
60	C_3H_6NO	62	$C_3H_4D_2O$
100	$C_5H_{10}NO$	106	$C_5H_4D_6NO$

Table 2 Continued

m/e N-t-B.A.	Proposed elemental formula of fragment peaks in the N-t-B.A. mass spectrum	Proposed analogous nominal mass in the N-t-B.A. d_9 mass spectrum	Proposed analogous elemental formula of fragment peaks in the N-t-B.A. d_9 mass spectrum
115	$C_6H_{13}NO$	126	$C_6H_4D_9NO$

N-t-B.A. is N-t-butylacetamide, and N-t-B.A. d_9 is N-t-butyl-d_9-acetamide. These symbols will be used in tables where necessary.

B) N-t-butyl-α-chloroacetamide

Table 3

A compilation of m/e, $\%\Sigma_{36}$, proposed elemental formula and proposed structural formula for peaks in the mass spectrum of N-t-butyl-α-chloroacetamide

m/e	$\%\Sigma_{36}$	Proposed elemental formula	Proposed structural formula
36	0.8	HCl	$[H\text{-}Cl]^{+\cdot}$
39	2.1	C_3H_3	
41	6.8	C_3H_5 (88%)	$CH_3\text{-}\overset{+}{C}{=}CH_2$
42	3.2	C_2H_4N (84%)	$CH_3\text{-}C{\equiv}\overset{+}{N}\text{-}H$
49	1.8	CH_2Cl	$^{+}CH_2Cl$
55	1.2	C_4H_7	
56	4.4	C_4H_8	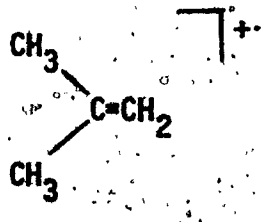
57	8.7	C_4H_9	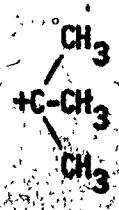

Table 3 Continued

m/e	$\%\Sigma_{36}$	Proposed elemental formula	Proposed structural formula
58	28.2	$C_3H_8N^+$	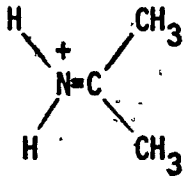
59	1.3	C_3H_8N (75%) a ^{13}C isotope of m/e 58	
		C_3H_7O (17%)	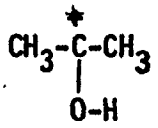
77	1.1	C_2H_2ClO	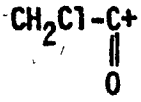
94	7.9	C_2H_5NOCl	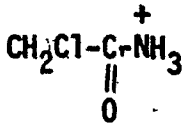
96	2.5	a ^{37}Cl isotope of m/e 94	
114	1.0	$C_6H_{12}NO$	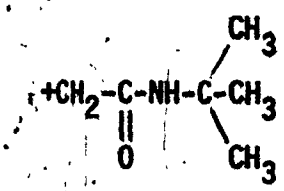
134	9.7	C_5H_9NOCl	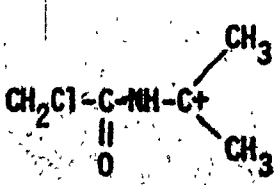
136	3.3	a ^{37}Cl isotope of m/e 134	

Table 3 Continued

m/e	$\%\Sigma_{36}$	Proposed elemental formula	Proposed structural formula
149	5.2	$C_6H_{12}NOCl$	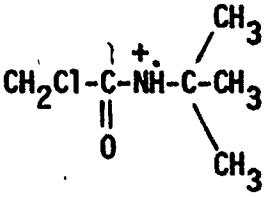
151	1.7	a ^{37}Cl isotope of m/e 149	

The peaks tabulated account for 91.1% of the ion current.

Table 4

A comparison of the mass spectra of N-t-butyl-α-chloroacetamide and N-t-butyl-d_9-α-chloroacetamide for peak identification purposes

m/e N-t-B.ClA.	Proposed elemental formula of fragment peaks in the N-t-B. ClA. mass spectrum	Proposed analogous nominal mass in the N-t-B.ClA. d_9 mass spectrum	Proposed analogous elemental formula of fragment peaks in the N-t-B.ClA. d_9 mass spectrum
39	C_3H_3	42	C_3D_3
41	C_3H_5	46	C_3D_5
42	C_2H_4N	45	C_2HD_3N
49	CH_2Cl	49	CH_2Cl
55	C_4H_7	62	C_4D_7
	C_3H_5N	59	C_3D_4NH
56	C_4H_8	64	C_4D_8
57	C_4H_9	66	C_4D_9
58	C_3H_8N	64	$C_3H_2D_6N$
59	C_3H_8N	65	$C_3H_2D_6N$
	a ^{13}C isotope of m/e 58		
59	C_3H_7O	66	C_3HD_6O
77	C_2H_2OCl	77	C_2H_2OCl

Table 4 Continued

m/e N-t-B.ClA.	Proposed elemental formula of fragment peaks in the N-t-B. ClA. mass spectrum	Proposed analogous nominal mass in the N-t-B.ClA. d_9 mass spectrum	Proposed analogous elemental formula of fragment peaks in the N-t-B.ClA. d_9 mass spectrum
94	C_2H_5NOCl	96	$C_2H_3D_2NOCl$
96	C_2H_5NOCl a ^{37}Cl isotope of m/e 94	98	$C_2H_3D_2NOCl$
114	$C_6H_{12}NO$	123	$C_6D_9H_3NO$
134	C_5H_9NOCl	140	$C_5H_3D_6NOCl$
136	C_5H_9NOCl a ^{37}Cl isotope of m/e 134	142	$C_5H_3D_6NOCl$
149	$C_6H_{12}NOCl$	158	$C_6H_3D_9NOCl$
151	$C_6H_{12}NOCl$ a ^{37}Cl isotope of m/e 149	160	$C_6H_3D_9NOCl$

N-t-B.ClA. is N-t-butyl-α-chloroacetamide and N-t-butyl-d_9-α-chloroacetamide is represented by N-t-B.ClA. d_9. These symbols will be used in the tables where necessary.

(2) N-t-butyl-α,α-dichloroacetamide

Table 5

A tabulation of m/e, $\%\Sigma_{36}$, proposed elemental formula, and proposed structural formula for peaks in the mass spectrum of N-t-butyl-α,α-dichloroacetamide

m/e	$\%\Sigma_{36}$	Proposed elemental formula	Proposed structural formula
36	1.9	HCl	$[HCl]^{+\cdot}$
39	2.7	C_3H_3	
41	9.7	C_3H_5	$CH_3-\overset{+}{C}=CH_2$
42	4.8	C_2H_4N	$CH_3-C\equiv\overset{+}{N}-H$
55	1.2	C_4H_7	
56	3.7	C_4H_8	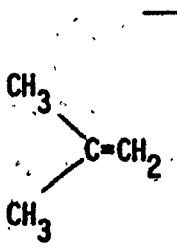
57	32.2	C_4H_9	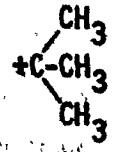
58	17.0	C_3H_8N	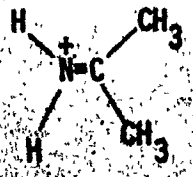

Table 5 Continued

m/e	$\%\Sigma_{36}$	Proposed elemental formula	Proposed structural formula
59	1.3	C_3H_7O	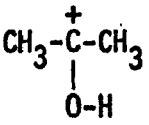
83	1.7	$CHCl_2$	
100	4.2	$C_5H_{10}NO$	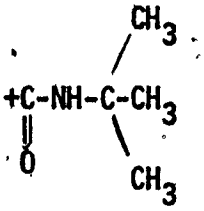
128	0.9	$C_2H_4NOCl_2$	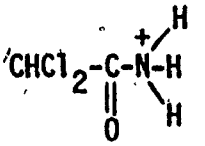
168	4.1	$C_5H_8NOCl_2$	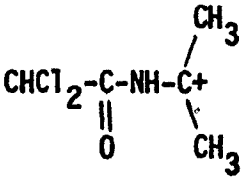
170	2.6	a ^{37}C isotope of m/e 168	
183	0.5	$C_6H_{11}NOCl_2$	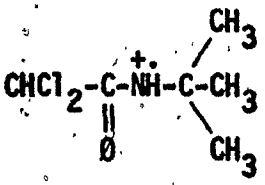

The peaks tabulated account for 89.2% of the ion current above m/e 36.

Table 6

A comparison of the mass spectra of N-t-butyl-α,α-dichloroacetamide and N-t-butyl-d_9-α,α-dichloroacetamide for peak identification purposes

m/e N-t-B.Cl_2A.	Proposed elemental formula of fragment peaks in the N-t-B.Cl_2A. mass spectrum	Proposed analogous nominal mass in the N-t-B.Cl_2A.d_9 mass spectrum	Proposed analogous elemental formula of fragment peaks in the N-t-B.Cl_2A.d_9 mass spectrum
36	HCl	36	HCl
39	C_3H_3	42	C_3D_3
41	C_3H_5	46	C_3D_5
42	C_2H_4N	45	C_2D_3HN
55	C_4H_7	62	C_4D_7
56	C_4H_8	64	C_4D_8
57	C_4H_9	66	C_4D_9
58	C_3H_8N	64	$C_3H_2D_6N$
59	C_3H_7O	65	C_3HD_6O
83	$CHCl_2$	83	$CHCl_2$
100	$C_5H_{10}NO$	109	C_5HD_9NO
128	$C_2H_4NOCl_2$	130	$C_2H_2D_2NOCl_2$
168	$C_5H_8NOCl_2$	174	$C_5H_2D_6NOCl_2$

Table 6 Continued

m/e N-t-B.Cl_2A.	Proposed elemental formula of fragment peaks in the N-t-B.Cl_2A. mass spectrum	Proposed analogous nominal mass in the N-t-B.Cl_2A.d_9 mass spectrum	Proposed analogous elemental formula of fragment peaks in the N-t-B.Cl_2A.d_9 mass spectrum
170	$C_5H_8NOCl_2$ a ^{37}Cl isotope of m/e 168	176	$C_5H_2D_6NOCl_2$
183	$C_6H_{11}NOCl_2$	192	$C_6H_2D_9NOCl_2$

N-t-B.Cl_2A. is N-t-butyl-α,α-dichloroacetamide and N-t-B.Cl_2A.d_9 is N-t-butyl-d_9-α,α-dichloroacetamide. These abbreviations will be used in tables where necessary.

D) N-t-butyl-α,α,α-trichloroacetamide

Table 7

A tabulation of m/e, $\%\Sigma_{36}$, proposed elemental formula, and proposed structural formula for peaks in the mass spectrum of N-t-butyl-α,α,α-trichloroacetamide

m/e	$\%\Sigma_{36}$	Proposed elemental formula	Proposed structural formula
36	1.4	HCl	$[H\text{-}Cl]^{+\cdot}$
39	1.6	C_3H_3	
41	10.0	C_3H_5	$CH_3\text{-}\overset{+}{C}{=}CH_2$
42	4.2	C_2H_4N	$CH_3\text{-}C{\equiv}\overset{+}{N}\text{-}H$
55	1.3	C_4H_7	
56	3.7	C_4H_8	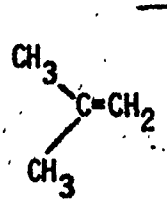
57	37.8	C_4H_9	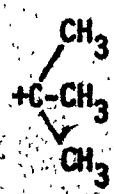

Table 7 Continued

m/e	$\%\Sigma_{36}$	Proposed elemental formula	Proposed structural formula
58	2.7	C_3H_8N (38%) a ^{13}C isotope of m/e 57 (82%)	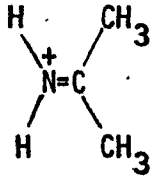
59	1.8	C_3H_7O	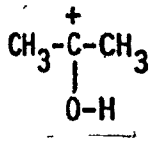
77	0.7	C_3H_6Cl	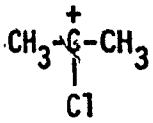
82	0.9	CCl_2	$[CCl_2]^{+\cdot}$
84	0.9	C_4H_6NO	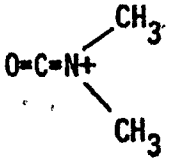
98	1.0	CH_2NCl_2	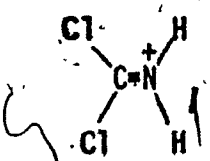
100	3.0	$C_5H_{10}NO$	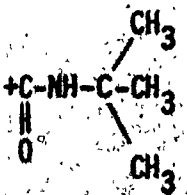

Table 7 Continued

m/e	$\%\Sigma_{36}$	Proposed elemental formula	Proposed structural formula
110	0.6	C_2OCl_2	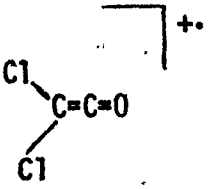
117	1.4	CCl_3	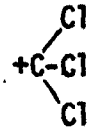
119	1.4	a ^{37}Cl isotope of m/e 117	
138	1.0	$C_4H_6NCl_2$	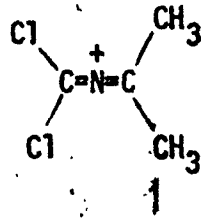
140	0.6	a ^{37}Cl isotope of m/e 138	
162	0.7	$C_2H_3NCl_3$	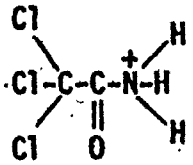
182	0.4	$C_6H_{10}NOCl_2$	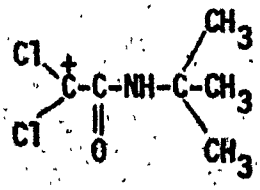
202	4.4	$C_5H_7NOCl_3$	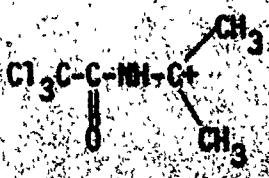

Table 7 Continued

m/e	$\%\Sigma_{36}$	Proposed elemental formula	Proposed structural formula
204	4.1	a ^{37}Cl isotope of m/e 202	
206	1.3	a ^{37}Cl isotope of m/e 202	
217	0.2	$C_6H_{10}NOCl_3$	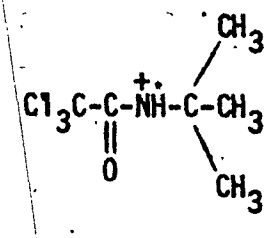

The peaks tabulated account for 84.7% of the ion current above m/e 36.

Table 8

A comparison of the mass spectra of N-t-butyl-α,α,α-trichloroacetamide and N-t-butyl-d_9-α,α,α-trichloroacetamide for peak identification purposes

m/e N-t-B.Cl_3A.	Proposed elemental formula of fragment peaks in the N-t-B.Cl_3A. mass spectrum	Proposed analogous nominal mass in the N-t-B.Cl_3A.d_9 mass spectrum	Proposed analogous elemental formula of fragment peaks in the N-t-B.Cl_3A.d_9 mass spectrum
36	HCl	36	HCl
39	C_3H_3	42	C_3D_3
41	C_3H_5	46	C_3D_5
42	C_2H_4N	45	CHD_3N
55	C_4H_7	62	C_4D_7
56	C_4H_8	64	C_4D_8
57	C_4H_9	66	C_4D_9
58	C_3H_8N	64	C_3HD_6N
		65	C_3HD_7N
59	C_3H_7O	65	C_3HD_6O

Table 8 Continued

m/e N-t-B.Cl_3A.	Proposed elemental formula of fragment peaks in the N-t-B.Cl_3A. mass spectrum	Proposed analogous nominal mass in the N-t-B.Cl_3A.d_9 mass spectrum	Proposed analogous elemental formula of fragment peaks in the N-t-B.Cl_3A.d_9 mass spectrum
77	C_3H_6Cl	83	CD_6Cl
82	CCl_2	82	CCl_2
84	C_4H_6NO	90	C_4D_6NO
98	$C_2H_2NCl_2$	99	C_2HDNCl_2
100	$C_5H_{10}NO$	109	C_5HD_9NO
110	$COCl_2$	110	$COCl_2$
117	CCl_3	117	CCl_3
119	CCl_3 a ^{37}Cl isotope of m/e 117	119	CCl_3
138	$C_4H_6NCl_2$	144	$C_4D_6NCl_2$
202	$C_5H_7NOCl_3$	208	$C_5HD_6NOCl_3$

Table 8 Continued

m/e N-t-B.Cl_3A.	Proposed elemental formula of fragment peaks in the N-t-B.Cl_3A. mass spectrum	Proposed analogous nominal mass in the N-t-B.Cl_3Ad_9 mass spectrum	Proposed analogous elemental formula of fragment peaks in the N-t-B.Cl_3A.d_9 mass spectrum
204	$C_5H_7NOCl_3$ a ^{37}Cl isotope of m/e 202	210	$C_5HD_6NOCl_3$
206	$C_5H_7NOCl_3$ a ^{37}Cl isotope of m/e 202	212	$C_5HD_6NOCl_3$
217	$C_6H_{10}NOCl_3$	226	$C_6HD_9NOCl_3$

Part II Identification of peaks

A) N-t-butyl-α-fluoroacetamide

Table 9

A tabulation of m/e, $\%\Sigma_{36}$, proposed elemental formula, and proposed structural formula for peaks in the N-t-butyl-α-fluoroacetamide mass spectrum

m/e	$\%\Sigma_{36}$	Proposed elemental formula	Proposed structural formula
39	1.5	C_3H_3	
*41	3.7	C_3H_5	$CH_3-\overset{+}{C}=CH_2$
*42	2.2	C_2H_4N	$CH_3-\overset{+}{C}\equiv N-H$
*55	1.4	C_4H_7	
56	3.8	C_4H_8	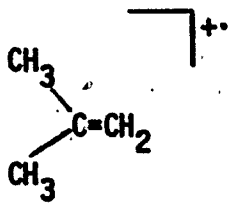
57	5.0	C_4H_9	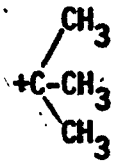
58	18.0	C_3H_8N	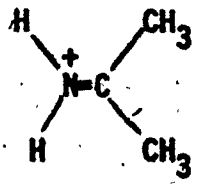

Table 9 Continued

m/e	$\%\Sigma_{36}$	Proposed elemental formula	Proposed structural formula
*59	1.2	C_3H_7O (50%) a ^{13}C isotope of m/e 58 (50%)	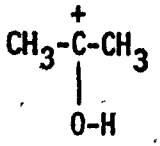
61	1.5	C_2H_2OF	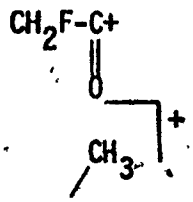
72	1.0	$C_4H_{10}N$	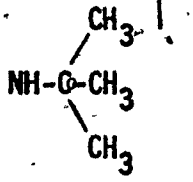
77	1.4	C_2H_4NOF	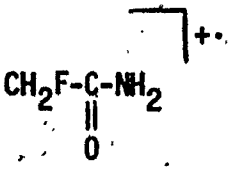
78	6.5	C_2H_5NOF	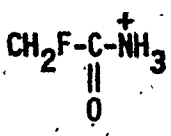
118	18.1	C_5H_9NOF	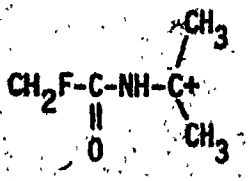

Table 9 Continued

m/e	$\%\Sigma_{36}$	Proposed elemental formula	Proposed structural formula
119	1.4	a ^{13}C isotope of m/e 118	
133	6.9	$C_6H_{12}NOF$	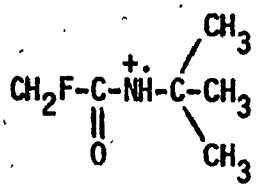

The peaks tabulated account for 73.6% of the ion current above m/e 36.

Table 10

A comparison of the mass spectra of N-t-butyl-α-fluoroacetamide and N-t-butyl-d_9-α-fluoroacetamide for the purpose of peak identification

m/e N-t-B.F.A.	Proposed elemental formula of fragment peaks in the N-t-B.F.A. mass spectrum	Proposed analogous nominal mass in the N-t-B.F.A.d_9 mass spectrum	Proposed analogous elemental formula of fragment peaks in the N-t-B.F.A. d_9 mass spectrum
39	C_3H_3	42	C_3D_3
56	C_4H_8	64	C_4D_8
57	C_4H_9	66	C_4D_9
58	C_3H_8N	64	$C_3H_2D_6N$
61	C_2H_2OF	61	C_2H_2OF
72	$C_4H_{10}N$	81	C_4HD_9N
77	C_2H_4NOF	78	C_2H_3DNOF
78	C_2H_5NOF	80	$C_2H_3D_2NOF$
118	C_5H_9NOF	124	$C_5H_3D_6NOF$
133	$C_6H_{12}NOF$	142	$C_6H_3D_9NOF$

N-t-B.F.A. is N-t-butyl-α-fluoroacetamide and N-t-B.F.A.d_9 is N-t-butyl-d_9-α-fluoroacetamide. These symbols will be used where necessary.

B) N-t-butyl-α,α-difluoroacetamide

Table II

A compilation of m/e, $\%\Sigma_{36}$, proposed elemental formula, and proposed structural formula for peaks in the N-t-butyl-α,α-difluoroacetamide mass spectrum

m/e	$\%\Sigma_{36}$	Proposed elemental formula	Proposed structural formula
39	3.6	C_3H_3	
41	10.4	C_3H_5	$CH_3-\overset{+}{C}=CH_2$
42	6.8	C_2H_4N	$CH_3-C\equiv\overset{+}{N}-H$
51	5.1	CHF_2	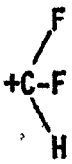
*55	1.4	C_4H_7	
*56	6.9	C_4H_8	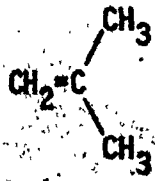
57	10.3	C_4H_9	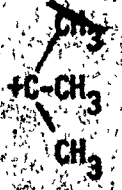

Table 11 Continued

m/e	$\%\Sigma_{36}$	Proposed elemental formula	Proposed structural formula
58	16.7	C_3H_8N	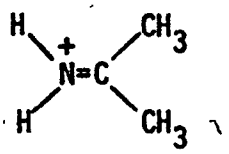
*59	5.6	C_3H_7O	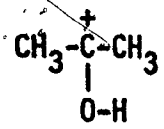
76	1.3	C_2H_3NOF	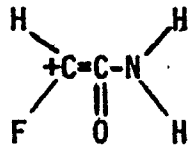
96	4.9	$C_2H_4NOF_2$	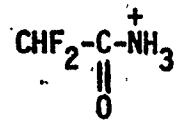
136	16.6	$C_5H_8NOF_2$	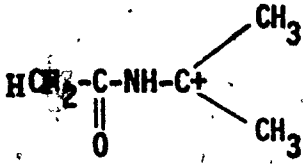
137	1.0	a ^{13}C isotope of m/e 136	
151	2.4	$C_6H_{11}NOF_2$	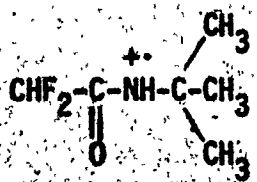

The peaks tabulated account for 93.0% of the ion current above m/e 36.

Table 12

A comparison of the mass spectra of N-t-butyl-α,α-difluoroacetamide and N-t-butyl-d_9-α,α-difluoroacetamide for the purpose of peak identification

m/e N-t-B.F_2A.	Proposed elemental formula of fragment peaks in the N-t-B.F_2A. mass spectrum	Proposed analogous nominal mass in the N-t-B.F_2A.d_9 mass spectrum	Proposed analogous elemental formula of fragment peaks in the N-t-B.F_2A.d_9 mass spectrum
39	C_3H_3	42	C_3D_3
41	C_3H_5	46	C_3D_5
42	C_2H_4N	45	C_2D_3HN
51	CHF_2	51	CHF_2
57	C_4H_9	66	C_4D_9
58	C_3H_8N	64	CH_2D_6N
76	C_2H_3NOF	77	C_2H_2DNOF
96	$C_2H_4NOF_2$	98	$C_2H_2D_2NOF_2$
136	$C_5H_8NOF_2$	142	$C_5H_2D_6NOF_2$

Table 12 Continued

m/e N-t-B.F_2A.	Proposed elemental formula of fragment peaks in the N-t-B.F_2A. mass spectrum	Proposed analogous nominal mass in the N-t-B.F_2A.d_9 mass spectrum	Proposed analogous elemental formula of fragment peaks in the N-t-B.F_2A.d_9 mass spectrum
137	$C_5H_8NOF_2$ a ^{13}C isotope of m/e 136		
151	$C_6H_{11}NOF_2$	160	$C_6H_2D_9NOF_2$

N-t-B.F_2A. is N-t-butyl-α,α-difluoroacetamide and N-t-B.F_2A.d_9 is N-t-butyl-d_9-α,α-difluoroacetamide. These symbols will be used where necessary.

C) N-t-butyl-α,α,α-trifluoroacetamide

Table 13

A tabulation of m/e, $\%\Sigma_{36}$, proposed elemental formula, and proposed structural formula for peaks in the N-t-butyl-α,α,α-trifluoroacetamide

m/e	$\%\Sigma'_{36}$	Proposed elemental formula	Proposed structural formula
39	0.9	C_3H_3	
*41	4.7	C_3H_5	$CH_3-\overset{+}{C}=CH_2$
*42	4.0	C_2H_4N	$CH_3-C\equiv\overset{+}{N}-H$
*55	1.3	C_4H_7	
56	15.4	C_4H_8	$CH_2=C(CH_3)-CH_3^{+\cdot}$
57	5.3	C_4H_9	$(CH_3)_2\overset{+}{C}-CH_3$
59	20.2	C_3H_7O	$CH_3-\overset{+}{C}(-O-H)-CH_3$

Table 13 Continued

m/e	$\%\Sigma_{36}$	Proposed elemental formula	Proposed structural formula
60	0.8	a ^{13}C isotope of m/e 59	
69	3.9	CF_3	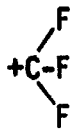
84	1.7	C_4H_6NO	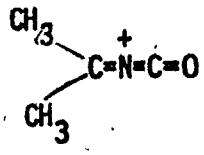
94	2.3	$C_2H_2ONF_2$	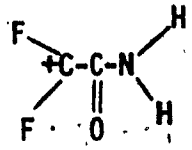
100	0.7	$C_5H_{10}NO$	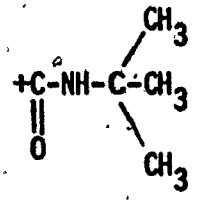
114	7.8	$C_2H_3ONF_3$	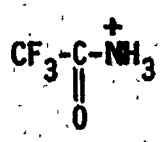
154	23.2	$C_5H_7NOF_3$	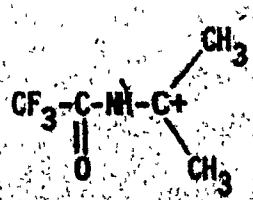

Table 13 Continued

m/e	$\%\Sigma_{36}$	Proposed elemental formula	Proposed structural formula
155	1.5	a ^{13}C isotope of m/e 154	
169	1.5	$C_6H_{10}NOF_3$	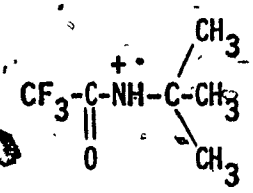

Table 14

A comparison of the mass spectra of N-t-butyl-α,α,α-trifluoroacetamide and N-t-butyl-d_9-α,α,α-trifluoroacetamide peak identification purposes

m/e N-t-B.F_3A.	Proposed elemental formula of fragment peaks in the N-t-B.F_3A. mass spectrum	Proposed analogous nominal mass in the N-t-B.F_3A.d_9 mass spectrum	Proposed analogous elemental formula of fragment peaks in the N-t-B.F_3A. d_9 mass spectrum
39	C_3H_3	42	C_3D_3
56	C_4H_8	64	C_4D_8
57	C_4H_9	66	C_4D_9
59	C_3H_7O	65	C_3HD_6O
60	C_3H_7O a ^{13}C isotope of m/e 59		
69	CF_3	69	CF_3
84	C_4H_6NO	90	C_4D_6NO
94	$C_2H_2NOF_2$	95	C_2HDNOF_2
100	$C_5H_{10}NO$	109	C_5HD_9NO
114	$C_2H_3NOF_3$	116	$C_2HD_2NOF_3$

Table 14 Continued

m/e N-t-B.F_3A.	Proposed elemental formula of fragment peaks in the N-t-B.F_3A. mass spectrum	Proposed analogous nominal mass in the N-t-B.F_3A.d_9 mass spectrum	Proposed analogous elemental formula of fragment peaks in the N-t-B.F_3A.d_9 mass spectrum
154	$C_5H_7NOF_3$	160	$C_5HD_6NOF_3$
155	$C_5H_7NOF_3$ a ^{13}C isotope of m/e 154		
169	$C_6H_{10}NOF_3$	178	$C_6HD_9NOF_3$

N-t-B.F_3A. is N-t-butyl-α,α,α-trifluoroacetamide and N-t-B.F_3A.d_9 is N-t-butyl-d_9-α,α,α-trifluoroacetamide. These symbols will be used in tables where necessary.

Part III Spectra Analysis

A) Fragments common to the N-t-butyl-α-chloroacetamide mass spectra

Table 15 lists fragments common to the members of the N-t-butyl-α-chloroacetamide series. Definite trends for fragment peaks at m/e 41, m/e 57, m/e 58 and m/e 59 can be seen.

It is assumed in all cases that the peak at m/e 57 arises from the molecular ion by a direct cleavage process. The observation of the appropriate metastable transitions confirms that the peak at m/e 41, in all cases, results from the peak at m/e 57. Intensities of both fragment peaks, m/e 57 and m/e 41, are seen to increase with increasing chlorination, particularly the fragment peak at m/e 57. An increasing electron withdrawing tendency of the acyl portion of the molecule, with increasing chlorination in the amide, may favor the formation of a positively charged alkyl ion. As expected, the trend in the intensity of the peak at m/e 41 parallels the intensity for the peak at m/e 57.

The fragment peak observed at m/e 56 is seen to decrease slightly with increasing chlorination, however there is not a firm trend. Although the formation of the peak at m/e 56 is not completely understood, the possible presence of metastable transitions in the spectra of N-t-butyl-α-chloroacetamide and N-t-butyl-α,α-dichloroacetamide, and the definite presence of a metastable transition in the spectra of N-t-butyl-α,α,α-trichloroacetamide, all seem to indicate that at least part of the peak at m/e 56, results from the process $M^+ \longrightarrow$ m/e 56.

A gradual decrease in the intensity of the peak at m/e 58 throughout the series is attributed to the fact that there are fewer hydrogen atoms available for transfer to the nitrogen atom. The mechanism

for this rearrangement is demonstrated with the parent fragment ion, which originated from a molecular ion of N-t-butylacetamide.

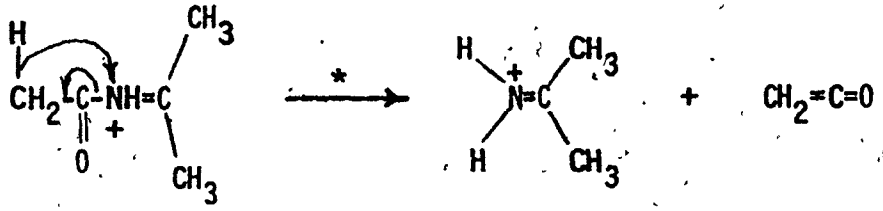

m/e 100 m/e 58

For a statistical distribution, one would have expected the results; 36.1% for N-t-butylacetamide, 24.0% for N-t-butyl-α-chloroacetamide, 12.0% for N-t-butyl-α,α-dichloroacetamide and 0.0% for N-t-butyl-α,α,α-trichloroacetamide (all results were given in $\%\Sigma_{36}$.) Observed results decreased in intensity only approximately in the same fashion, and gave results that were higher than the statistical distribution predicted. In the compound N-t-butyl-α,α,α-trichloroacetamide all hydrogen atoms that migrate to the nitrogen atom resulting in the peak at m/e 58, must come from the tertiary butyl group. The fragment peak 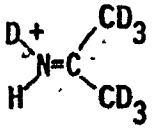 observed at m/e 65, has been noted in the spectrum of the deuterated analogue.

The proposed rearrangement that produces the peak at m/e 59 is illustrated in conjunction with the mass spectrum of N-t-butyl-α,α-dichloroacetamide.

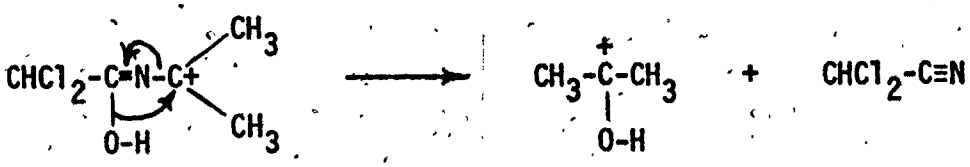

m/e 168 m/e 59

The intensity of the peak at m/e 59 increases with increasing chlorination throughout the series.

Simple cleavage of the molecular ion, to give the peak at m/e 100, shows no definite trend in intensity throughout the series.

Table 15

Fragments common to the N-t-butyl-α-chloroacetamide mass spectra

m/e	$\%\Sigma_{36}$ N-t-B.A.	$\%\Sigma_{36}$ N-t-B.ClA.	$\%\Sigma_{36}$ N-t-B.Cl_2A.	$\%\Sigma_{36}$ N-t-B.Cl_3A.
39 (C_3H_3)	1.4	2.1	2.7	1.6
41 (C_3H_5)	4.1	6.8	9.7	10.0
42 (C_2H_4N)	3.9	3.2	4.8	4.2
55 (C_4H_7)	1.0	1.2	1.2	1.3
56 (C_4H_8)	3.6	4.4	3.7	3.7
57 (C_4H_9)	3.8	8.7	32.2	37.8
58 (C_3H_8N)	36.1	28.2	17.0	1.0
59 (C_3H_7O)	0.9	0.2	1.3	1.9
100 ($C_5H_{10}NO$)	--	0.4	4.2	3.0

B) Fragments common to the N-t-butyl-α-fluoroacetamide mass spectra

Definite trends in the values of $\%\Sigma_{36}$ of Table 16 can be observed only for the peaks at m/e 56, m/e 57, m/e 58, and m/e 59. The rearrangement peak at m/e 56 increases in intensity as the number of fluorine atoms incorporated into the amide increases, it was noted previously that a definite increase in $\%\Sigma_{36}$ for the peak at m/e 56 for the chlorine containing compounds was not observed. Differences between the two observations would seem to result from the fluorine atoms having a greater electronegativity than the chlorine atoms. As noted for the N-t-butyl-α-chloroacetamides, the peak at m/e 56 is thought to arise from a rearrangement process.

Intensity of the peak at m/e 57 increases as fluorination increases throughout the series, although there is a drop in intensity for N-t-butyl-α,α,α-trifluoroacetamide.

The fragment peak at m/e 58 in the N-t-butyl-α-fluoroacetamides is noted to decrease in intensity as fluorination increases throughout the series. This rearrangement ion has a smaller chance of occurring as fluorination increases, because the hydrogen atom that is transferred comes from the acyl part of the molecule. Although the trend is the same for both series of amides, the $\%\Sigma_{36}$ for m/e 58 in the N-t-butyl-α-chloroacetamides is greater than the $\%\Sigma_{36}$ in the N-t-butyl-α-fluoroacetamides.

The rearrangement process that results in the formation of the peak at m/e 59, is more prominent in the N-t-butyl-α-fluoroacetamides, than in the similar N-t-butyl-α-chloroacetamides. The proposed process is most evident for N-t-α,α,α-trifluoroacetamide, for which the peak at

m/e 59 has a $\%\Sigma_{36}$ of 20.2. It is likely that the trend noted is not as prominent in the N-t-butylchloroacetamides, as the chlorine atoms in these molecules do not have as strong an electron withdrawing effect as ~~do~~ the fluorine atoms in the analogous N-t-butyl-α-fluoroacetamides.

Table 16 indicates that there is no definite trend in the intensity for the fragment peak at m/e 100. Peak intensity for the fragment at m/e 100 in the N-t-butyl-α-fluoroacetamides is much less than the comparable intensities in the analogous N-t-butyl-α-chloroacetamides.

Table 16

Fragments common to the N-t-butyl-α-fluoroacetamide mass spectra

m/e	N-t-B.A.	N-t-B.FA.	N-t-B.F_2A.	N-t-B.F_3A.
39 (C_3H_3)	1.4	1.5	3.6	0.9
41 (C_3H_5)	4.1	3.7	10.4	4.8
42 (C_2H_4N)	3.9	2.2	6.8	4.0
55 (C_4H_7)	1.0	1.4	1.4	1.3
56 (C_4H_8)	3.6	3.8	6.9	15.4
57 (C_4H_9)	3.8	5.0	10.3	5.3
58 (C_3H_8N)	36.1	18.0	16.7	0.4
59 (C_3H_7O)	0.9	1.2	5.6	20.2
100 ($C_5H_{10}NO$)	---	0.2	0.2	0.7

C) Analogous fragments in the N-t-butyl-α-chloroacetamide mass spectra

The process by which the peaks at m/e 43, m/e 77, m/e 111 and m/e 145, listed in Table 17, arise is not certain; but it can be seen that the formation of a fragment peak of the type $R-C\equiv O^{+}$ is not a favored process.

The rearrangement peak of the type shown at m/e 60, m/e 94, m/e 128 and m/e 162 (listed in Table 17) is found in both the N-t-butyl-α-chloroacetamides and the N-t-butyl-α-fluoroacetamides. Formation of these peaks results from a mechanism that is most favored when there are no chlorine atoms present in the amide; it is proposed that all of the protonated chloroacetamide fragments arise directly from the corresponding molecular ion giving the appropriate peak.

Peak intensities for the peaks at m/e 49, m/e 83, and m/e 117 (listed in Table 17) are observed to decrease with increasing chlorination suggesting that the number of chlorine atoms in the fragment R+ increases, the fragment is less likely to be a positively charged species.

Chlorination seems to have little effect upon the formation of the analogous fragments at m/e 114, m/e 148 and m/e 182. All of these fragments have low abundance.

Formation of the peak at $[M-15]^{+}$ in the N-t-butyl-α-chloroacetamides is not affected in a regular fashion by the presence of chlorine atoms. It is proposed that these peaks result from a direct cleavage process from the molecular ion.

Molecular ion intensity in the N-t-butyl-α-chloroacetamides is noted to be strongly dependent upon the number of chlorine atoms present. As the number of chlorine atoms present in the series increases, the observed intensity of the molecular ion decreases.

Table 17

Analogous fragments in the N-t-butyl-α-chloroacetamides

m/e	Fragment	$\%\Sigma_{36}$
43	$R\text{-}C{\equiv}O^{+}$	8.2
77		1.0
111		0.0
145		0.0
60	$R\text{-}\underset{\underset{O}{\|}}{C}\text{-}NH_3^{+}$	13.8
94		7.9
128		0.9
162		0.7
49	R^{+}	1.8
83		1.8
117		1.4
114	$[M\text{-}Cl]^{+}$	1.0
148		0.1
182		0.4
100	$[M\text{-}15]^{+}$	3.4
134		9.7

Table 17 Continued

m/e	Fragment	$\%\Sigma_{36}$
168	$[M-15]^+$	4.1
	(continued)	
202		5.0
115	$[M]^+$	12.7
149		5.3
183		0.5
217		0.2

R in Table 17 and in all other following work is used to correspond to CH_xCl_y, where x and y may be 0,1,2 or 3 and $x + y = 3$. The symbol R must then be adapted to each compound under consideration.

D) Analogous fragments in the N-t-butyl-α-fluoroacetamide mass spectra

Analogous fragments at m/e 43, m/e 61, m/e 79, m/e 97 (listed in Table 18) are observed to follow a definite trend. As fluorination increased in the series, the fragment peaks decrease in intensity; the N-t-butyl-α-chloroacetamides gave the same pattern.

Protonated acetamide type fragments at m/e 60, m/e 78, m/e 96, and m/e 114 result from the same rearrangement process as described for the N-t-butyl-α-chloroacetamides. With the increase of fluorination, the analogous fragments at m/e 60, m/e 78, m/e 96 and m/e 114 are observed to increase in intensity, except in the case of m/e 114.

The process that gives rise to the analogous fragments at m/e 33, m/e 51, and m/e 69, is not known, although this process seems to be less favored as fluorination increases. A comparable trend was noted for the fragments $+CH_2Cl$, $+CHCl_2$ and $+CCl_3$.

Fragments at m/e 58, m/e 76, and m/e 94 are observed in the mass spectra of the N-t-butyl-α-fluoroacetamides whereas comparable fragments are not observed in the N-t-butyl-α-chloroacetamide mass spectra. A proposed mechanism is the loss of HF from the corresponding protonated fluoroacetamides to give the observed peaks. Saxby[7] first mentioned this mechanism, but he did not observe the corresponding metastable transition. Loss of HF becomes more likely as fluorination increases, the proposed mechanism, using the mass spectrum of N-t-butyl-α,α,α-trifluoroacetamide as an example, is then:

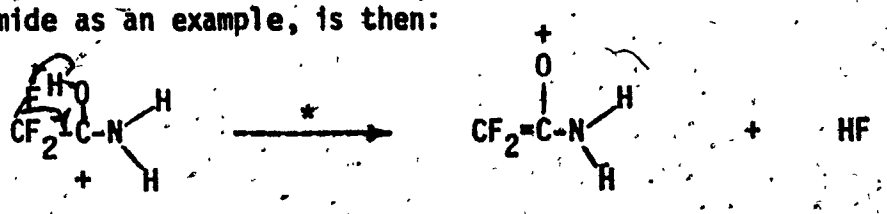

m/e 114 m/e 94

The peaks at m/e 58, and m/e 76 increased in intensity as fluorination increased.

Direct cleavage gives the analogous peaks at m/e 100, m/e 118, m/e 136 and m/e 154 but a particular trend in intensity was not observed as fluorination increased in the series. A similar observation was made for the analogous fragments in the N-t-butyl-α-chloroacetamide series.

Intensity of the molecular ion in the series m/e 115, m/e 133, and m/e 169 decreases as fluorination increases. The same tendency was noted in the N-t-butyl-α-chloroacetamides.

Table 18

Analogous fragments in the N-t-butyl-α-fluoroacetamides

m/e	Fragment ion	$\%\Sigma_{36}$
43	$R\text{-}\overset{+}{C}{=}O$	8.2
61		1.4
79		0.1
97		0.0
60	$R\text{-}\overset{\overset{O}{\|}}{C}\text{-}\overset{+}{N}H_3$	13.8
78		6.5
96		4.9
114		7.8
33	R+	---
51		5.1
69		3.9
58	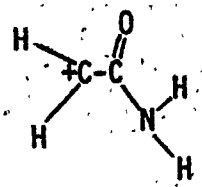	---
76		1.3
94		2.3

Table 18. Continued

m/e	Fragment ion	$\%\Sigma_{36}$
100	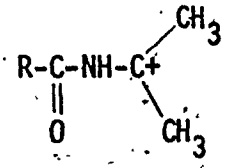	3.4
118		18.1
136		16.6
154		23.2
115	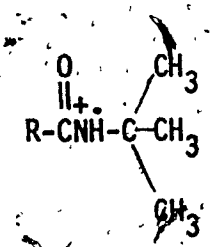	12.7
133		7.0
151		2.4
169		1.4

E) Peaks resulting from cleavage or rearrangement processes

The proposed fragmentation pattern for each compound is presented in this section. The fragment peaks for each of the proposed fragmentation patterns are grouped into two categories, those that originated through the process of cleavage and those that resulted from a rearrangement process. Each of the categories (peaks resulting from cleavage, and peaks resulting from rearrangement) are discussed.

Compounds of the N-t-butyl-α-chloroacetamide series are presented first, followed by the appropriate discussion on cleavage peaks and rearrangement peaks. The same sequence is repeated for the N-t-butyl-α-fluoroacetamide series.

N-t-butylacetamide

Fragmentation pattern of N-t-butylacetamide

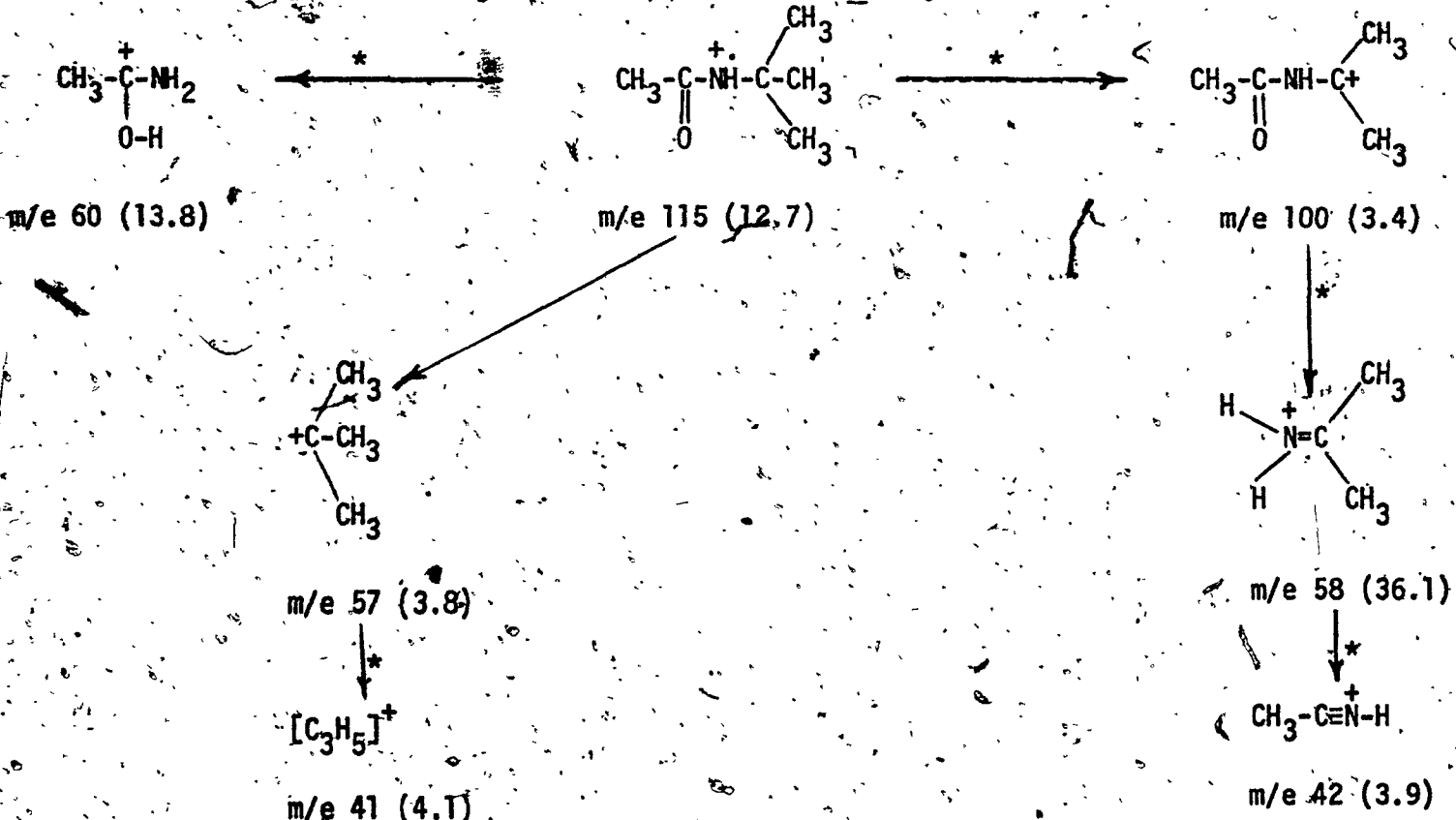

* indicates metastable peak observed at predicted m/e

( ) indicates the $\%\Sigma_{36}$ for a particular peak

a) Peaks arising by cleavage

The following peaks probably arise by a direct cleavage process

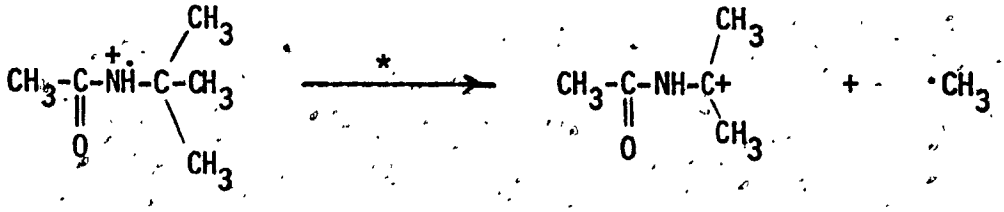

m/e 115 m/e 100

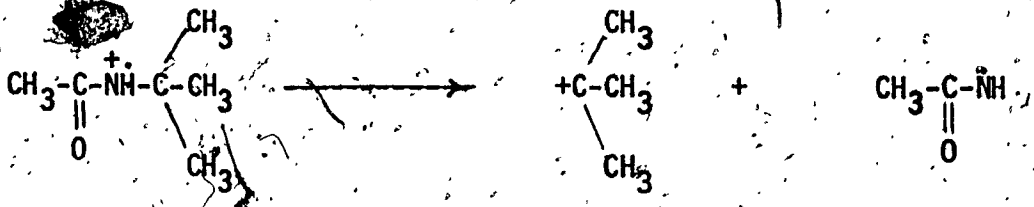

m/e 115 m/e 57

b) Peaks arising by rearrangement

The following peaks probably arise via a rearrangement process

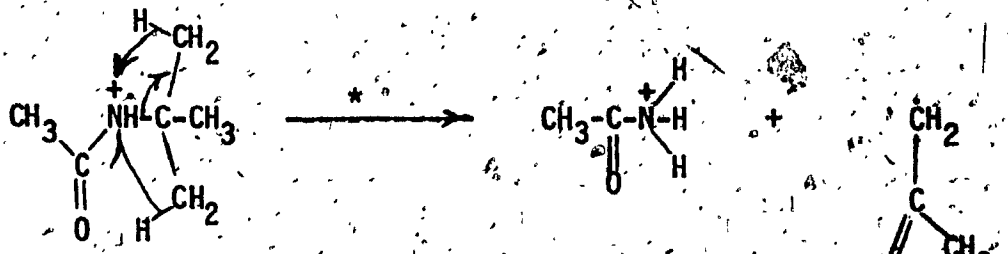

m/e 115 m/e 60

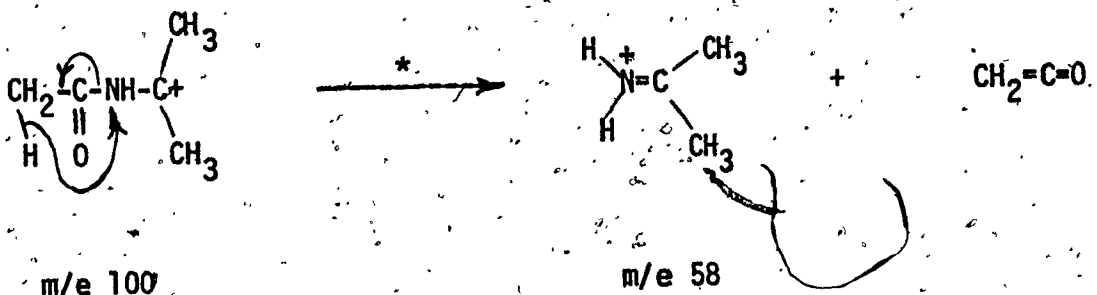

m/e 100 m/e 58

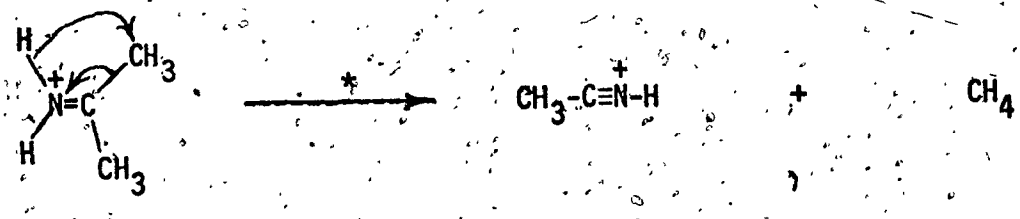

m/e 58 m/e 42

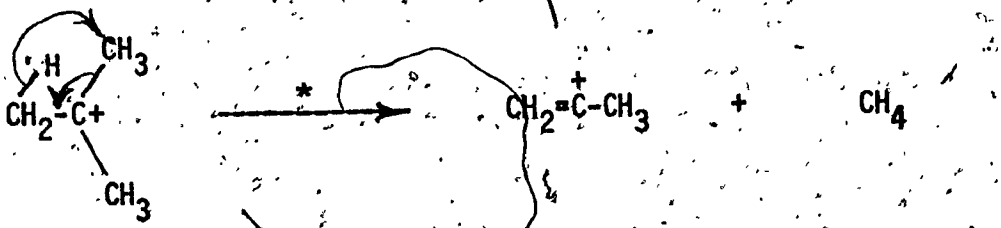

m/e 57 m/e 41

N-t-butyl-α-chloroacetamide.

Fragmentation pattern of N-t-butyl-α-chloroacetamide

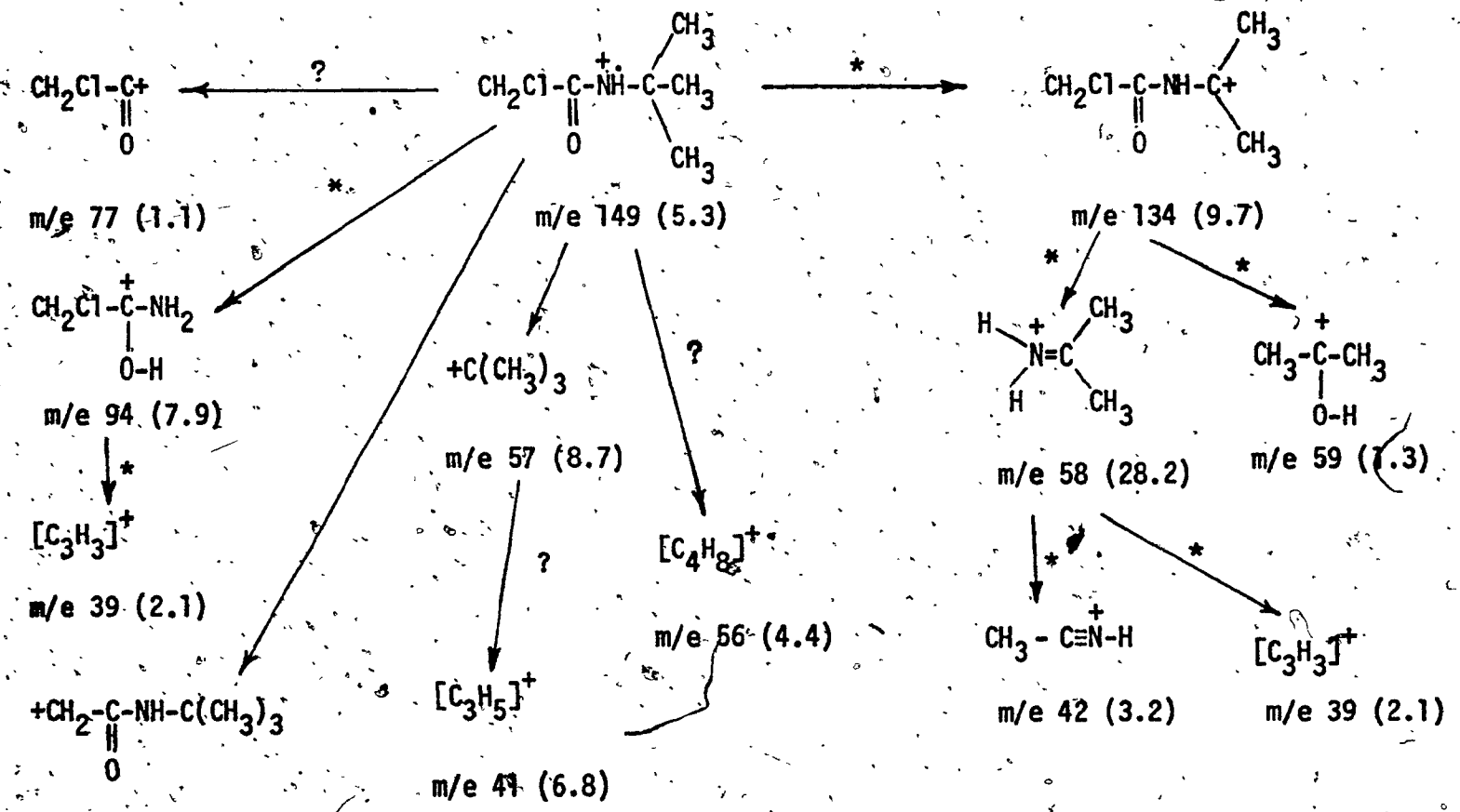

a) Peaks arising by cleavage

The following peaks probably result via direct cleavage.

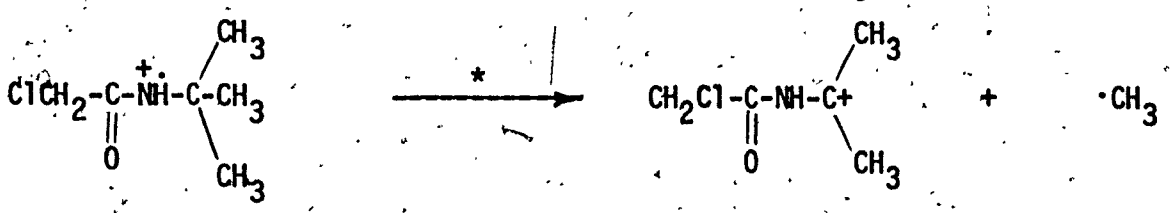

m/e 149 m/e 134

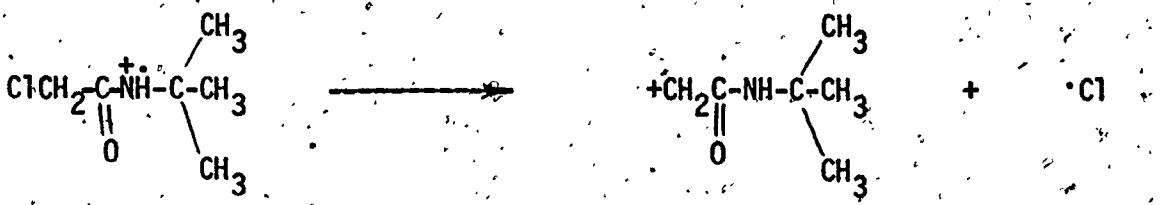

m/e 149 m/e 114

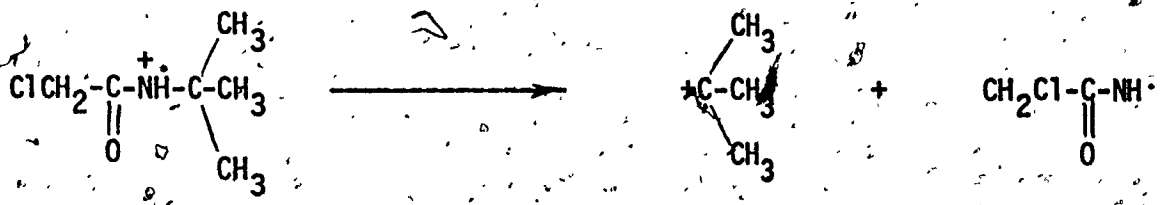

m/e 149 m/e 57

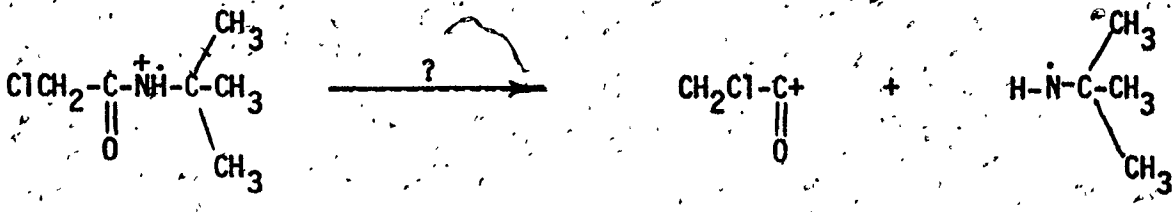

m/e 149 m/e 77

b) Peaks arising by rearrangement

The following peaks probably arise via the rearrangement processes shown

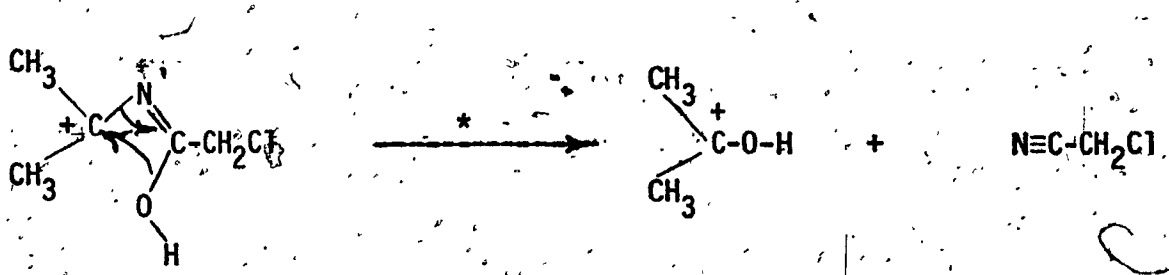

m/e 134 m/e 59

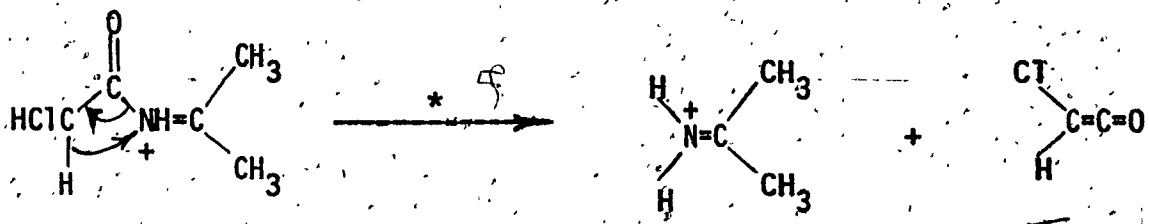

m/e 134 m/e 58

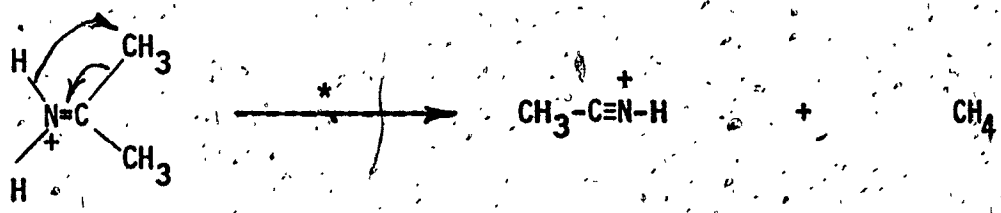

m/e 58 m/e 42

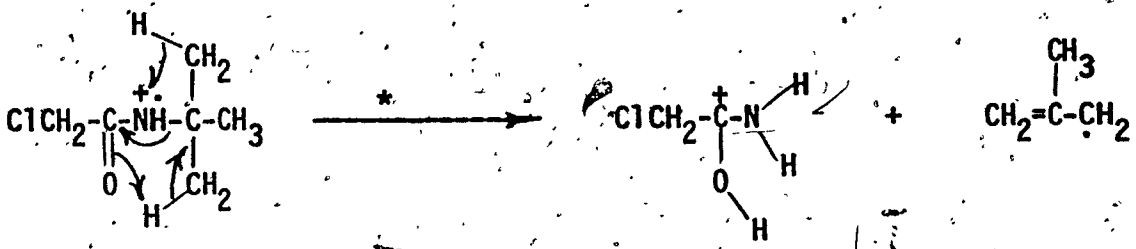

m/e 149 m/e 94

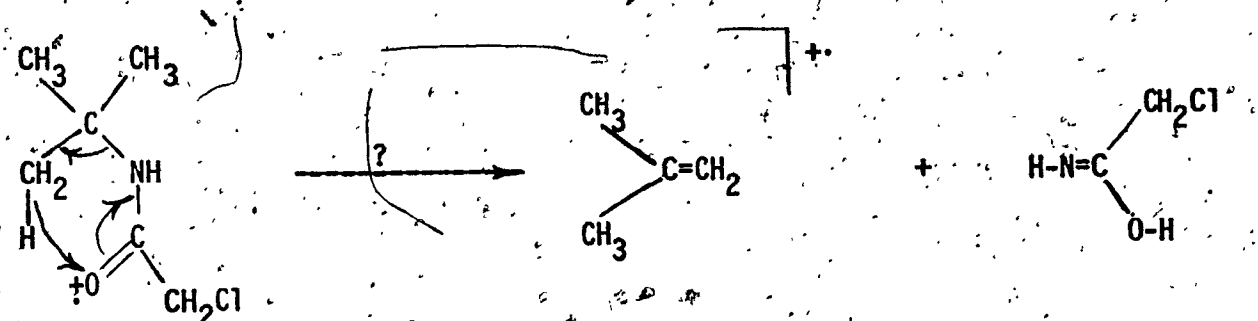

m/e 149 m/e 56

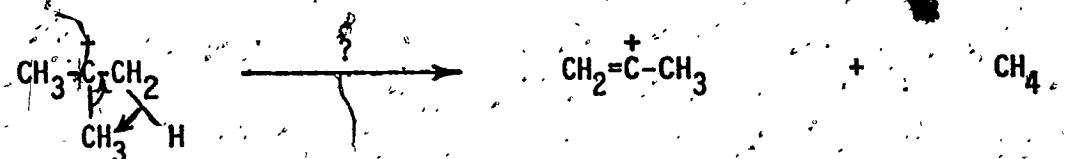

m/e 57 m/e 41

The peak at m/e 39 is seen to arise from two processes in the fragmentation pattern, m/e 94 $\xrightarrow{*}$ m/e 39 and m/e 58 $\xrightarrow{*}$ m/e 39. It is assumed that this occurs via a rearrangement process in both cases.

N-t-butyl-α,α-dichloroacetamide

Fragmentation pattern of N-t-butyl-α,α-dichloroacetamide

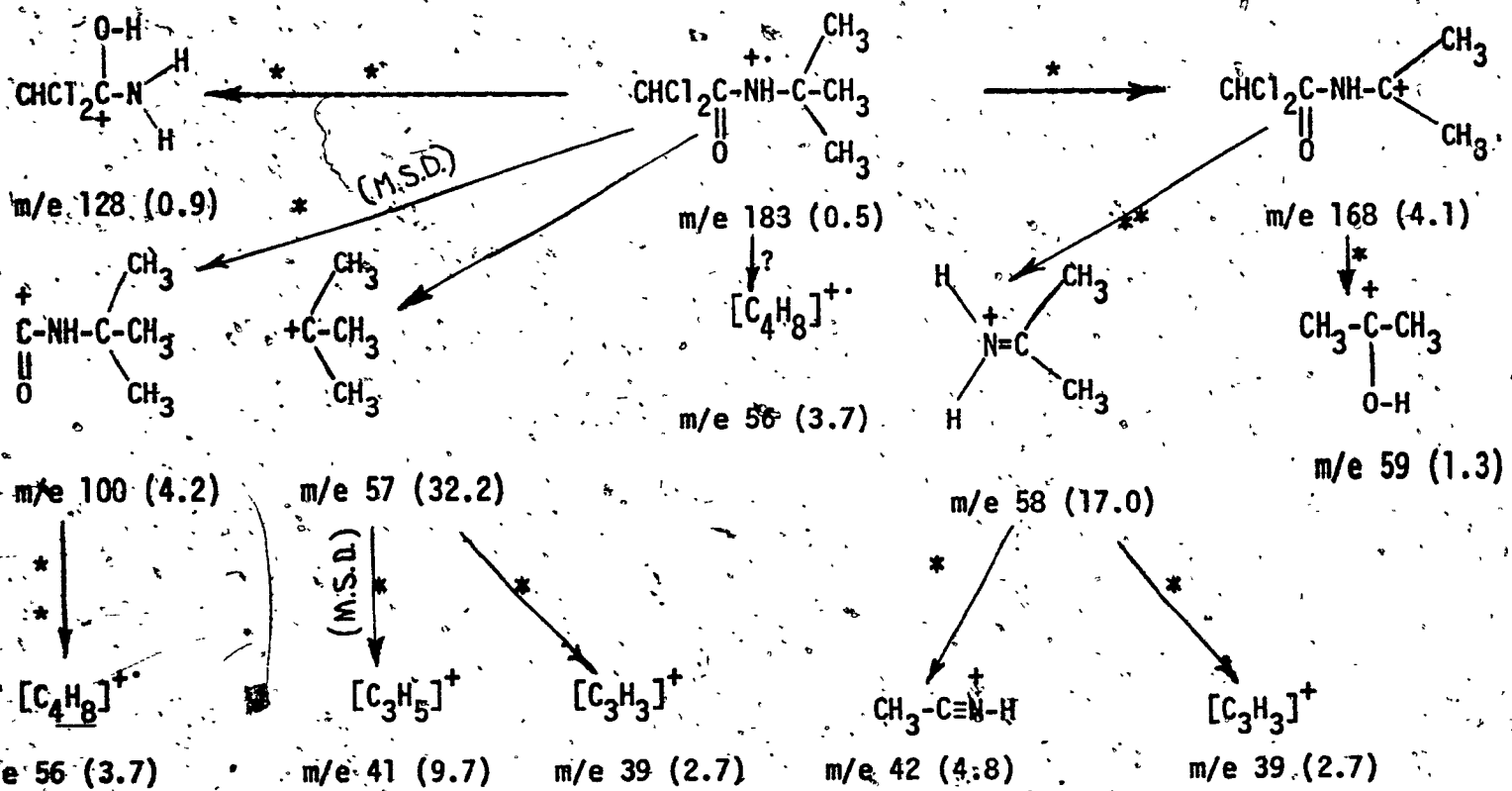

** observed in d_9 analog only

(M.S.D.) transition confirmed by metastable defocussing

a) Peaks arising by cleavage

The following peaks probably arise via simple cleavage.

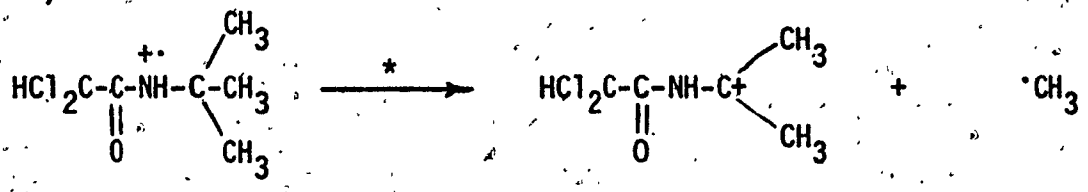

m/e 183 m/e 168

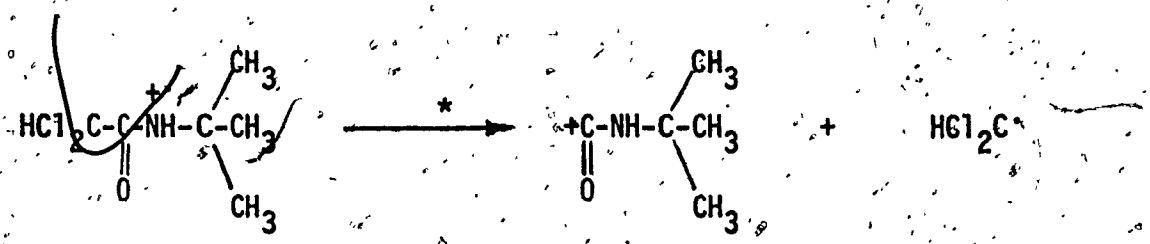

m/e 183 m/e 100

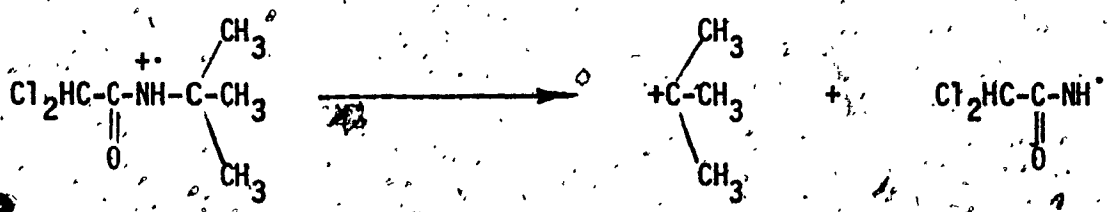

m/e 183 m/e 57

b) Peaks arising by rearrangement

The following peaks probably arise via the rearrangement processes shown.

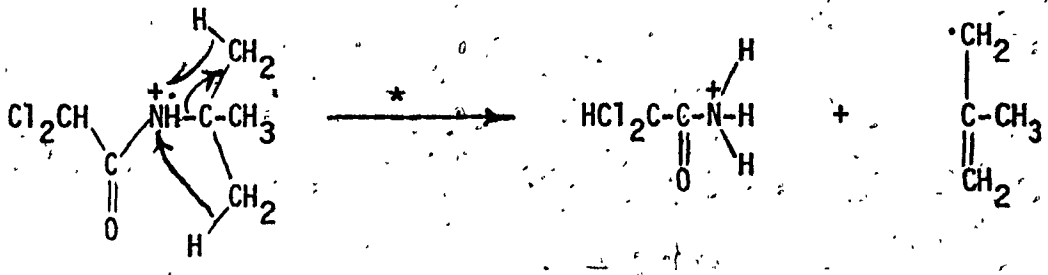

m/e 183 m/e 128

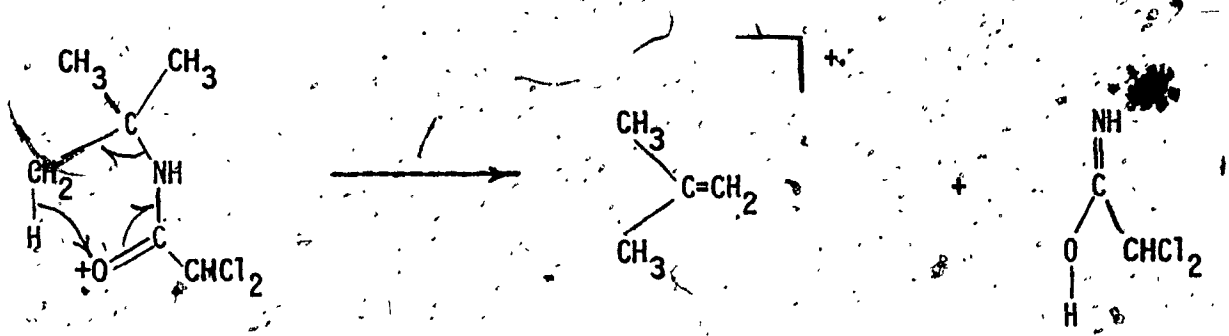

m/e 183 m/e 56

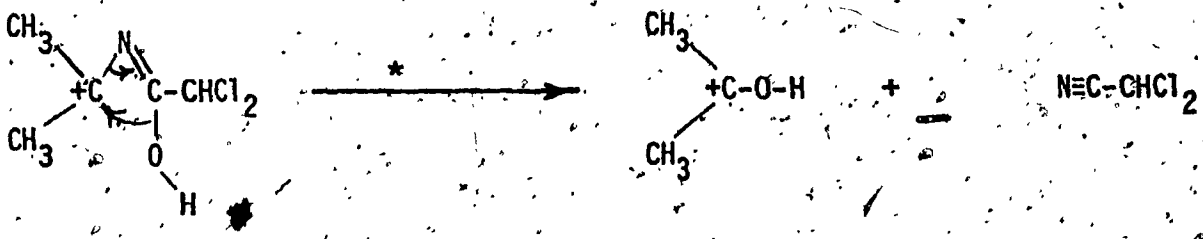

m/e 168 m/e 59

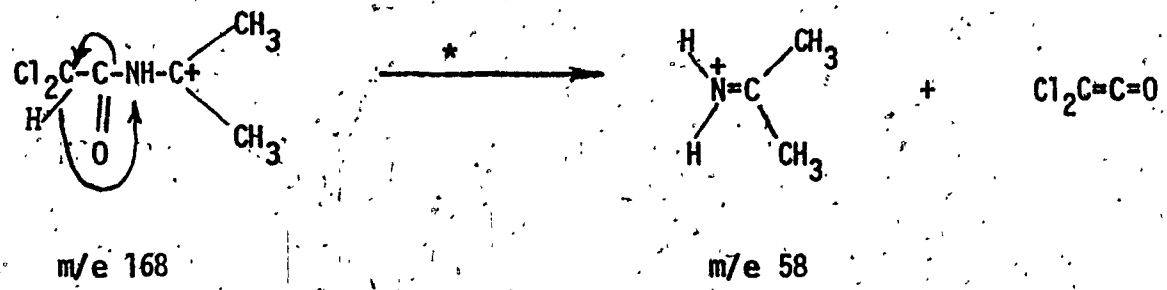

m/e 168 m/e 58

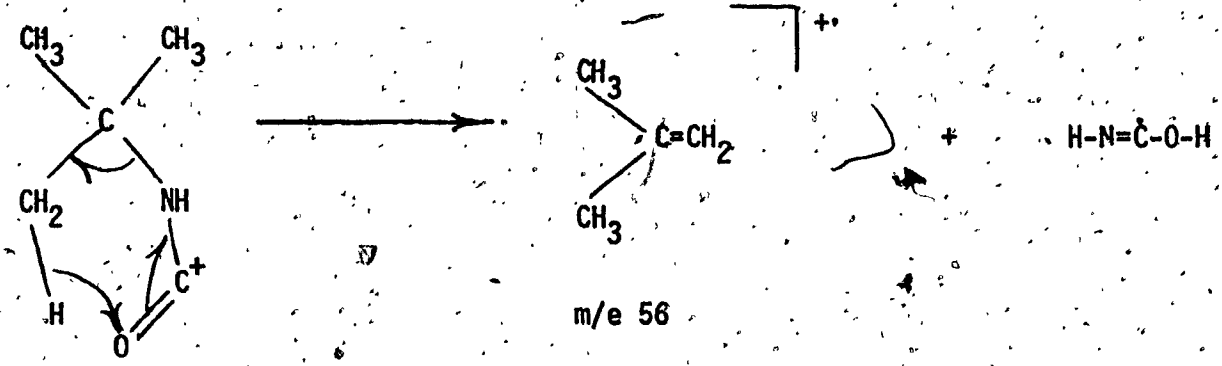

m/e 100 m/e 56

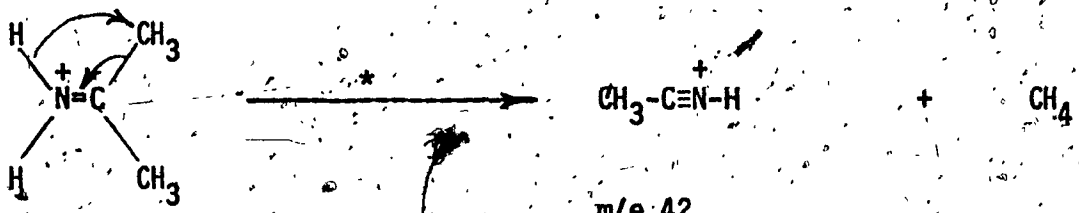

m/e 58 m/e 42

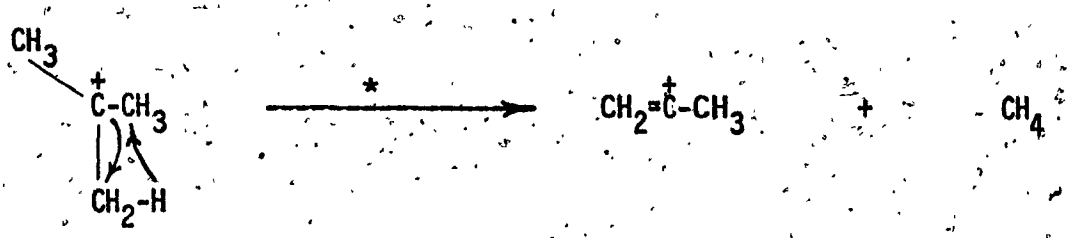

m/e 57 m/e 41

The peak at m/e 39 is seen to arise from two processes in the fragmentation pattern, m/e 57 $\xrightarrow{*}$ m/e 39 and m/e 58 $\xrightarrow{*}$ m/e 39. It is assumed that both of these processes are rearrangements.

N-t-butyl-α,α,α-trichloroacetamide

Fragmentation pattern for N-t-butyl-α,α,α-trichloroacetamide

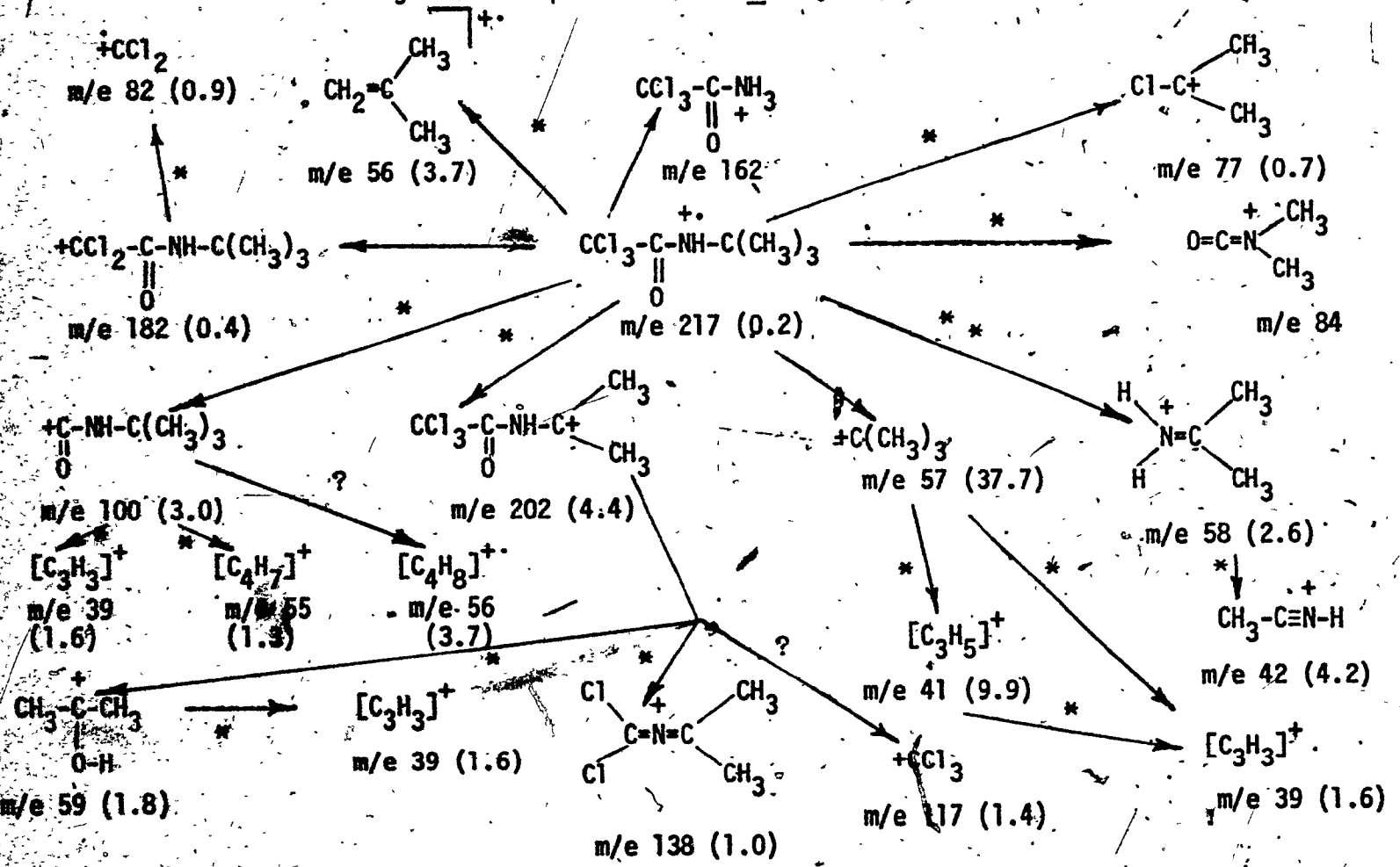

a) Peaks arising by cleavage

The following peaks probably arise by simple cleavage.

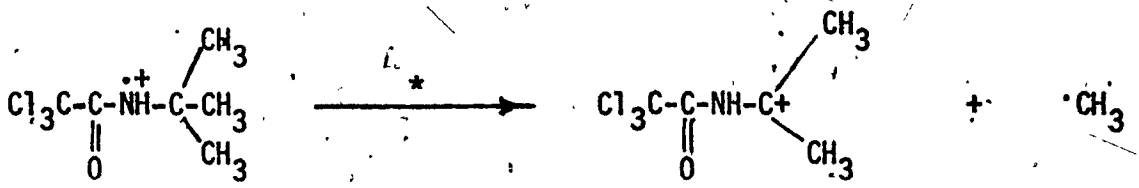

m/e 217 m/e 202

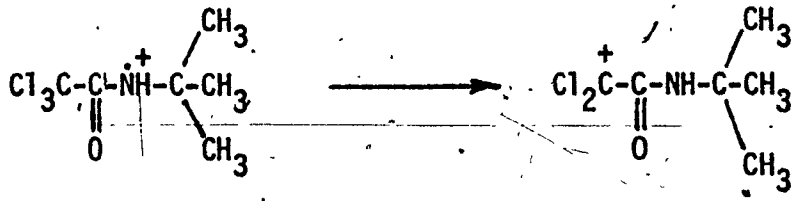

m/e 217 m/e 182

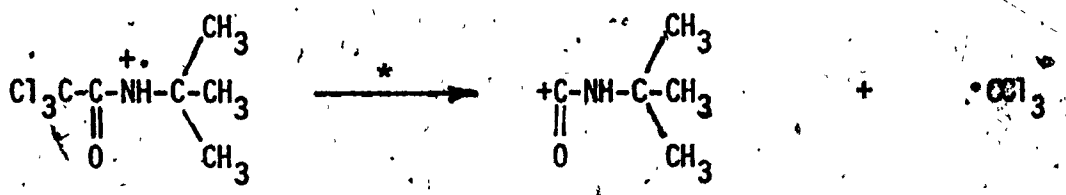

m/e 217 m/e 100

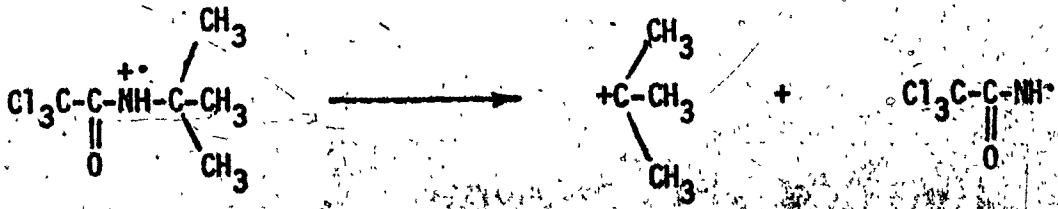

m/e 217 m/e 57

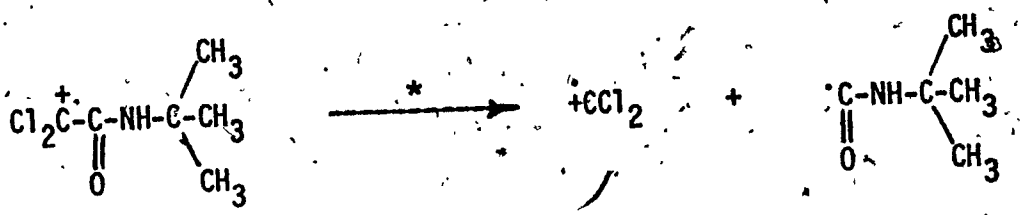

m/e 182

m/e 82

b) Peaks arising via rearrangement

The following peaks probably arise by a rearrangement process.

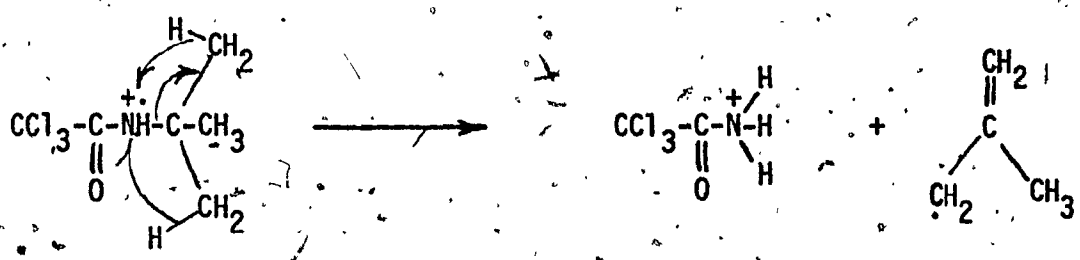

m/e 217 m/e 162

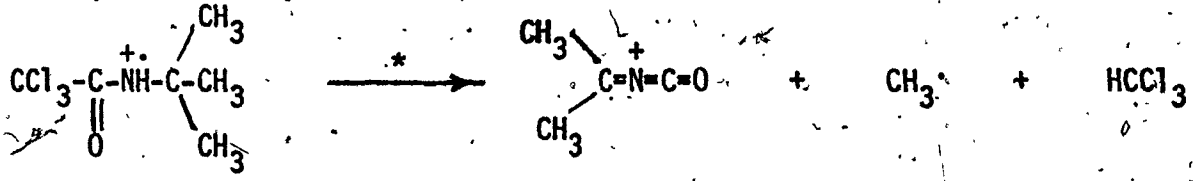

m/e 217 m/e 84

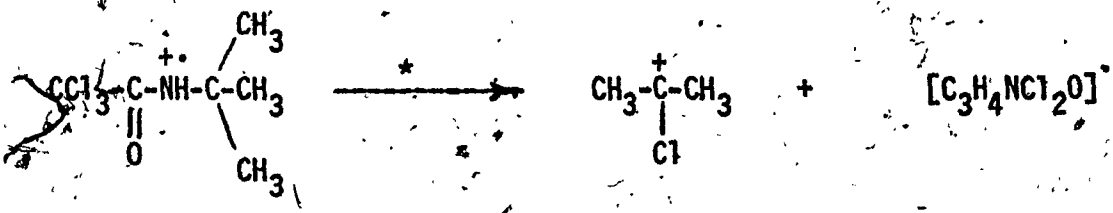

m/e 217 m/e 77

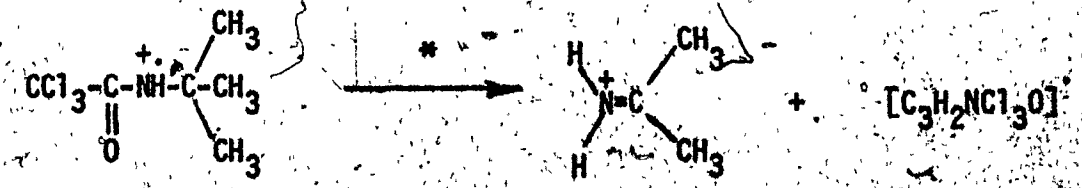

This process is observed in the d_9 analog only

m/e 217 m/e 58

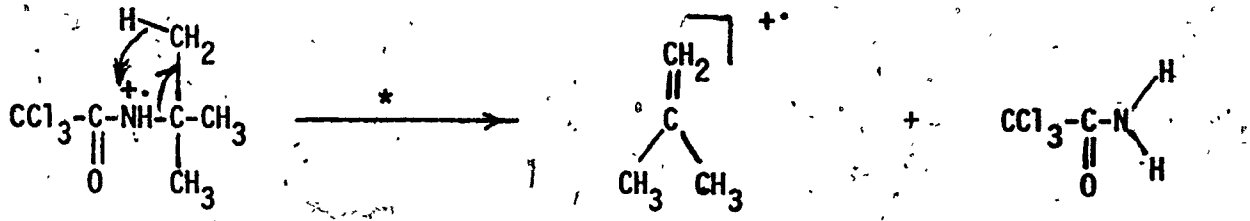

m/e 217 m/e 56

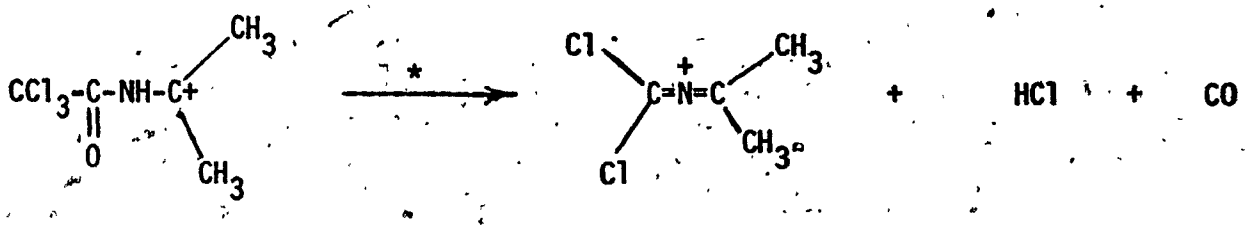

m/e 202 m/e 138

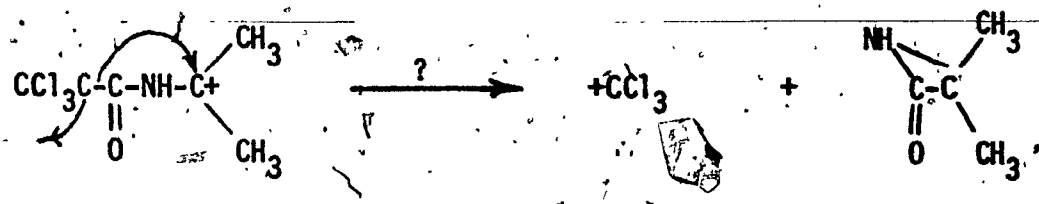

m/e 202 m/e 117

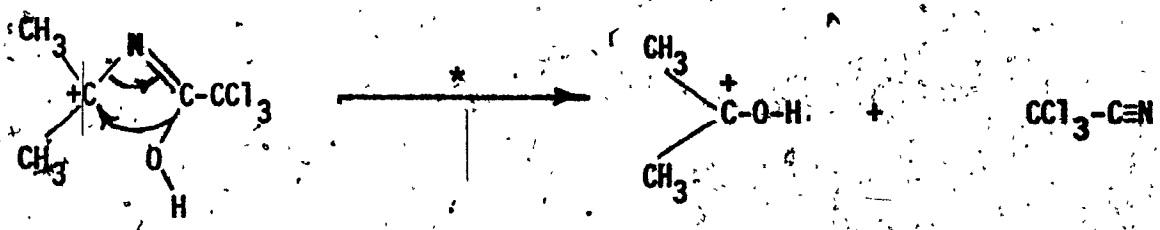

m/e 202 m/e 59

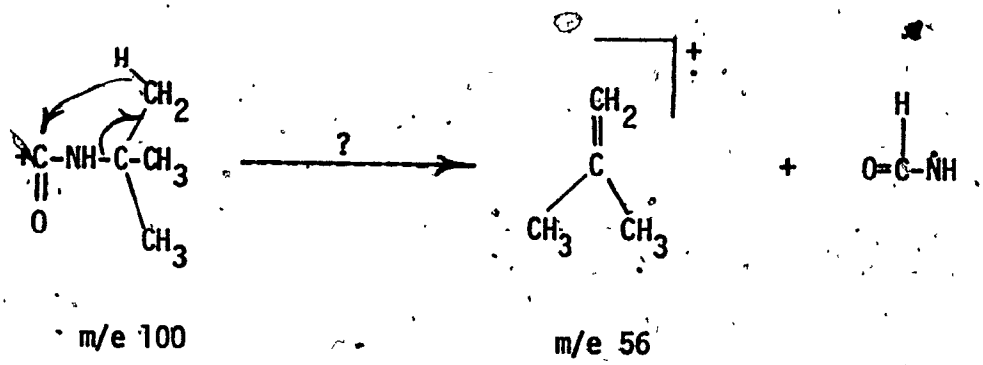

m/e 100 m/e 56

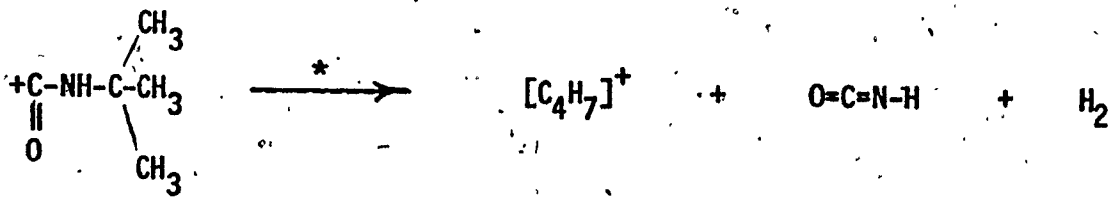

m/e 100 m/e 55

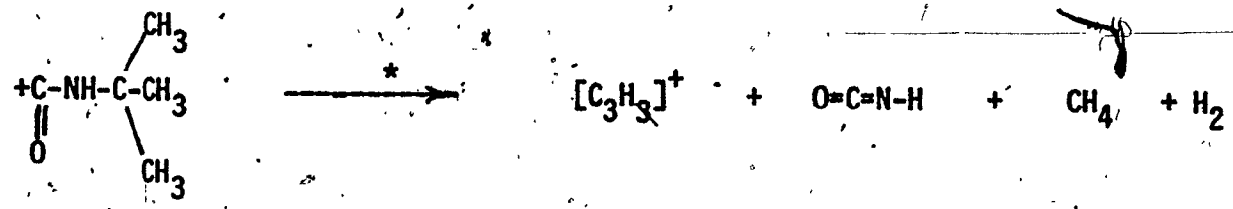

m/e 100 m/e 89

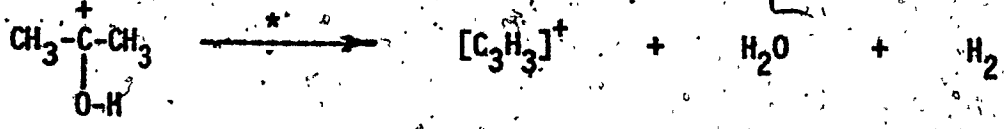

m/e 59 m/e 89

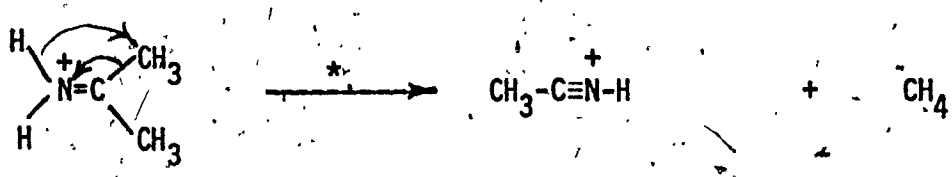

m/e 58 m/e 42

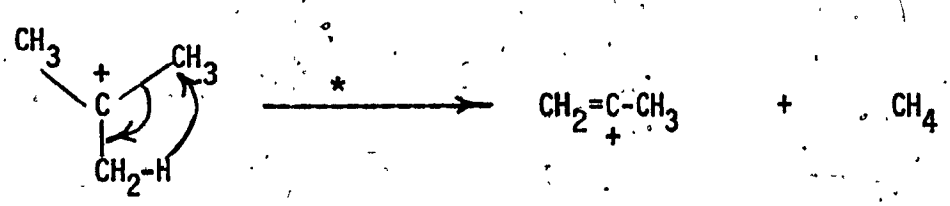

m/e 57 m/e 41

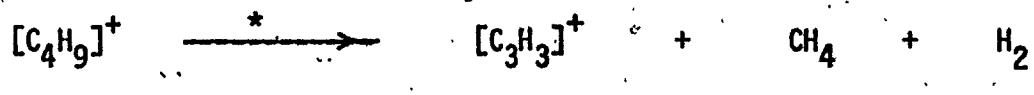

m/e 57 m/e 39

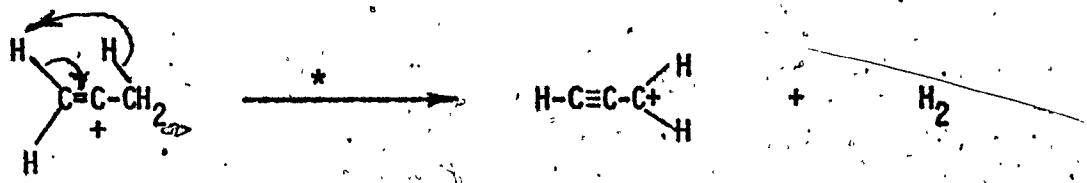

m/e 41 m/e 39

i) Primary cleavage peaks in the N-t-butyl-α-chloroacetamide mass spectra

Peaks that result from primary cleavage are of considerable interest in the mass spectra of the N-t-butyl-α-chloroacetamides. Primary cleavage peaks that are common to the N-t-butyl-α-chloroacetamide series are the peaks at m/e 57 and at m/e 100. The source of the peak at m/e 57 is thought to be the molecular ion. Metastable transitions have not been found to support this assumption, however similar compounds have been observed to fragment in the proposed manner, and a metastable transition was observed [9]. Prox and Schmid observed the cleavage process presented below:

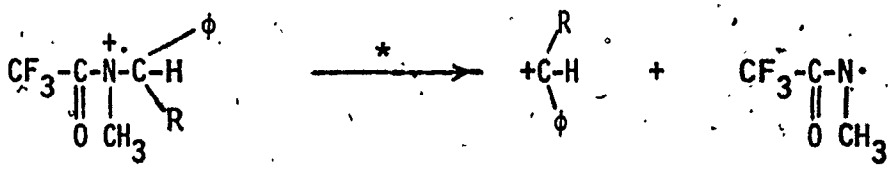

The proposed cleavage process, that gives the peak at m/e 57, occurs between a tertiary carbon and the nitrogen atom. There is a definite trend in the formation of the peak at m/e 57, throughout the N-t-butyl-α-chloroacetamide series; as chlorination increases throughout the series, the peak at m/e 57 increases in intensity. Formation of the alkyl fragment would seem to be a more favorable process as chlorination increases because the chlorine atoms tend to withdraw electrons from the carbonyl and nitrogen functions, thus giving a greater electron shortage between the tertiary carbon and the nitrogen atom. As fragmentation occurs between the nitrogen and the t-butyl function, it would seem that the t-butyl fragment would be more able to stabilize a positive charge.

The formation of the peak at m/e 100 ($C_4H_{10}N$) is observed to occur in the mass spectra of N-t-butylchloroacetamide and N-t-butyl-α,α,α-trichloroacetamide. Metastable transitions are observed for both of the cleavage processes that lead to the formation of the peaks at m/e 100 for each of the above compounds. There seems to be no trend in intensity visible for the peak at m/e 100 in the N-t-butyl-α-chloroacetamide series. The peak at m/e 100 originates from the molecular ion in both cases, a proposed cleavage process is:

$$[M]^{+\cdot} \longrightarrow {}^{+}NH\text{-}C(CH_3)_3 + R\text{-}C{=}O$$

Comparable processes have been observed by Saxby [6] in the compound N-ethyl-α,α,α-trifluoroacetamide

$$[CF_3\text{-}\overset{\overset{O}{\|}}{C}\text{-}NH\text{-}CH_2\text{-}CH_3]^{+\cdot} \longrightarrow {}^{+}NH\text{-}CH_2CH_3 + CF_3\text{-}C{=}O$$

The probable cleavage process that gives the analogous peaks m/e 100, m/e 134, m/e 168 and m/e 202 is;

$$[CH_xCl_y\text{-}\overset{\overset{O}{\|}}{C}\text{-}NH\text{-}C(CH_3)_3]^{+\cdot} \longrightarrow CH_xCl_y\text{-}\overset{\overset{O}{\|}}{C}\text{-}NH\text{-}\overset{+}{C}(CH_3)_2 + {}^{\cdot}CH_3$$

(for m/e 100, 134, 168, 202)

Formation of the analogous peaks $[M\text{-}Cl]^+$ (m/e 114, m/e 148 and m/e 182), is also thought to be a primary cleavage process. No metastable transitions have been observed to reinforce this proposal, however

all of the observed peaks are just 35 mass units less than the molecular ion, which would suggest that a chlorine atom has been lost from the molecular ion. No definite trend is observable for the $\%\Sigma_{36}$ values, as the number of chlorine atoms increases throughout the N-t-butylchloroacetamide series.

The formation of the peak $R\text{-}\overset{+}{C}{=}O$ was affected by the presence of chlorine atoms, if no chlorine atom was present in the ion $R\text{-}\overset{+}{C}{=}O$, the $\%\Sigma_{36}$ was 8.2, however with the introduction of a chlorine atom into the amide, the $\%\Sigma_{36}$ falls considerably. Pelah [5] suggested that the formation of the peak at m/e 43 $[C_2H_3O]^+$ for the compound n-butylacetamide was a result of a fission process. Saxby [7] mentioned that this fission process was absent in all of the trifluoroacetamides he studied. A metastable transition is not observed for any of the transitions $[M]^{+\cdot} \longrightarrow R\text{-}\overset{+}{C}{=}O$ in this work.

ii) Rearrangement peaks in the N-t-butyl-α-chloroacetamide mass spectra

Rearrangement peaks that are common to the N-t-butylchloroacetamide spectra, are the peaks at m/e 39, m/e 41, m/e 42, m/e 56, m/e 58 and m/e 59. The identification of these peaks was discussed previously for each compound.

The peak at m/e 39 (C_3H_3), originates from different sources in the series of N-t-butyl-α-chloroacetamides. The source of m/e 39 in N-t-butylacetamide is not known. For N-t-butyl-α-chloroacetamide m/e 39 was found to originate from two sources; m/e 94 $\xrightarrow{*}$ m/e 39, and m/e 58 $\xrightarrow{*}$ m/e 39. It is difficult to understand how these processes occur, in terms of a mechanism. The pathway by which the peak at m/e 39 arises in the compound N-t-butyl-α,α-dichloroacetamide also is difficult to describe. Metastable transitions appear to support the transitions m/e 58 $\xrightarrow{*}$ m/e 39, and m/e 57 $\xrightarrow{*}$ m/e 39 in N-t-butyl-α,α-dichloroacetamide. The following processes are seen to give the peak at m/e 39 in N-t-butyl-α,α,α-trichloroacetamide; m/e 100 $\xrightarrow{*}$ m/e 39, m/e 59 $\xrightarrow{*}$ m/e 39, and m/e 57 $\xrightarrow{*}$ m/e 39. As with the previously discussed compounds it is difficult to visualize how the peak at m/e 39 originates.

The origin of the peak at m/e 41 (C_3H_5) is thought to be from the fragment C_4H_9 (m/e 57). A metastable observed at m/e 29.5 that substantiates the proposed pathway is observed in N-t-butylacetamide, and all of the N-t-butyl-α-chloroacetamide mass spectra. The proposed mechanism is then;

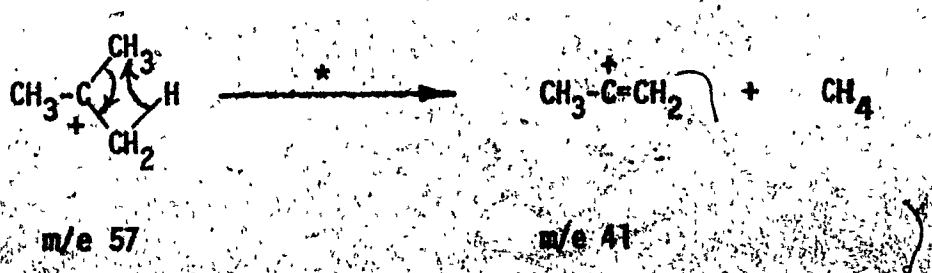

This process has been confirmed by the metastable defocussing technique for N-t-butyl-α,α-dichloroacetamide.

The peak at m/e 42 (C_2H_4N), results from the transition m/e 58 $\xrightarrow{*}$ m/e 42. This suggested process is compatible with the observation of a metastable ion at m/e 30.4 in the spectra of N-t-butylacetamide and the N-t-butyl-α-chloroacetamides. A mechanism for the production of m/e 42 is:

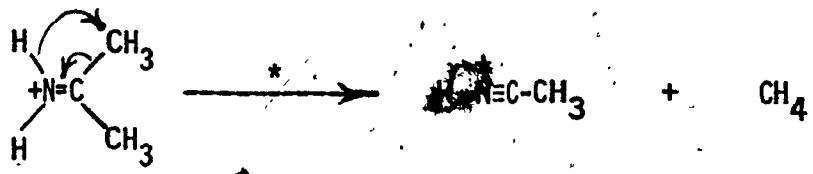

m/e 58 m/e 42

An analogous system observed by Prox [9] is;

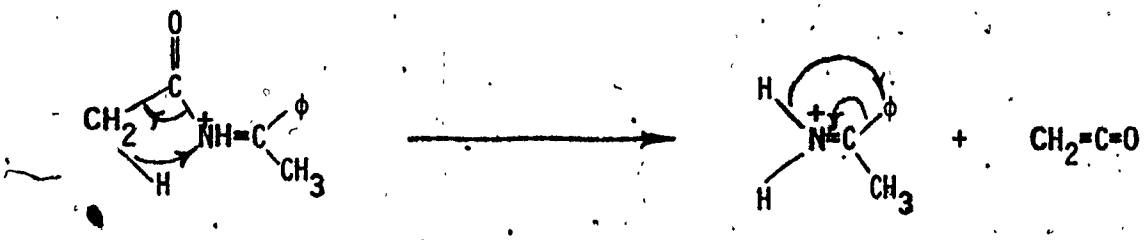

m/e 162 m/e 120

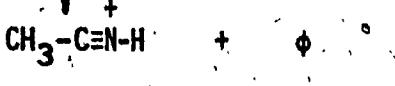

m/e 42

It is proposed that the peak at m/e 56 arises from the molecular ion by the process;

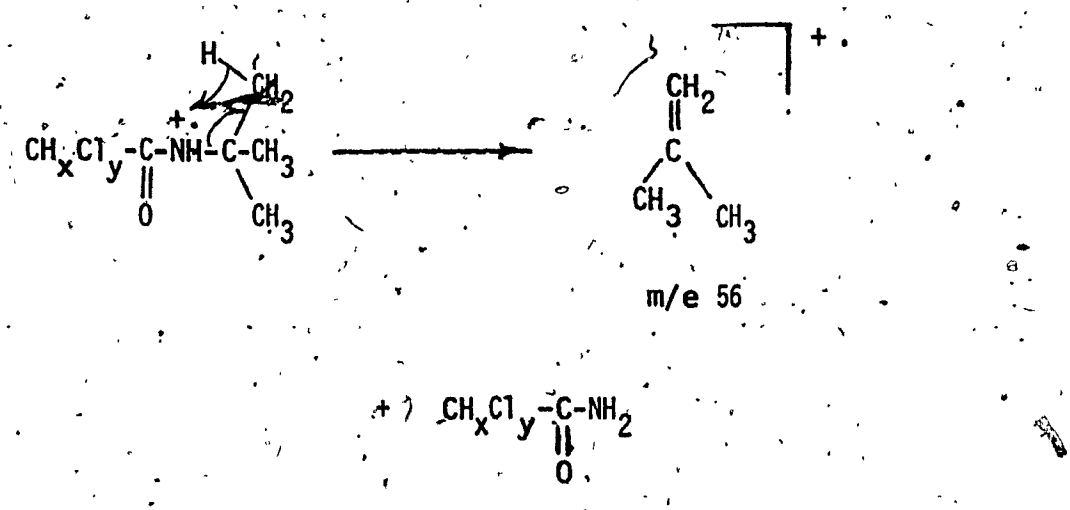

m/e 56

Possible metastable transitions appear in the mass spectra of N-t-butyl-α-chloroacetamide and N-t-butyl-α,α-dichloroacetamide, but a definite metastable transition is noted in N-t-butyl-α,α,α-trichloroacetamide, for the transition $M^+ \longrightarrow$ m/e 56. A similar process given by Saxby [7] for the peak at m/e 56 in N-n-butyl-α,α,α-trifluoroacetamide is;

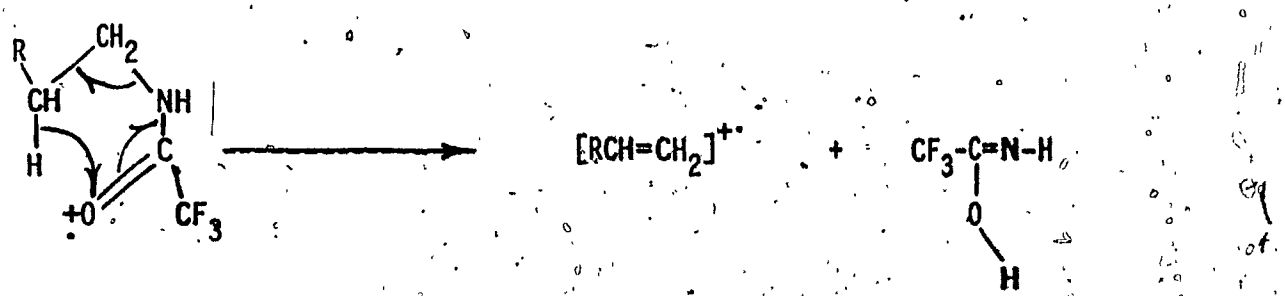

m/e 169 m/e 56

The peak at m/e 58 (C_3H_8N), is suggested to result from the process $[M-15]^+ \longrightarrow$ m/e 58. This process has been confirmed by the metastable defocussing technique for the compound N-t-butyl-α,α-dichloroacetamide. The proposed pathway is further established by the observation of metastable ions in the compounds N-t-butylacetamide and N-t-butyl-α-chloroacetamide. Formation of the peak at m/e 58 is in accordance with process II proposed

by Gilpin;

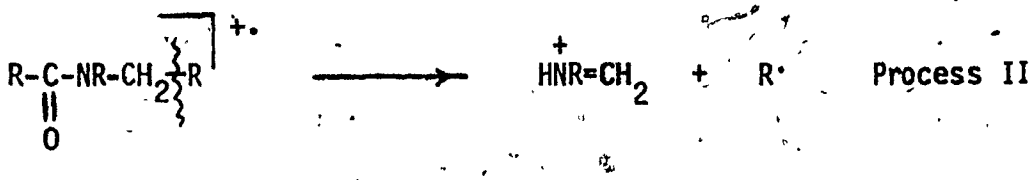

Process II

The study of N-ethylacetamide by Gilpin [1], showed the peak at m/e 30 to be $\overset{+}{H}NH=CH_2$. Pelah [5] clarified the mechanism of processII by studying the mass spectrum of N-n-butyl-d_3-acetamide. The peak at m/e 30 was observed to change to m/e 31 in the mass spectrum of the deuterated amide.

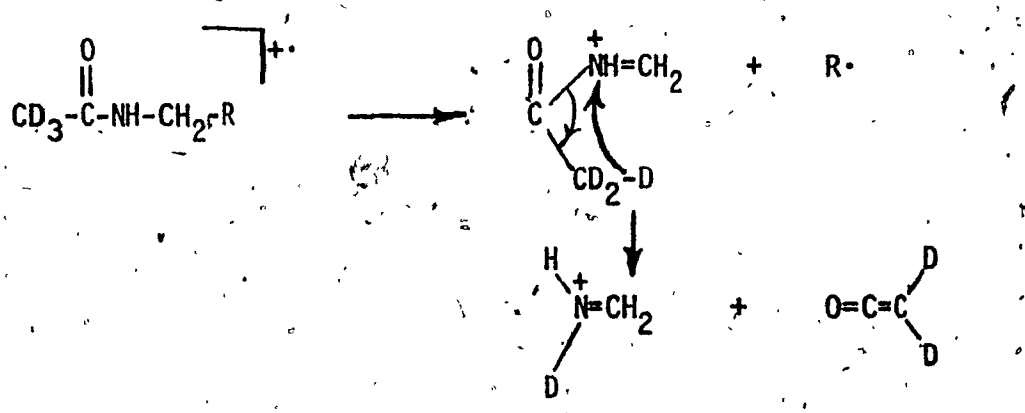

m/e 31

An analogous rearrangement has been observed by Prox [9]. The rearrangement is:

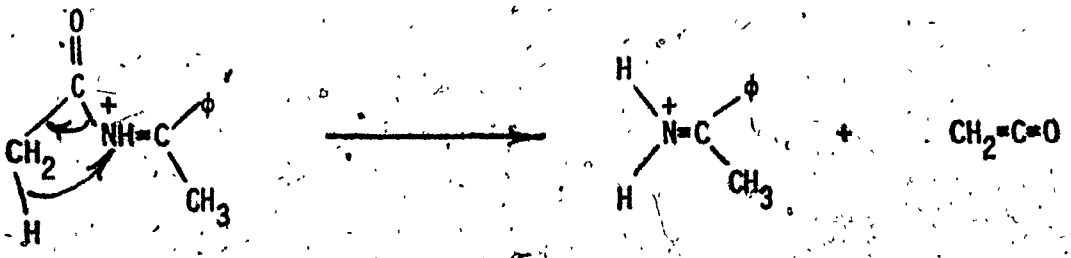

m/e 162 m/e 120

The peak at m/e 59 is observed in the mass spectra of N-t-butyl-acetamide and the N-t-butyl-α-chloroacetamides. The proposed process is;

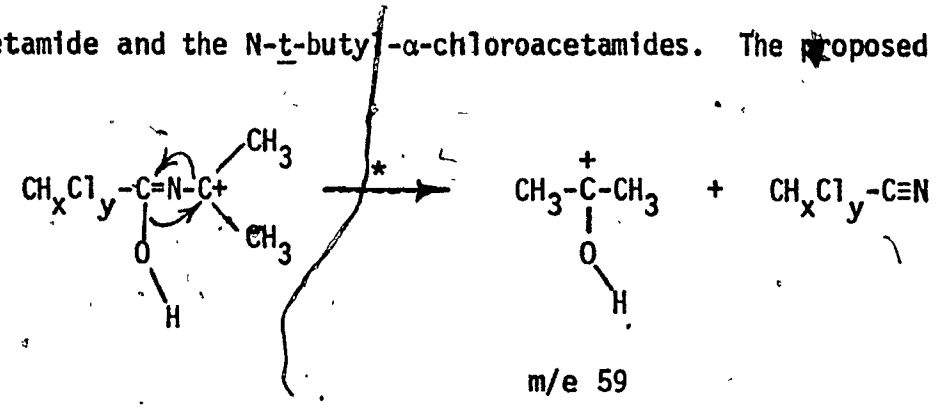

m/e 59

Metastable transitions were observed for the process $[M-15]^+ \longrightarrow$ m/e 59, for the N-t-butyl-α-chloroacetamides. The proposed rearrangement is consistent with the rearrangement proposed by Saxby [7], for the compound N-t-butyl-α,α,α-trifluoroacetamide.

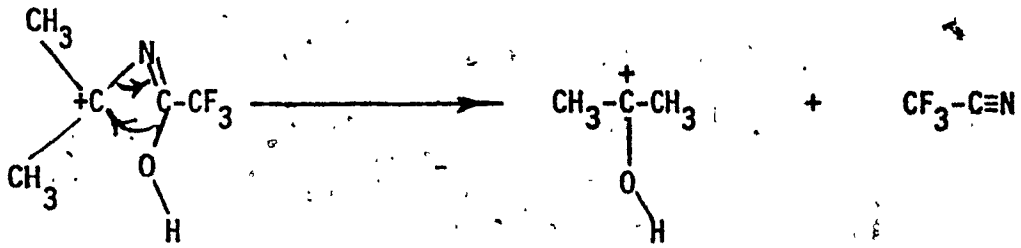

m/e 154, m/e 59

The probable rearrangement process that gives the analogous peaks; m/e 60, m/e 94, m/e 128, and m/e 162 is;

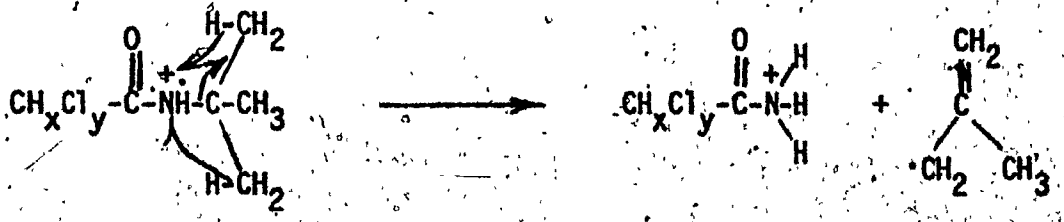

$[M]^+$ (m/e 60, 94, 128, 162)

The proposed pathway is substantiated by the observation of metastable transitions in the mass spectra of N-t-butylacetamide, N-t-α-chloroacetamide and N-t-butyl-α,α-dichloroacetamide, for the rearrangement

$$[M]^+ \longrightarrow CH_xCl_y\overset{\overset{O}{\|}}{C}-\overset{+}{N}H_3 .$$

The formation of the peaks at m/e 84 (C_4H_6NO), m/e 98 (CH_2NCl_2), and m/e 138 ($C_4H_6NCl_2$), is found only in the mass spectra of N-t-butyl-α,α,α-trichloroacetamide. It would seem that these peaks are all formed by rearrangement processes; for the peak at m/e 138, it is postulated that the process generating it involves the peak at m/e 202. A metastable transition was observed that supports this proposal; most likely the rearrangement process is a concerted one involving the loss of CO and HCl.

No useful information could be gained as to the origin of the peak at m/e 98 in the spectra of N-t-butyl-α,α,α-trichloroacetamide. Even though there seems to be metastable transitions for m/e 217 ⟶ m/e 77 and m/e 217 ⟶ m/e 58 it is extremely difficult to give meaningful mechanisms that would support these proposals.

N-t-butyl-α-fluoroacetamide

Fragmentation pattern for N-t-butyl-α-fluoroacetamide

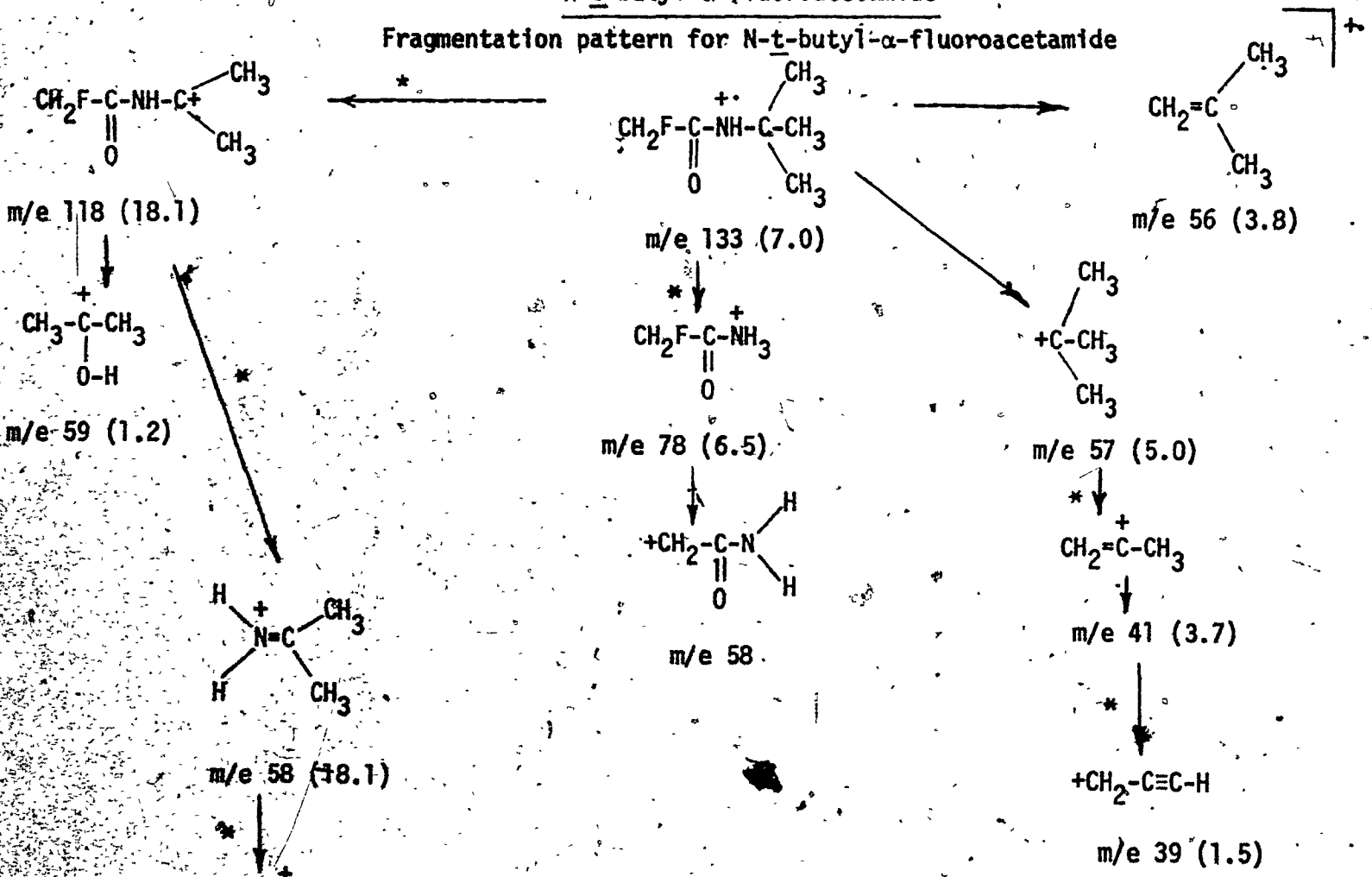

a) Peaks arising via simple cleavage.

The following fragment peaks most likely arise through a direct cleavage process.

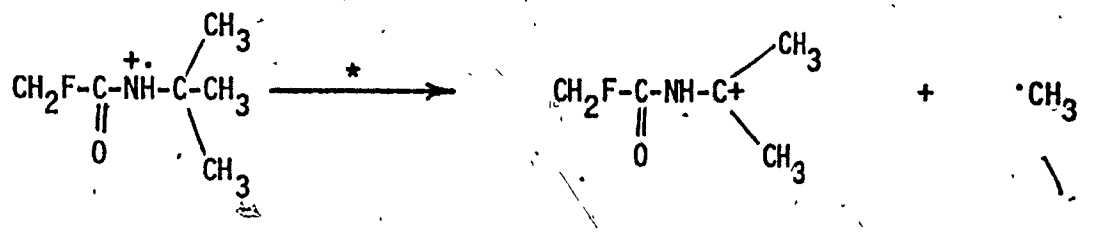

m/e 133 m/e 118

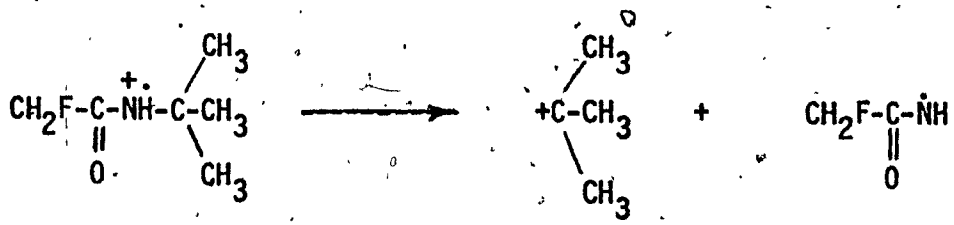

m/e 133 m/e 57

b) Peaks arising via a rearrangement process.

The following peaks most likely result from a rearrangement process.

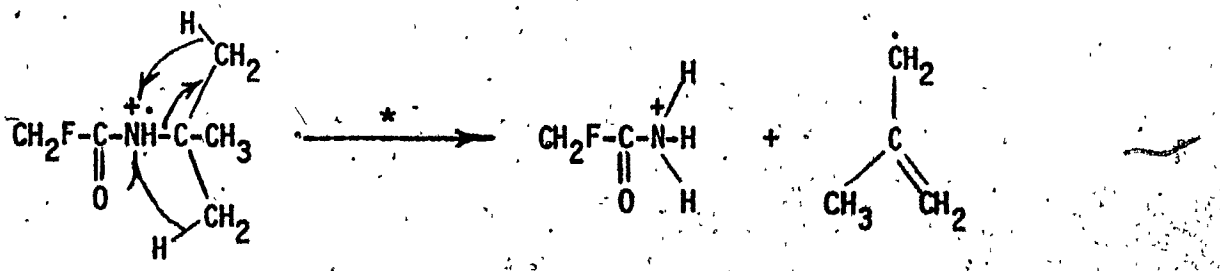

m/e 133 m/e 78

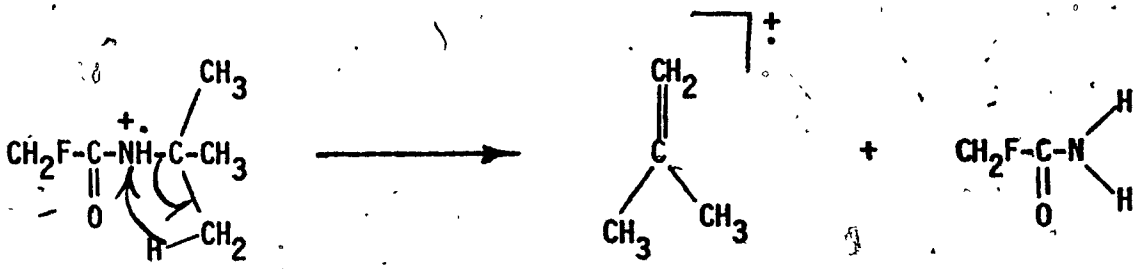

m/e 133 m/e 56

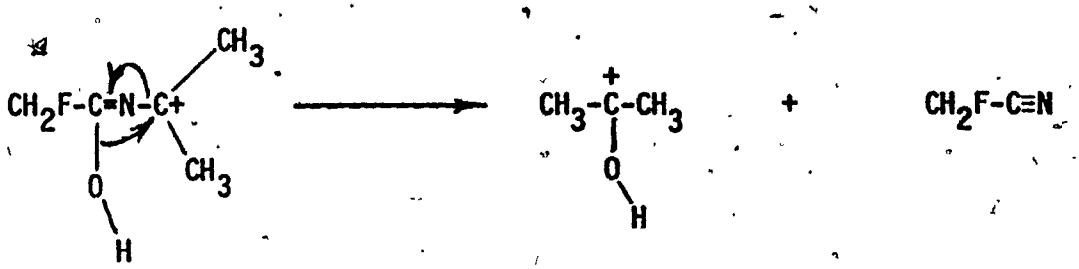

m/e 118 m/e 59

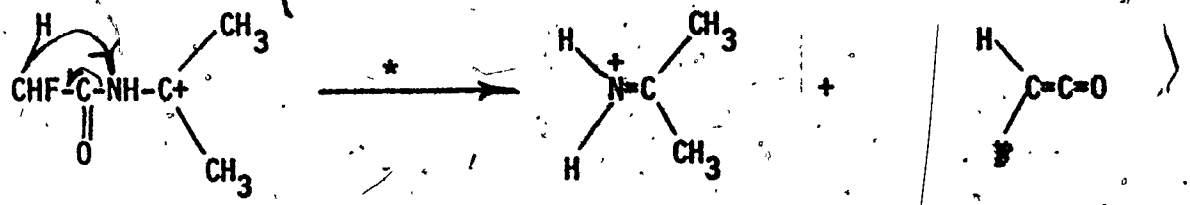

m/e 118 m/e 58

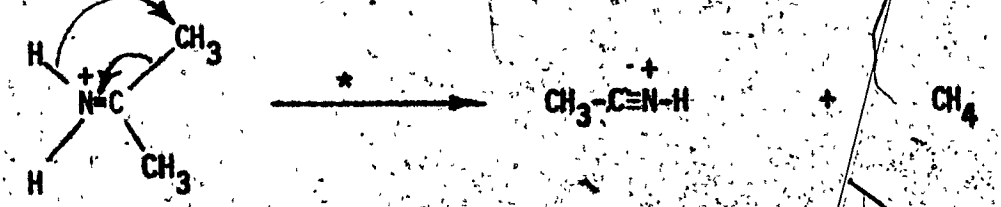

m/e 58 m/e 42

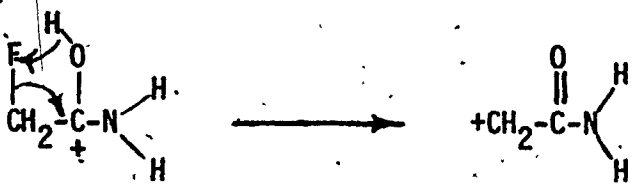

m/e 78 m/e 58

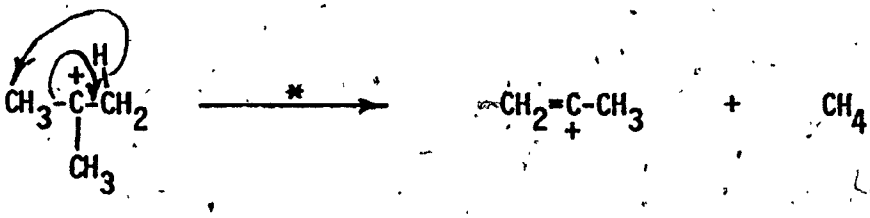

m/e 57 m/e 41

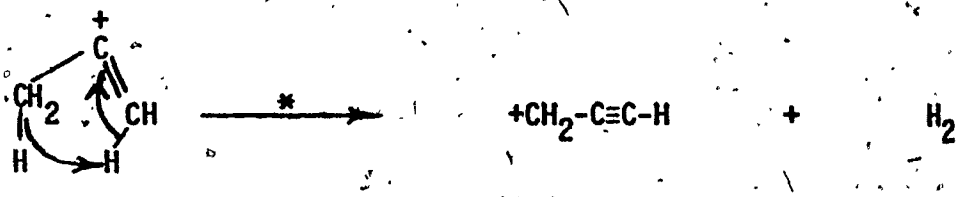

m/e 41 m/e 39

N-t-butyl-α,α-difluoroacetamide

Fragmentation pattern for N-t-butyl-butyl-α,α-difluoroacetamide

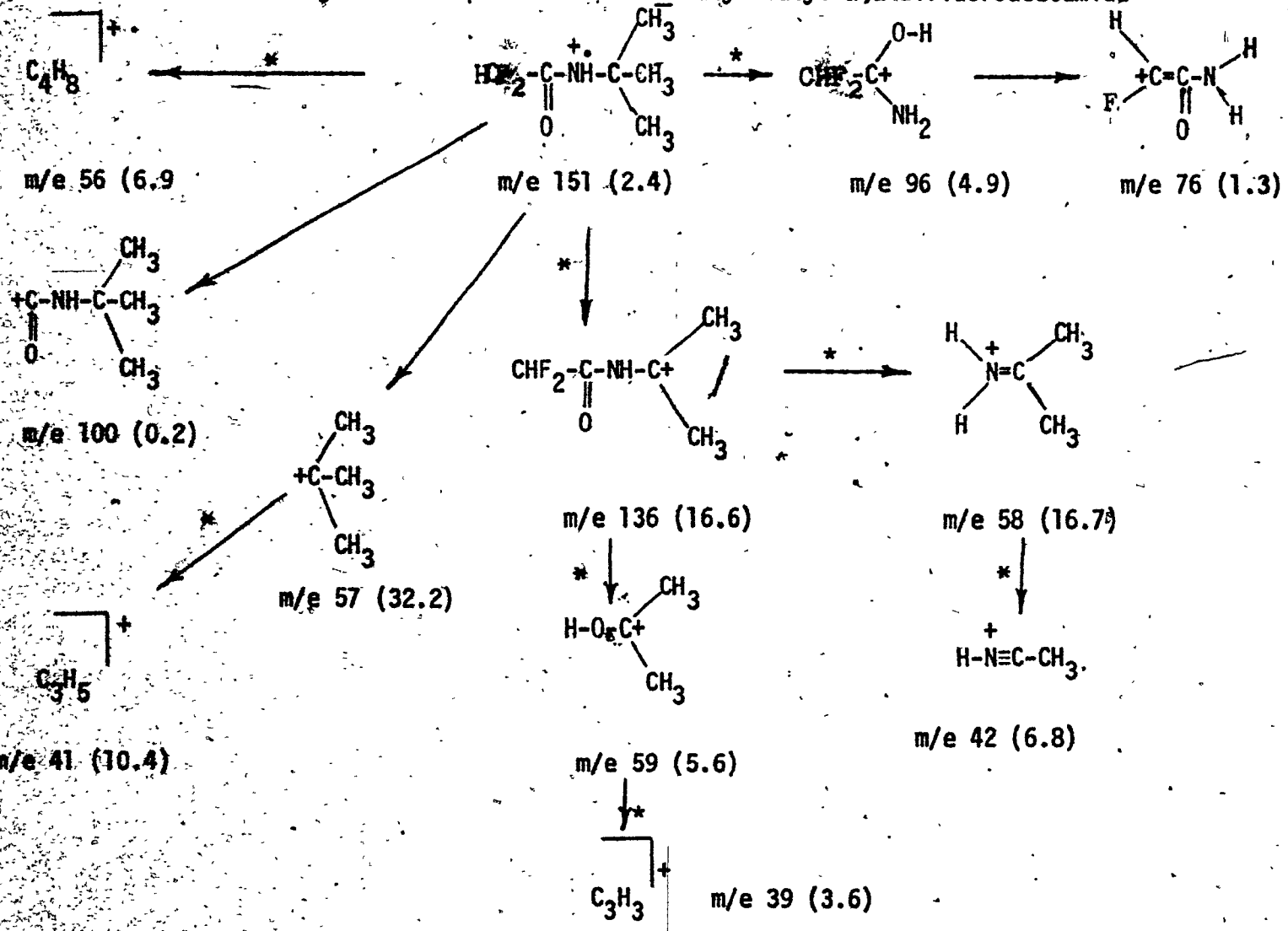

a) Peaks resulting from simple cleavage

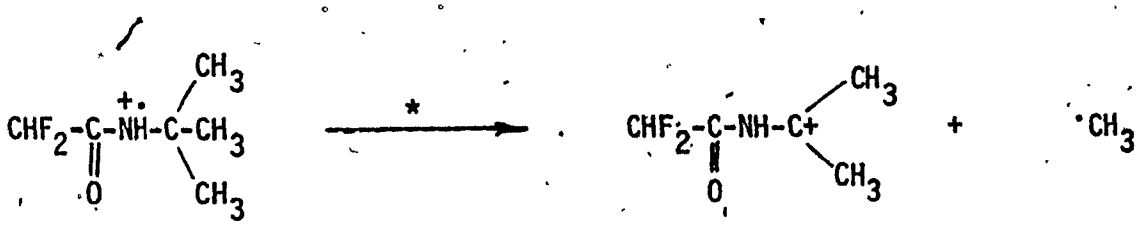

m/e 151 m/e 136

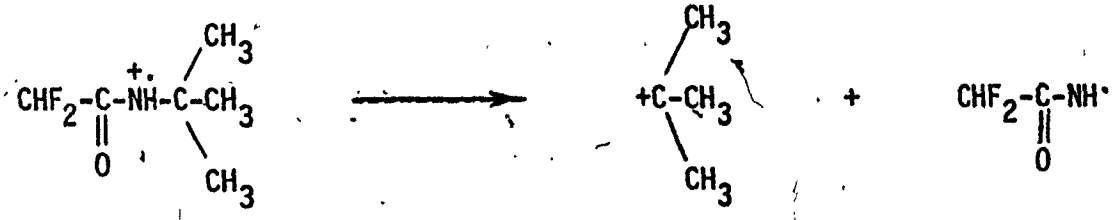

m/e 151 m/e 57

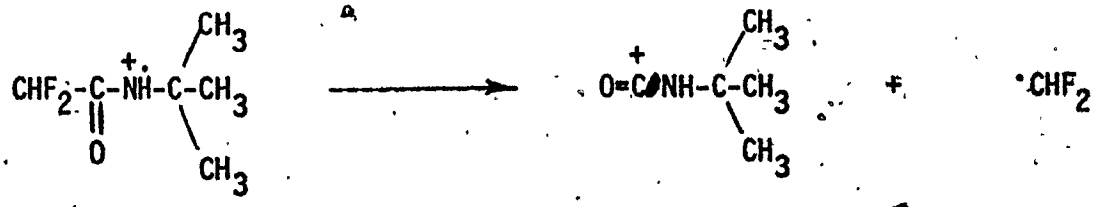

m/e 151 m/e 100

b) Peaks formed by rearrangement

The fragment peaks that result from a rearrangement process are given in the postulated scheme shown below:

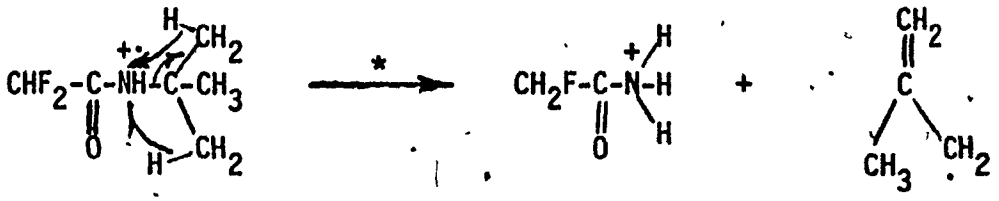

m/e 151 m/e 96

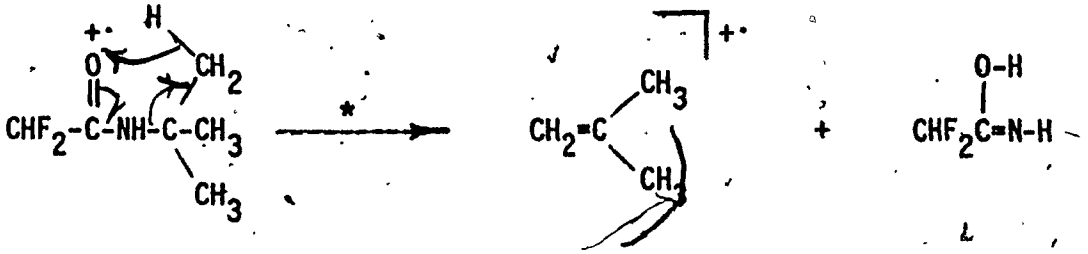

m/e 151 m/e 56

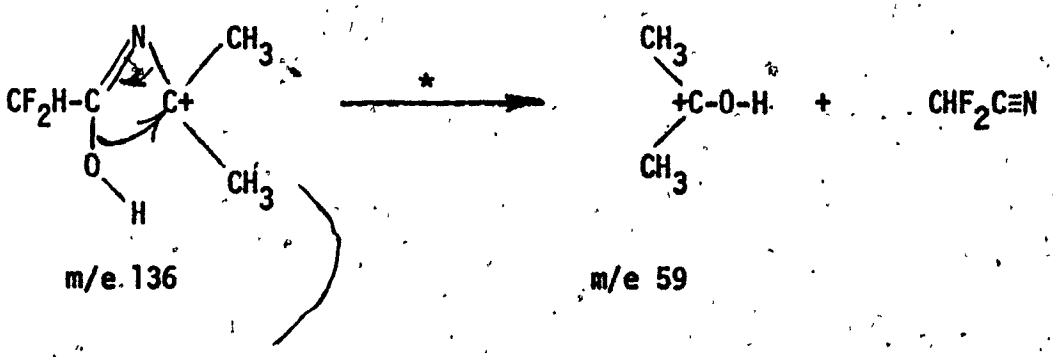

m/e 136 m/e 59

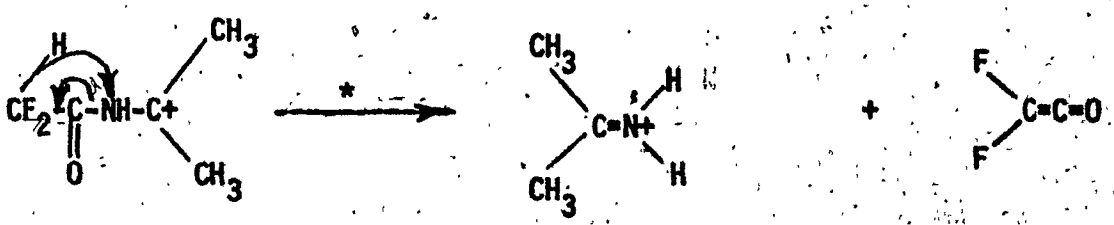

m/e 136 m/e 58

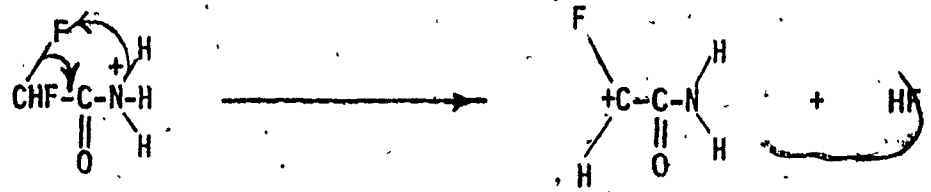

m/e 96 m/e 76

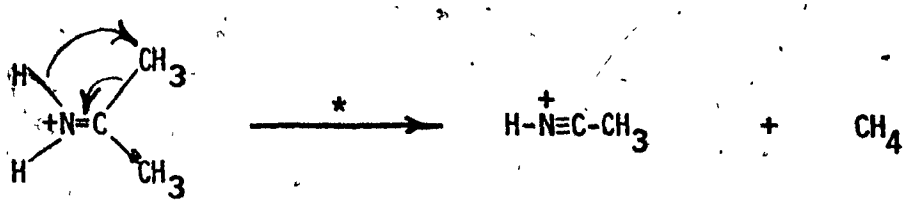

m/e 58 m/e 42

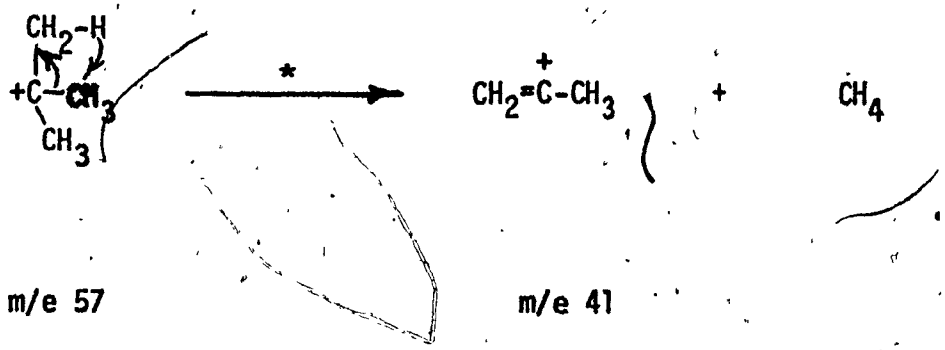

m/e 57 m/e 41

The transitions m/e 136 $\xrightarrow{*}$ m/e 42 and m/e 59 $\xrightarrow{*}$ m/e 39 are difficult to visualize in terms of a mechanistic process, however it is most likely that they are rearrangement processes.

N-t-butyl-α,α,α-trifluoroacetamide

Fragmentation pattern for N-t-butyl-α,α,α-trifluoroacetamide

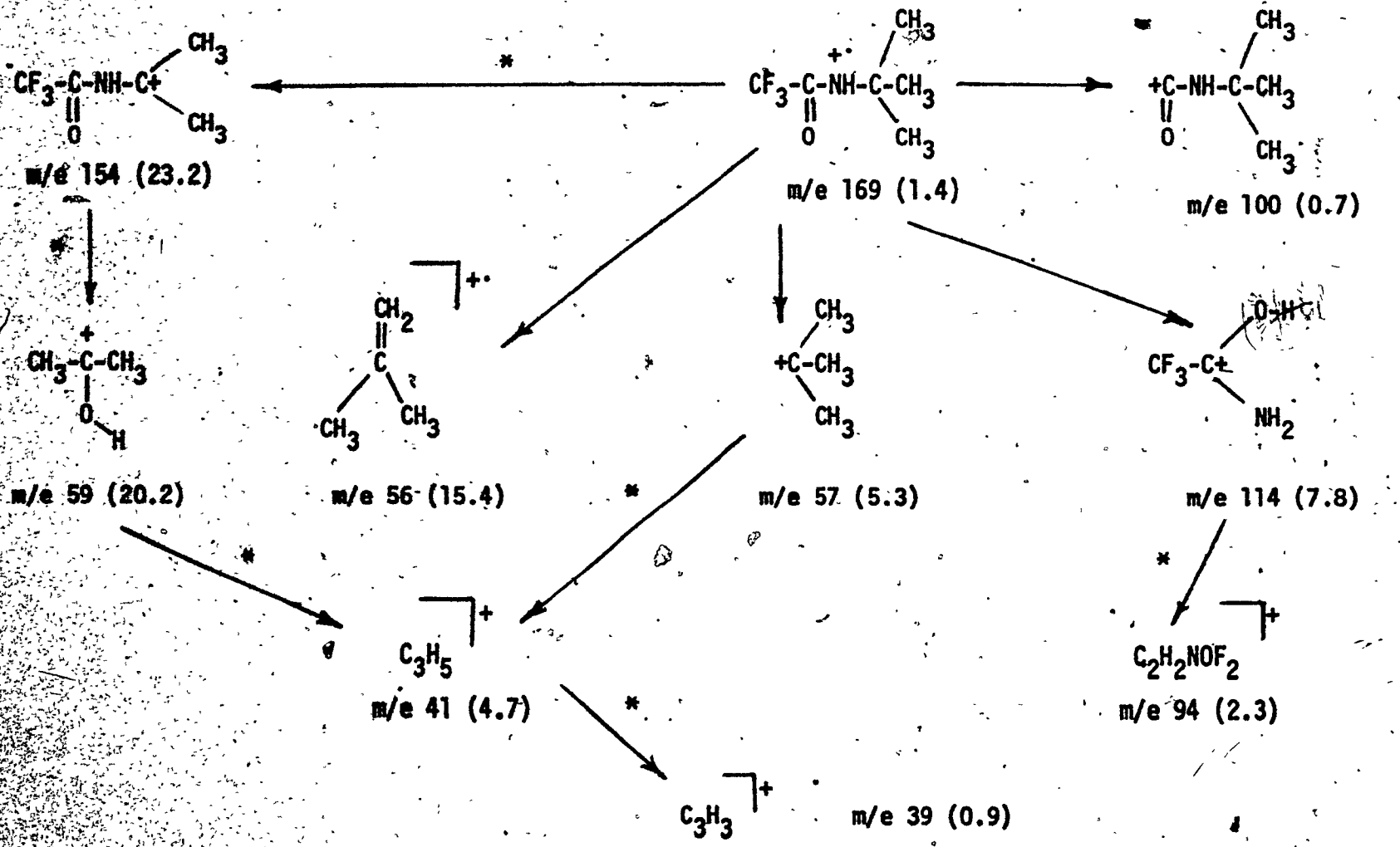

a) Peaks arising via simple cleavage

The following peaks most likely arise through a direct cleavage process.

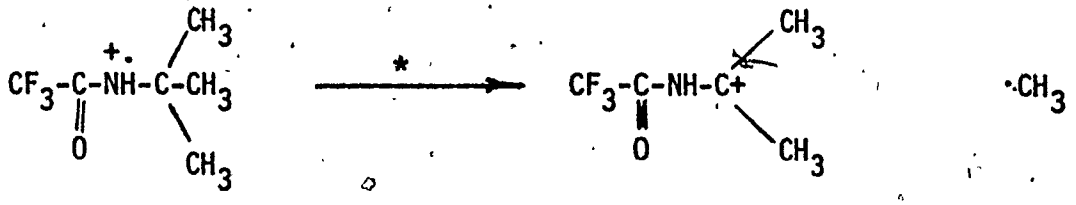

m/e 169 m/e 154

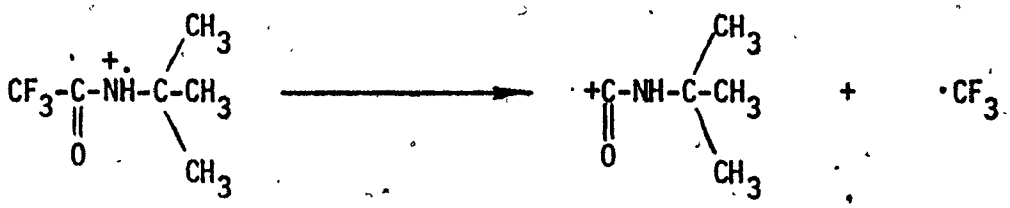

m/e 169 m/e 100

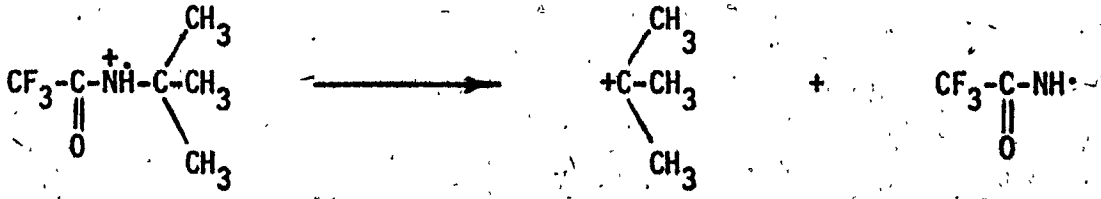

m/e 169 m/e 57

b) Peaks resulting from a rearrangement process

The following fragment peaks are thought to arise via the postulated routes shown below

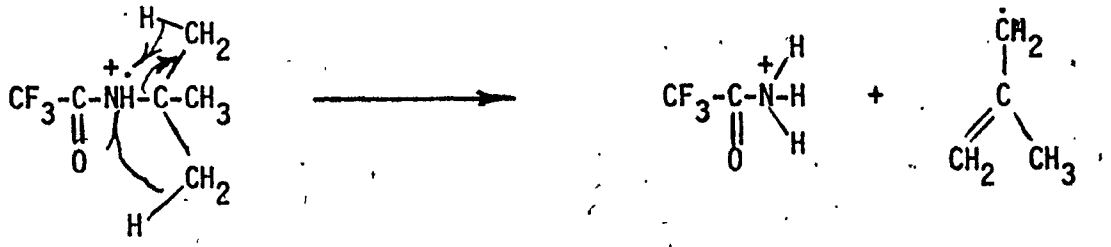

m/e 169 m/e 114

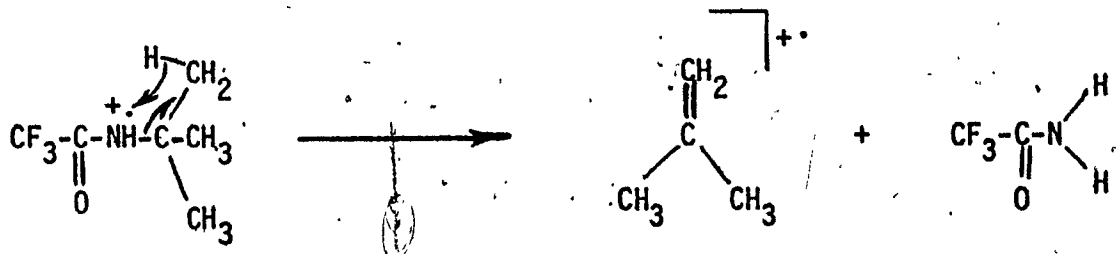

m/e 169 m/e 56

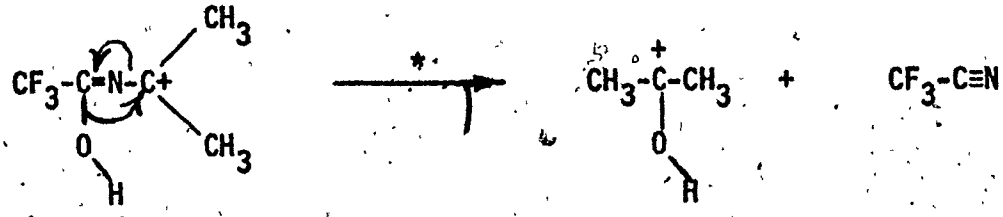

m/e 154 m/e 59

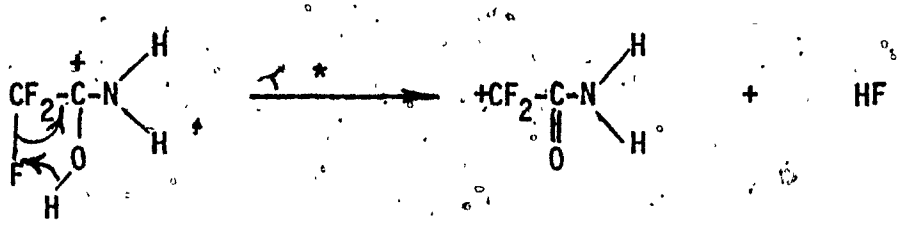

m/e 114 m/e 94

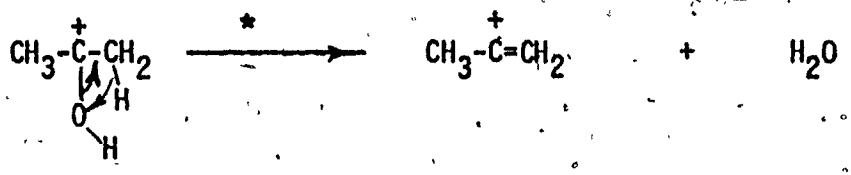

m/e 59 m/e 41

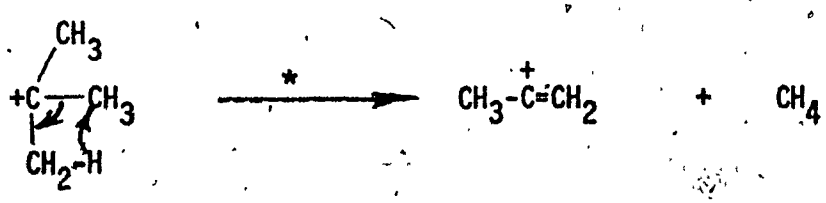

m/e 57 m/e 41

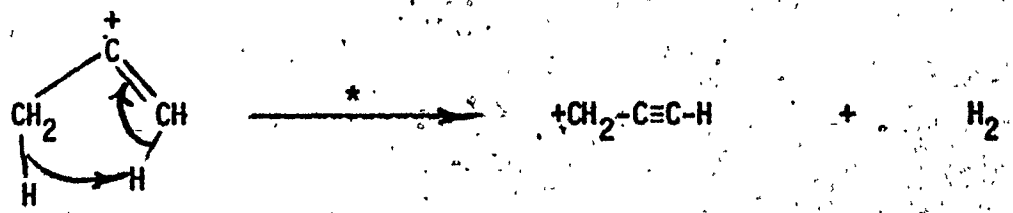

m/e 41 m/e 39

iii) Primary cleavage peaks in the N-t-butyl-α-fluoroacetamide mass spectra

Primary cleavage peaks that are common in the N-t-butyl-α-fluoroacetamide mass spectra are the peaks at m/e 57 and m/e 100. The peak at m/e 57 (C_4H_9) is thought to be derived from the molecular ion, but as in the N-t-butyl-α-chloroacetamide mass spectra, no metastable transitions were observed that would confirm this proposed process. It has been mentioned previously, that comparable cleavage processes have been observed by other workers. There seems to be a trend to increasing values of $\%\Sigma_{36}$ for the peak at m/e 57 in the N-t-butyl-α-fluoroacetamide mass spectra, with the exception of N-t-butyl-α,α,α-trifluoroacetamide.

The peak at m/e 100 occurs, however the values of $\%\Sigma_{36}$ are very low, the highest being noted in the spectrum of N-t-butyl-α,α,α-trifluoroacetamide (0.7). Formation of the fragment peak at m/e 100 is seen to be of much less significance in the N-t-butyl-α-fluoroacetamide spectra, as compared to the N-t-butyl-α-butylchloroacetamide mass spectra. As in the N-t-butyl-α-chloroacetamide series, the peak at m/e 100 is thought to be derived from the molecular ion.

Peaks at m/e 118, m/e 136 and m/e 154 are analogous peaks that are all assumed to result from a cleavage process; metastable transitions have been observed for the transition $[M]^+ \longrightarrow [M-15]^+$ for all cases. As previously noted in the section for cleavage ions of the N-t-butyl-α-chloroacetamide series, transitions of this nature have been observed by other investigators.

The formation of the analogous peaks $[M-F]^+$ and $R-\overset{+}{C}=O$ is noticably missing in the N-t-butyl-α-fluoroacetamide series. Saxby [7] made a similar comment, when referring to the peak $R-\overset{+}{C}=O$, in his study of a number of homologous trifluoroacetamides; perhaps this process does not occur because the fluorine atoms on the acyl function have such an electron withdrawing effect that the acyl function can not stabilize a positive charge.

iv) Rearrangement peaks in the N-t-butyl-α-fluoroacetamide mass spectra

Rearrangement peaks that are common to the N-t-butyl-α-fluoroacetamide mass spectra, are the peaks at m/e 39, m/e 41, m/e 42, m/e 56, m/e 58, and m/e 59. Identification of these peaks was discussed previously for each compound.

The peak at m/e 39 (C_3H_3), originates from various sources in the N-t-butyl-α-fluoroacetamide series, one source of m/e 39 in the observed mass spectra is from the peak at m/e 41. A possible mechanism for this transition in N-t-butyl-α-fluoroacetamide is:

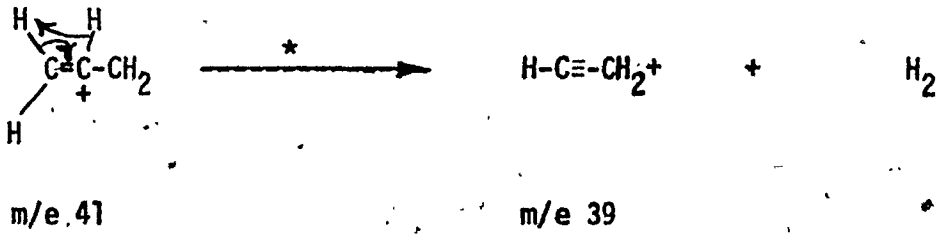

A similar means of production of the peak at m/e 39 is thought to occur in the compound N-t-butyl-α,α,α-trifluoroacetamide. The most likely source of the peak at m/e 39 in the mass spectrum of N-t-butyl-α,α-difluoroacetamide is the process m/e 59 $\xrightarrow{*}$ m/e 39; it is difficult to visualize this process in terms of a mechanism.

A common source for the origin of the peak at m/e 41 is thought to result from the fragment C_4H_9 (m/e 57). Mass spectra of all of the N-t-butyl-α-fluoroacetamides show metastable transitions to support this proposal. A possible mechanism that involves the formation of the neutral molecule methane is:

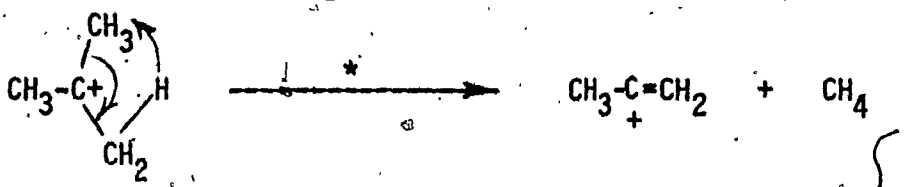

m/e 57 m/e 41

The peak at m/e 42 (C_2H_4N), is thought to result from the process:

m/e 58 m/e 42

A metastable transition that would support the proposal for this process has been observed in the mass spectra of the compounds N-t-butyl-α-fluoroacetamide and N-t-butyl-α,α-difluoroacetamide. As mentioned previously a similar process has been reported by Prox [9].

For the mass spectra of the N-t-butyl-α-fluoroacetamides the peak at m/e 56 is thought to result from the process:

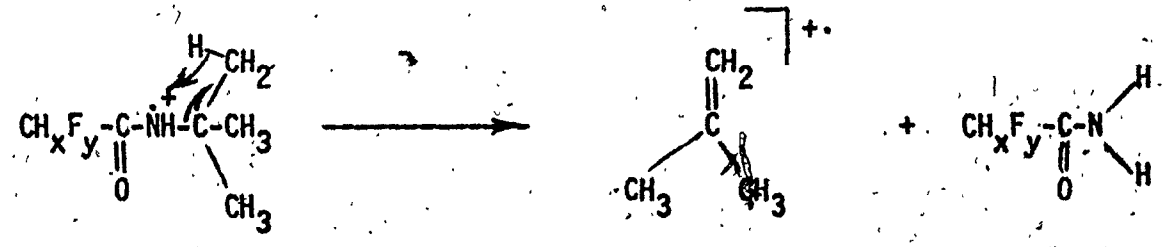

m/e $[M]^+$ m/e 56

A metastable transition was noted for the compound N-t-butyl-α,α-difluoroacetamide, in reference to the proposed process. As previously noted, Saxby [7] proposed a similar process for the peak at m/e 56 in N-t-butyl-α,α,α-trifluoroacetamide.

The peak at m/e 58 (C_3H_8N) is suggested to result from the process $[M-15]^+ \longrightarrow$ m/e 58, as the mass spectra of N-t-butyl-α-fluoroacetamide and N-t-butyl-α,α-difluoroacetamide show metastable transitions that support this proposal. The proposed process conforms to process I postulated by Gilpin [1].

The probable rearrangement process that produces the peak at m/e 59 is:

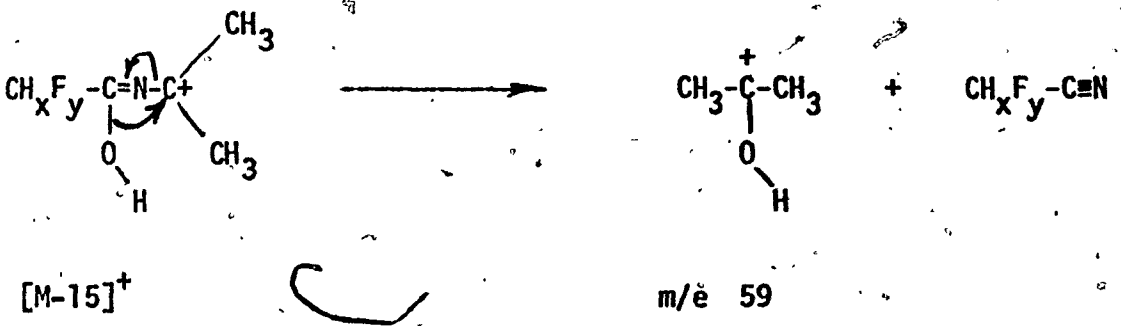

$[M-15]^+$ m/e 59

Metastable transitions that would suggest this process to occur, are found in the mass spectra of N-t-α,α-difluoroacetamide and N-t-butyl-α,α,α-trifluoroacetamide. Saxby [7] has also proposed this mechanism for N-t-butyl-α,α,α-trifluoroacetamide.

Analogous peaks at m/e 60, m/e 78, m/e 96 and m/e 114 are probably all produced by the same type of rearrangement:

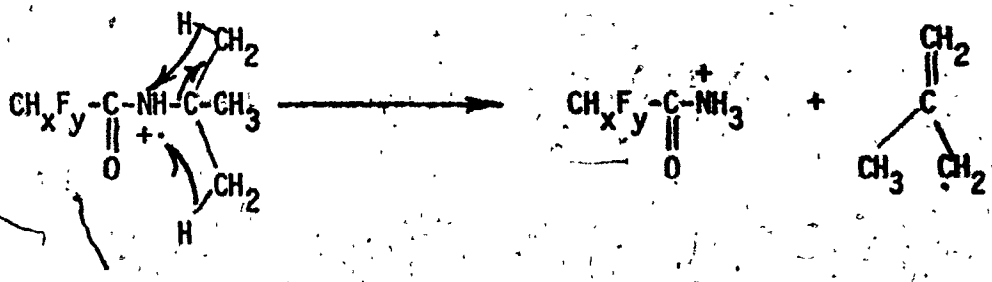

The proposed pathway is substantiated by metastable transitions in the mass spectra of N-t-butyl-α-fluoroacetamide and N-t-butyl-α,α-difluoroacetamide.

Formation of the analogous peaks at m/e 58, m/e 76, and m/e 94 in the N-t-butyl-α-fluoroacetamide mass spectra does not have a comparable process in the N-t-butyl-α-chloroacetamide mass spectra. The observed analogous peaks are postulated to result from a process that involves the loss of HF from the protonated fluoroacetamide, an example of this process is:

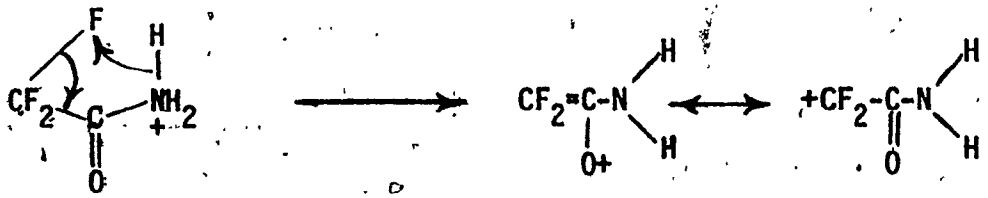

m/e 114 m/e 94

Saxby [7] proposed this scheme in the mass spectrum of the compound N-t-butyl-α,α,α-trifluoroacetamide. In the mass spectrum of N-t-butyl-α-fluoroacetamide the above process is an extremely weak one, and almost all of the peak at m/e 58 is attributed to the species C_3H_8N.

The rearrangement peak at m/e 84, C_4H_6NO, is characteristic of only the N-t-butyl-α,α,α-trifluoroacetamide mass spectrum. No information could be obtained to suggest how this peak resulted.

F) Ratio of $\%\Sigma_{36}$ for daughter and parent ions in the N-t-butyl-α-chloroacetamide mass spectra

The ratio of the $\%\Sigma_{36}$ for the daughter to the parent ion, generally shows that as chlorination is increased the ratio of the daughter ion to the parent ion increases in value; this is evident in the ratios 59/M-15, 56/M, 57/M, $R-\overset{\overset{O}{\|}}{C}-\overset{+}{N}H_3$/M and M-15/M. For each of the cases listed above (see Table 19) it would seem that as chlorination increases, the daughter ion becomes more stable and therefore more abundant than the parent ion.

For the cases 41/57, and 58/M-15, the parent peak is more intense than the daughter peak throughout the series. The ratio 41/57 decreases in value as chlorination increases in the mass spectra of the N-t-butyl-α-chloroacetamides; this happens as a result of the peak at m/e 57 increasing in intensity faster than the peak at m/e 41. The ratio 58/M-15 decreases in value as a result of the nature of the formation of the peak at m/e 58, since the peak at m/e 58 results from a rearrangement process that is less likely to occur as chlorination increases; the ratio would then be expected to decrease as chlorination increases. This can be seen from the proposed mechanism:

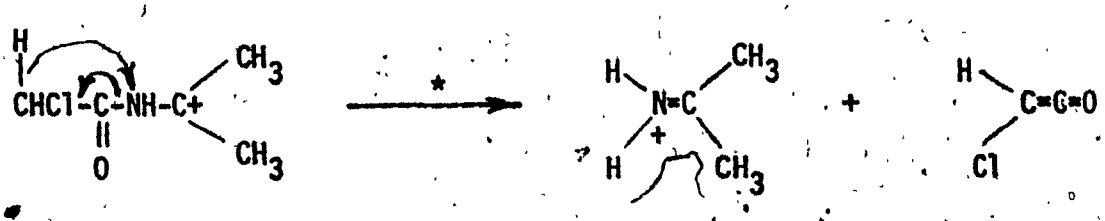

The ratios 42/58 and M-35/M are unaffected by alpha chlorination.

Table 19

Ratio of $\%\Sigma_{36}$ for daughter and parent peaks in the N-t-butyl-α-chloroacetamide mass spectra

Peak ratios	N-t-B.A.	N-t-B.ClA.	N-t-B.Cl_2A.	N-t-B.Cl_3A.
41/57	1.1	0.8	0.3	0.3
42/58	1.1	1.1	0.3	4.2
58/[M-15]	10.8	2.9	4.2	0.2
59/[M-15]	0.3	0.1	0.3	0.4
56/M	0.3	0.8	7.6	15.9
57/M	0.3	1.7	67.2	164.0
$R-\overset{\overset{O}{\parallel}}{C}-\overset{+}{N}H_3$/M	1.1	1.5	1.9	3.2
[M-35]/M	---	0.2	0.2	1.6
[M-15]/M	0.3	0.7	8.4	19.3

G) Ratio of $\%\Sigma_{36}$ for selected rearrangement peaks in the N-t-butyl-α-chloroacetamide mass spectra

Competition between various fragmentation routes that involve rearrangement peaks can be demonstrated by reviewing the ratio of $\%\Sigma_{36}$ for two rearrangement peaks. Formation of the peak at m/e 42 versus the peak at m/e 56 is shown in Table 20 to be unaffected by chlorination. No noticeable trend for the peak at m/e 58 versus the peak at $R\text{-}\overset{\overset{+}{}}{\underset{\underset{O}{\|}}{C}}\text{-}NH_3$ was found.

The ratio of the $\%\Sigma_{36}$ for two rearrangement peaks shows a definite trend for the ratios 56/58, 58/59, and 59/$R\text{-}\overset{\overset{+}{}}{\underset{\underset{O}{\|}}{C}}\text{-}NH_3$. For the rearrangement process that gives the peak at m/e 56 versus the peak at m/e 58, one can see that chlorination has a definite effect; as chlorination increases throughout the series, the value of the ratio falls, demonstrating that the process giving the ion at m/e 56 is a more favored one. The same analysis, and results, may be obtained for the ratio 59/$R\text{-}\overset{\overset{+}{}}{\underset{\underset{O}{\|}}{C}}\text{-}NH_3$. A ratio of the peaks at m/e 58 and 59 is interesting in the sense that they are both derived from the same parent ion, $[M\text{-}15]^+$. As chlorination is increased throughout the series, the value of the ratio 58/59 shows that the rearrangement process giving the peak at m/e 59 is more favorable. The ratio of 41/42 shows no consistent trend.

Table 20

Ratio of $\%\Sigma_{36}$ for selected rearrangement peaks in the N-t-butyl-α-chloroacetamide mass spectra

Rearrangement	N-t-B.A.	N-t-B.ClA.	N-5-B.Cl_2A.	N-t-B.Cl_3A.
41/42	0.1	2.1	2.0	2.4
42/56	1.1	0.7	1.3	1.2
56/58	0.1	0.2	0.2	3.7
58/59	42.0	127.0	12.9	0.5
58/$R-\overset{\overset{O}{\|\|}}{C}-NH_3^+$	2.6	3.6	19.0	1.4
59/$R-\overset{\overset{O}{\|\|}}{C}-NH_3^+$	0.1	0.1	1.5	2.5

H) Ratio of $\%\Sigma_{36}$ for selected fragment peaks of the N-t-butyl-α-chloroacetamide mass spectra

Table 21 shows the ratio of $\%\Sigma_{36}$ for fragment peaks (where it is understood that fragment peak means those peaks that are generated from a simple cleavage process) indicating that the ratios $57/CH_xCl_y$, 57/[M-15], and $57/CH_xCl_yC$ (=O) are affected by chlorination. In each of the above cases, it can be seen that the more stable fragment is the alkyl fragment, rather than the chlorine containing fragment. Perhaps this phenomenon results since the positive charge that is associated with the fragment is most readily stabilized by an electron donating group rather than one that is electron withdrawing.

The presence of a chlorine atom in a fragment peak does not produce a definite trend for the ratios $CH_xCl_y/100$, and $CH_xCl_y/[M-15]$.

Table 21

Ratio of $\%\Sigma_{36}$ for selected fragment peaks of the N-t-butyl-α-chloroacetamide mass spectra

Ratio of fragment peaks	N-t-B.A.	N-t-B.ClA.	N-t-B.Cl_2A.	N-t-B.Cl_3A.
$CH_xCl_y/100$	--	4.9	0.4	0.5
$57/CH_xCl_y$	--	4.9	18.7	26.6
57/[M-15]	1.1	0.9	7.7	12.5
$57/CH_xCl_y$-C(=O)	2.2	7.8	∞	∞
CH_xCl_y/[M-15]	--	0.2	0.4	0.3

I) Ratio of $\%\Sigma_{36}$ of fragment peak to rearrangement peak for the N-t-butyl-α-chloroacetamide mass spectra

A comparison of the intensities of peaks formed by fragmentation versus those that arise via a rearrangement process shows that chlorination effects the ratios 57/56, 57/58, 57/R-C(=O)-$\overset{+}{N}H_3$ and [M-15]/R-C(=O)-$\overset{+}{N}H_3$. In all of the ratios previously mentioned, it is noted that the ion resulting from simple cleavage becomes more intense throughout the series. This is of special significance for the ratios 57/56, 57/R-C(=O)-$\overset{+}{N}H_3$, and [M-15]/R-C(=O)-$\overset{+}{N}H_3$ as each of the ions in the ratio pair result from the same parent peak. It would seem then, as chlorination increases throughout the series, simple cleavage is the preferred process of breakdown rather than a rearrangement process for ions resulting from the molecular ion.

For the ratio 57/59 there is only a noticeable trend for the chlorine containing compounds. The ratio shows that as chlorination increases throughout the series, the rearrangement ion at m/e 59 becomes more important, although not as important as the ion at m/e 57.

Chlorination does not have an effect upon the ratio [M-35]/R-C(=O)-$\overset{+}{N}H_3$.

Table 22

Ratio of $\%\Sigma_{36}$ of fragment peak to rearrangement peak for the N-t-butyl-α-chloroacetamide mass spectra

Ratio of fragment peak to rearrangement peak	N-t-B.A.	N-t-B.ClA.	N-t-B.Cl_2A.	N-t-B.Cl_3A.
57/56	1.0	2.0	8.1	10.2
57/58	0.1	0.3	1.9	37.7
57/59	4.2	43.5	24.8	19.8
$\frac{57}{R\text{-}\overset{\overset{O}{\|}}{C}\text{-}\overset{+}{N}H_3}$	0.3	1.1	35.8	53.9
$\frac{[M-35]}{CH_xCl_y\text{-}\overset{\overset{O}{\|}}{C}\text{-}\overset{+}{N}H_3}$	--	0.1	0.8	0.5
$\frac{[M-15]}{CH_xCl_y\text{-}\overset{\overset{O}{\|}}{C}\text{-}\overset{+}{N}H_3}$	0.2	1.2	4.6	6.0

J) Ratio of $\%\Sigma_{36}$ for daughter ions and parent ions for the N-t-butyl-α-fluoroacetamide mass spectra

As for the N-t-butyl-α-chloroacetamides, the N-t-butyl-α-fluoroacetamide mass spectra show many significant trends in the value of the ratio of intensities for the daughter peak to the parent peak. These trends are found for the following cases, 59/[M-15], $R-\overset{\overset{O}{\|}}{C}-\overset{+}{N}H_3/[M]$, and [M-15]/M (see Table 23). For each of the above ratios, the daughter peak became more intense than the parent peak. The same pattern was noted in the mass spectra of the N-t-butyl-α-chloroacetamides. As fluorination increases in the series, the daughter peak became the more abundant because it was a more stable species than the parent peak.

As was noted for the N-t-butyl-α-chloroacetamides the ratio of intensities for 58/[M-15] decreased; in the N-t-butylfluoroacetamides the ratio 58/[M-15] decreases for the same reason; that is, as fluorination increases the rearrangement process that gives the peak at m/e 58 has a much smaller chance of occurring.

There is no consistent change in the value of the ratio of daughter peak to parent peak to parent peak for 56/[M] and 41/57.

Table 23

Ratio of $\%\Sigma_{36}$ for daughter ions and parent ions for the N-t-butyl-α-fluoroacetamide mass spectra

Ratio of daughter peak to parent peak	N-t-B.A.	N-t-B.FA.	N-t-B.F_2A.	N-t-B.F_3A.
41/57	1.1	0.7	1.0	0.9
42/58	1.1	0.1	0.4	--
58/[M-15]	10.8	0.9	1.0	0.1
59/[M-15]	0.3	0.1	0.3	0.9
56/[M]	0.3	5.5	2.9	10.6
57/[M]	0.3	0.7	4.3	3.6
$\frac{R-\overset{\overset{O}{\|}}{C}-\overset{+}{N}H_3}{[M]}$	1.1	0.9	2.0	5.4

K) Ratio of $\%\Sigma_{36}$ for selected rearrangement peaks of the N-t-butyl-α fluoroacetamide mass spectra

The ratio of the peak intensities for 56/59, 58/59, and 58/$R-\overset{\overset{O}{\|}}{C}-\overset{+}{N}H_3$ all show a significant pattern; in each of 41/42, 56/58, and 59/$R-\overset{\overset{O}{\|}}{C}-\overset{+}{N}H_3$ (see Table 24) the effect of increasing fluorination is to increase the value of the ratio. The ratio value increases for 56/58 because the fragment peak at m/e 58 decreases sharply in intensity, as fluorination is increased. For 59/$R-\overset{\overset{O}{\|}}{C}-\overset{+}{N}H_3$, the value of the ratio increases because the process generating the ion fragment m/e 59 becomes more favorable.

Both of the ratios 58/59 and 58/$R-\overset{\overset{O}{\|}}{C}-\overset{+}{N}H_3$ show that as fluorination is decreasing through the series, the rearrangement peak at m/e 58 becomes less significant than the peak at m/e 59, and the analogous peak at $R-\overset{\overset{O}{\|}}{C}-\overset{+}{N}H_3$.

For the ratios 56/58, 58/59 and 59/$R-\overset{\overset{O}{\|}}{C}-\overset{+}{N}H_3$, the same trends were observed in the N-t-butyl-α-chloroacetamides. Only the ratio 42/56 shows no consistent effect upon the introduction of an increasing number of fluorine atoms into the prepared amides.

Table 24

Ratio of $\%\Sigma_{36}$ for selected rearrangement peaks in the N-t-butyl-α-fluoroacetamide mass spectra

Rearrangement peak ratios	N-t-B.A.	N-t-B.FA.	N-t-B.F_2A.	N-t-B.F_3A.
41/42	0.1	1.7	1.5	1.2
42/56	1.1	0.6	1.0	0.3
56/58	0.1	0.2	0.4	40.5
58/$R-\overset{\overset{O}{\|}}{C}-\overset{+}{N}H_3$	2.6	2.8	3.4	0.1
59/$R-\overset{\overset{O}{\|}}{C}-\overset{+}{N}H_3$	0.1	0.2	1.1	2.6

L) Ratio of $\%\Sigma_{36}$ for selected fragment ions of the N-t-butyl-α-fluoroacetamide mass spectra

An examination of Table 25 shows that the only ratio to give a consistent trend is for the case $57/[CH_xF_y\text{-}\overset{\overset{O}{\|}}{C}]$. This particular case demonstrates that the simple cleavage process that results in the formation of the peak at m/e 57 is a preferred process, compared to the process that would give the peak that would be observed at m/e $[CH_xF_y\text{-}\overset{\overset{O}{\|}}{C}]$.

The ratios 57/[M-15] and 57/100 show no definite trend. Not enough information is available to state whether or not a trend exists for the ratios $57/CH_xF_y$, $CH_xF_y/[M\text{-}15]$ and $CH_xF_y/100$.

Table 25

Ratio of $\%\Sigma_{36}$ for selected fragment ions of the N-t-α-fluoroacetamide mass spectra

Ratio of fragment ions	N-t-B.A.	N-T-B.FA.	N-t-B.F_2A.	N-t-B.F_3A.
$57/CH_xF_y$	--	--	2.0	1.4
57/[M-15]	1.1	0.3	0.6	0.2
$57/CH_xF_y-\overset{\overset{O}{\|\|}}{C}$	0.5	3.4	93.7	∞
CH_xF_y/[M-15]	--	--	0.3	0.2
CH_xF_y/100	--	--	23.3	5.7
57/100	--	21.6	47.0	7.7

M) Ratio of $\%\Sigma_{36}$ for fragment peaks to rearrangement peaks in the N-t-butyl-α-fluoroacetamide mass spectra

The ratio of the peak intensities for 57/58, 57/59, and [M-15]/R-$\overset{\overset{O}{\|}}{C}$-$\overset{+}{N}H_3$ (see Table 26) all show a consistent change with increasing fluorination. As in the mass spectra of the N-t-butyl-α-chloroacetamides, the ratio of 57/58 indicates that the more fluorinated the amide molecule becomes, the more abundant the peak at m/e 57 becomes with respect to the peak at m/e 58. The opposite trend becomes evident for the ratio 57/59, that is the peak at m/e 57 is more predominant than the rearrangement process giving the peak at m/e 59. This was not the case for the N-t-butyl-α-chloroacetamide series.

Ratios 57/56 and 57/R-$\overset{\overset{O}{\|}}{C}$-$\overset{+}{N}H_3$, which each contain a pair of ions that result from the same parent ion (the molecular ion), do not show the same definite trends that were noted for them in section I. Only the ratio [M-15]/CH_xF_y-$\overset{\overset{O}{\|}}{C}$-$\overset{+}{N}H_3$ shows a definite trend. This trend is as before, the cleavage fragment seems to be of greater importance than the rearrangement fragment.

Table 26

Ratio of $\%\Sigma_{36}$ for selected fragment peaks to rearrangement peaks in the N-t-butyl-α-fluoroacetamide mass spectra

Ratio of fragment peak to rearrangement peak	N-t-B.A.	N-t-B.FA.	N-t-B.F_2A.	N-t-B.F_3A.
57/56	1.1	1.3	1.5	0.3
57/58	0.1	0.3	0.6	13.5
57/59	4.4	4.3	1.9	0.3
57/$R-\overset{\overset{O}{\|\|}}{C}-\overset{+}{N}H_3$	0.3	0.8	2.1	0.7
$\frac{[M-15]}{CH_xF_y-\overset{\overset{O}{\|\|}}{C}-NH_3}^{+}$	0.2	2.8	3.4	3.0

Summary

In the preceding sections, fragmentation pathways common to a number of α-halo-N-tert-butyl acetamides have been described. Of particular interest in this work are those fragmentation processes which involve halogenated precursors; such processes may be (a) fragmentations of the molecular ion prior to rearrangement, (b) fragmentations of the rearranged molecular ion and (c) secondary fragmentations involving halogen containing species. The ease with which a particular fragmentation occurs will depend on the strength of the bond cleaved and on the stability of the product(s) formed. It is to be expected that both of these factors will be influenced by the presence of one or more α-halogen substituents in the precursor ion. We now consider six of the principal fragmentation processes in the compounds studied in an attempt to isolate and identify the role played by the substituent.

1. Fragmentations of the molecular ion prior to rearrangement:-

Two competitive dissociations of the molecular ion are observed in all of the compounds studied:

$$M^{+\cdot} \rightarrow {}^{+}C(CH_3) + R\text{-}\overset{O}{\overset{\|}{C}}\text{-}\dot{N}H \qquad [A]$$

$$M^{+\cdot} \rightarrow (M\text{-}15)^{+} + CH_3^{\cdot} \qquad [B]$$

Although the carbon-nitrogen bond is somewhat weaker than the carbon-carbon bond (on the basis of average bond energy values), these two dissociations are of approximately equal importance in the unsubstituted (R = CH_3) amide (Table 27). In the α-chloro series, the importance of [A] increases

significantly with increasing halogen substitution. Thus, the intensity ratio for (M/e57)/(M-15) increases in a regular fashion from approximately unity when R = CH_3 to a value of 8.5 for R = CCl_3; for the di- and trichloro compounds the peak at M/e 57 is the base peak. This trend is consistent with a weakening of the carbon-nitrogen bond as a result of the long range inductive effect of the chlorine atoms. The intensity of the (M-15) peak (expressed as $\%\Sigma_{36}$) remains essentially constant throughout this series; it is reasonable to expect that the inductive effect of the acyl chlorines on the carbon-carbon bond of the tert-butyl group will be considerably less than the effect on the carbon-nitrogen bond..

The effect of fluorine substitution on the two dissociations under consideration is somewhat surprising. Methyl radical loss from the molecular ion (process [B]) increases significantly in relative importance in going from the unsubstituted to the mono-substituted amide. Subsequent fluorine substitution, however, has only a minor influence on this dissociation. Thus the intensity of the (M-15) peak rises from 3.4 in the unsubstituted amide to 18.1 in the mono-fluoro compound; for the tri-fluoro amide the value is only 23.2. The increase in methyl radical elimination that results from mono-substitution is consistent with the inductive effect discussed previously; because of the greater electronegativity of fluorine one might expect the electron withdrawing influence to be felt farther from the site of substitution than would be the case for chlorine substitution. On this basis, a regular increase in methyl radical loss with increasing fluorine substitution might be expected; as indicated above such an increase was not observed.

A similar situation exists with regard to the intensity of the peak at M/e 57. By analogy with the α-chloro series a regular and significant increase in the intensity of this peak with increasing fluorine substitution

would be expected. The observed increase in the intensity, a factor of 2 - 3, is markedly less than the ten-fold increase observed in the α-chloro series, in spite of the considerable difference in electronegativity between fluorine and chlorine.

These results suggest that the inductive effect of the α-fluorine atoms is not felt solely at the carbon-nitrogen or carbon-carbon bond. With increasing electronegativity of the α-substituent rearrangement of the molecular ion prior to fragmentation becomes an effective competitive fate for the molecular ion.

2. Fragmentations of the molecular ion after rearrangement:-

Rearrangement of the molecular ion prior to cleavage is involved in the formation of the ions at M/e 56 and M/e (R+45) :-

$$M^{\ddagger} \quad R\text{-}\overset{O}{\overset{\|}{C}}\text{-}NH_3^{+} \quad + \quad CH_3\text{-}\overset{CH_2^{\cdot}}{\overset{|}{C}}\text{=}CH_2 \qquad [C]$$

$$M^{\ddagger} \quad R\text{-}\overset{O}{\overset{\|}{C}}\text{-}NH_2^{+} \quad + \quad (CH_3)_2C\text{=}CH_2 \qquad [D]$$

M/e 56

It is somewhat surprising that in the unsubstituted amide process [C], which involves transfer of two hydrogen atoms from the tert-butyl group, is favoured over the single atom transfer process, [D]. Presumably in this case the driving force is the greater stability of the products formed via [C].

In the α-chloro series there is a marked decrease in the intensity of the ion at M/e (R+45) with increasing halogen substitution, reflecting the preference for nitrogen-carbon bond cleavage as the fate for the molecular ion. The intensity of the peak at M/e 56 remains essentially constant throughout this series. The intensity of the peak at M/e (R+45) also de-

crease with increasing substitution in the α-fluoro series; however, there is only a 40% decrease in peak intensity in going from R = CH_3 to R = CF_3 compared to the 90% decrease observed in the chlorine compounds. Fluorine substitution results in a significant increase in the peak intensity at M/e 56, with the $\%\Sigma_{36}$ for this peak rising from a value of 3.6 in the unsubstituted amide to a value of 15.4 when R is CF_3. It should be noted that the major increase is observed on going from the di- to the tri-substituted members of the series.

These results are consistent with the greater electronegativity of fluorine as compared to that of chlorine, and with the strong electron withdrawing influence of α-halogen substituents. In the α-chloro compounds this influence is reflected in easier bond breaking, particularly at the nitrogen-carbon bond. In the α-fluoro series the nitrogen atom becomes progressively more and more "electron poor" with increasing substitution, thus favouring hydrogen atom transfer to the nitrogen.

3. Secondary fragmentations of halogen-containing species:-

The ion formed by methyl radical loss from the molecular ion undergoes a number of further fragmentations, usually accompanied by some rearrangement. We consider two of these secondary fragmentations here :

$$(M\text{-}15)^+ \rightarrow \underset{\text{M/e 59}}{HO\text{-}C^+(CH_3)_2} + R\text{-}C{\equiv}N \qquad [E]$$

$$(M\text{-}15)^+ \rightarrow H_2N{=}C^+(CH_3)_2 + CH_2{=}C{=}O \quad (R = CH_3)$$
$$(CHR'\text{-}C{=}O;\ R' = R - H) \qquad [F]$$

In both series of compounds, the intensity of the peak at M/e 58 decreases

with increasing α-substitution. This appears to be mainly a statistical effect, the number of hydrogen atoms available for transfer decreasing with increasing α-substitution. In the unsubstituted amide the peak at M/2 58 is approximately 18 times as intense as the peak at M/e 59; this presumably reflects both the greater stability of the product in [F] and the preference for a simple hydrogen atom transfer as opposed to the more complicated, group transfer required by pathway [E].

The intensity of the peak at M/e 59 remains essentially constant throughout the α-chloro series, but increases significantly in the fluorine substituted compounds. It should be noted that the largest increase is observed in going from the di-to the tri-fluoro compound; in the latter case the peak at M/e 59 has a $\%\Sigma_{36}$ of 20.2 and is the second most intense peak in the spectrum. A possible explanation of the observed results is indicated in the following scheme:

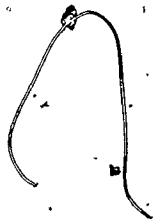

$$R\text{-}\overset{O}{\overset{\|}{C}}\text{-}\underset{H}{N}\text{-}C(CH_3)_2^{+} \rightarrow R\text{-}\overset{OH}{\overset{|}{C}}{=}N\text{-}C(CH_3)_2^{+} \rightarrow HO\text{-}C(CH_3)_2^{+} + R\text{-}C{\equiv}N$$

When R = CF_3 the α-carbon is "electron poor", and there will be a strong tendency for loss of an electron withdrawing substituent.

From the preceding it is clear that the difference observed between the α-chloro and the α-fluoro compounds is largely one of degree. In both cases the observed trends can be explained in terms of the electron withdrawing tendency of the α-halogen substituent. In the case of α-chlorine substitution, this inductive effect is reflected in the ease with which the nitrogen-carbon bond is cleaved. For the α-fluoro series, the greater electronegativity of the fluorine atoms leads to "electron poor" sites in

the molecular ion and/or in other precursor ions, with a resulting trend towards rearrangement processes rather than simple cleavages.

Suggestions for future work

Future investigation of similar compounds could be accomplished at a faster rate if speedier methods for identification of the fragment ions were available. This would be accomplished with the aid of a computer.

A surer stance could be taken on the proposing of a fragmentation pattern for certain molecules with much greater use of the metastable defocussing technique. Frequent use of this technique would be essential to future study of these same compounds.

The results of mass spectral fragmentation of the N-t-butyl-α-chloroacetamides and the N-t-butyl-α-fluoroacetamides could be compared to fragmentation products of the pyrolysis of these same compounds.

List of References

1. J.A. Gilpin, Anal. Chem., 31, 935 (1959).
2. Ng. Dinh Nguyen, R. Ryhage, S. Stallberg-Stenhagen and E. Stenhagen, Arkiv. Kemi., 18, 393 (1961).
3. R.S. Gohlke and F.W. McLafferty, Anal. Chem., 34, 1281 (1962).
4. F.W. McLafferty ibid. 29, 1782 (1957).
5. Z. Pelah, M.A. Kielczewski, J.M. Wilson, M. Ohashi, H. Budzikiewicz and C. Djerassi, J. Am. Chem. Soc., 85, 2470 (1963).
6. M.J. Saxby, Chem. & Ind. (London), 1316 (1968).
7. M.J. Saxby, Org. Mass Spectrom., 2, 33 (1969).
8. A. Prox and J. Schmid, Org. Mass Spectrom. 2, 105 (1969).
9. A. Prox and J. Schmid, Org. Mass Spectrom. 2, 121 (1969).
10. A. Zeman and I.P.G Wirotama, J. Anal. Chem., 247, 158 (1969).
11. K. Bieman, Mass Spectrometry Organic Chemical Applications, McGraw Hill, New York, 1962, p. 47.
12. H.M. Rosenstock, M.B. Wallenstein, A.L. Wahrhaftig, and H. Erying, Proc. Natl. Acad. Sci. U.S. 38, 667 (1952).
13. A.M. Struck and H.W. Major, Jr., "Enhanced Metastable Ion Measurement by Defocussed Operation of Double Focussing Mass Spectrometers", 17th Annual Meeting, ASTM Committee E-14 on Mass Spectrometry, Dallas, Texas, May 18-23, 1969.
14. J.M. Momigny, Bull. Soc. Roy. Sci. Liege 24, 111 (1955).
15. A.J. Speziale, P.C. Hamm, J. Am. Chem. Soc. 78, 2556 (1956).
16. A.C. Cope, M.A. LoBol, H.H. Lee, W.R. Moore, J. Am. Chem. Soc. 79, 4720 (1957).
17. F. Cramer, N. Hennrich, Chem. Ber., 94, 976 (1961).
18. E. Sawicki, J. Org. Chem., 376 (1956).

Appendix

Figures 1 to 7 show the $\%\Sigma_{36}$ for all peaks that occurred in each spectrum, if the peak was above the $0.8\%\Sigma_{36}$ level.

Tables 26 to 39 contain nominal m/e values, $\%\Sigma_{36}$ and % base peak. The values of $\%\Sigma_{36}$ were calculated by adding up the peak heights from the peak at m/e 36 to the parent peak; then the peak height at a particular value of m/e was calculated by putting the peak height over the total peak height and multiplying by 100%. The % base peak was found by putting the height of a particular peak over the height of the tallest peak in the spectrum, and then multiplying by 100%.

For purposes of spectra comparison only the values of $\%\Sigma_{36}$ can be used to compare spectra of different compounds, since different compounds may not have the same base peak.

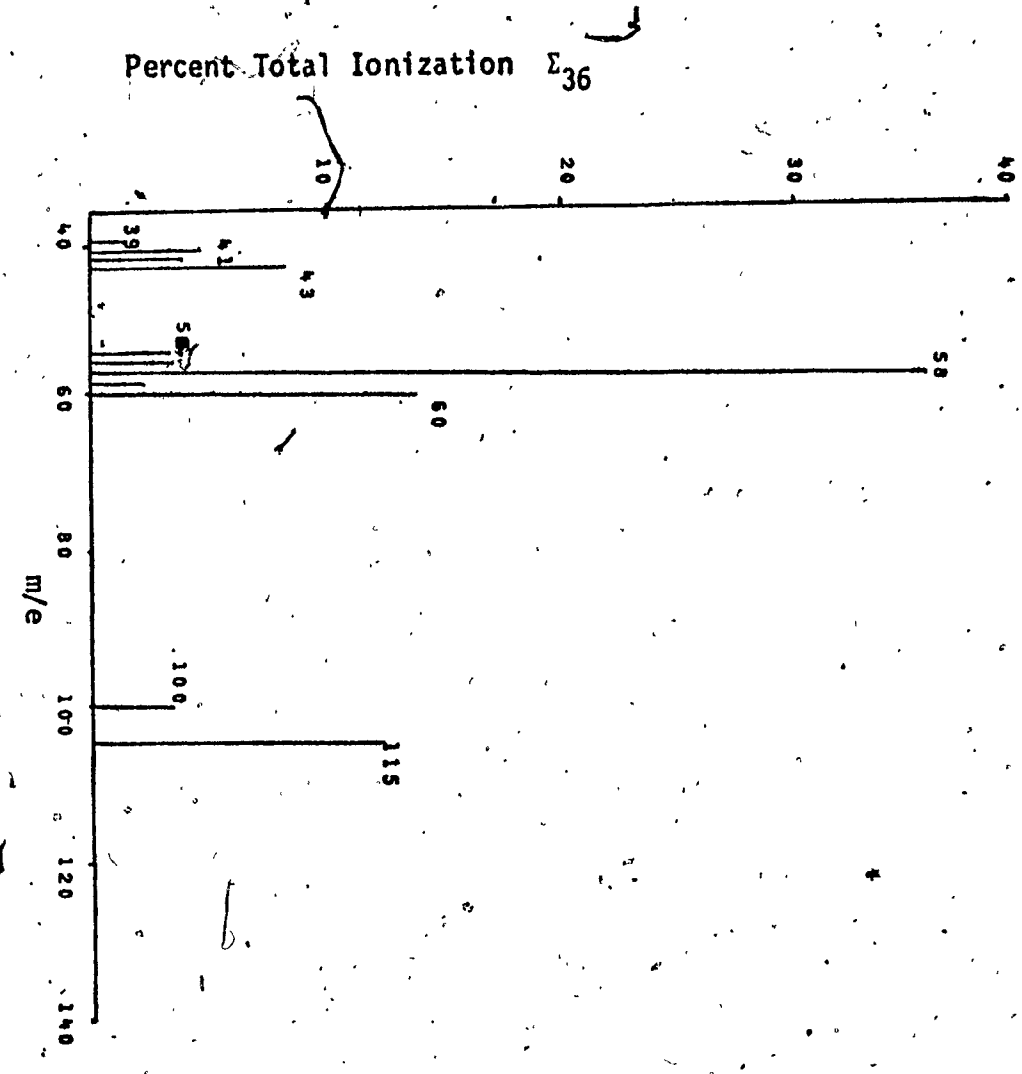

Figure 1

N-t-butylacetamide

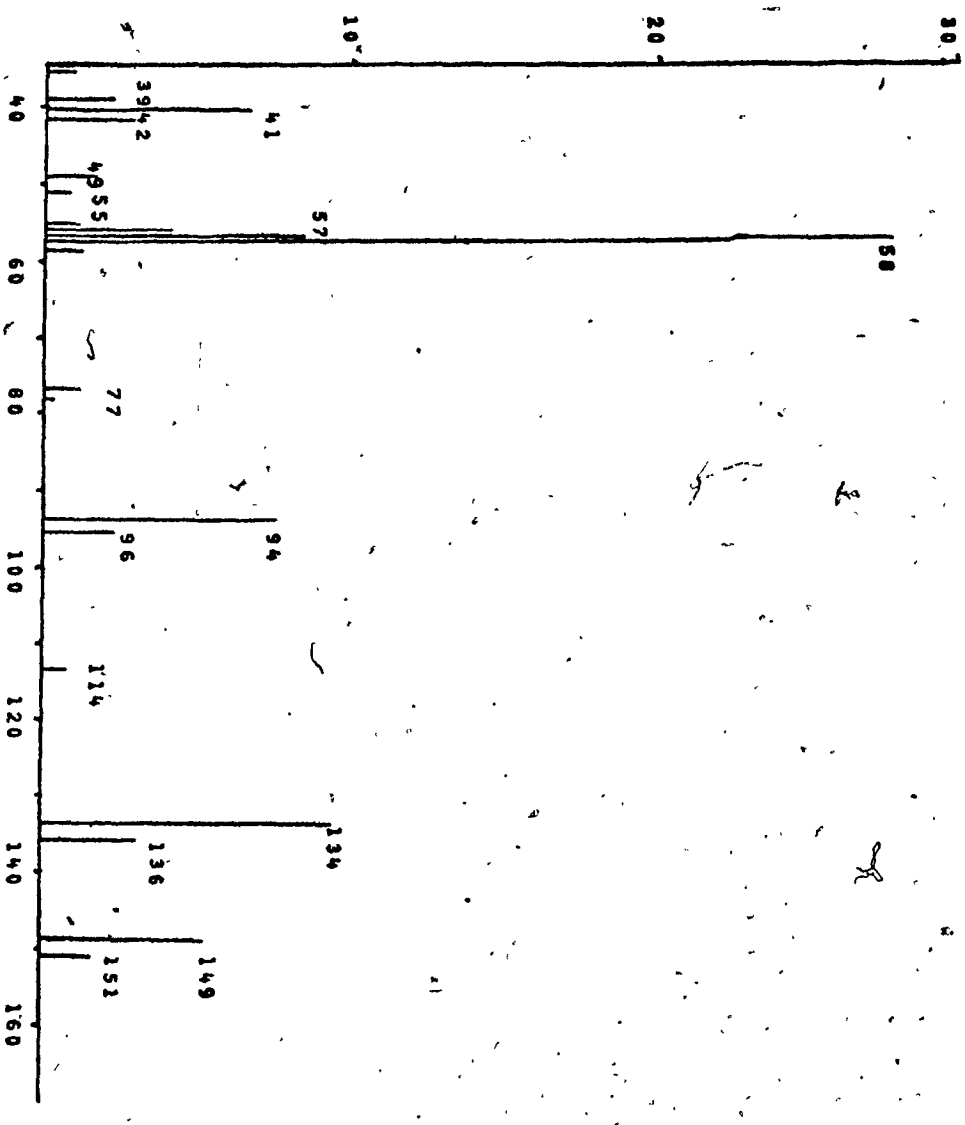

Figure 2

N-t-butyl-α-chloroacetamide

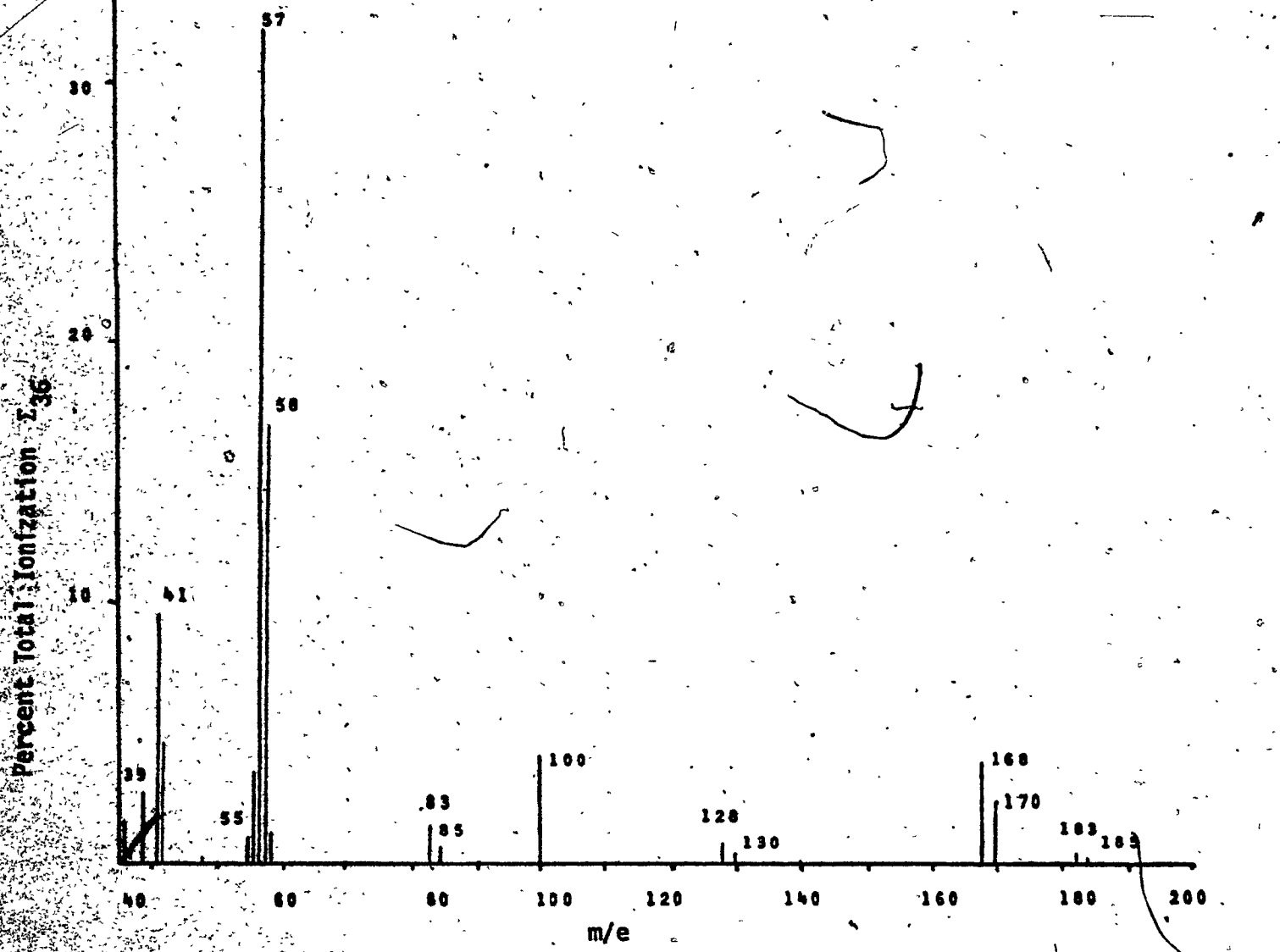

Figure 3
N-t-butyl-α,α-dichloroacetamide

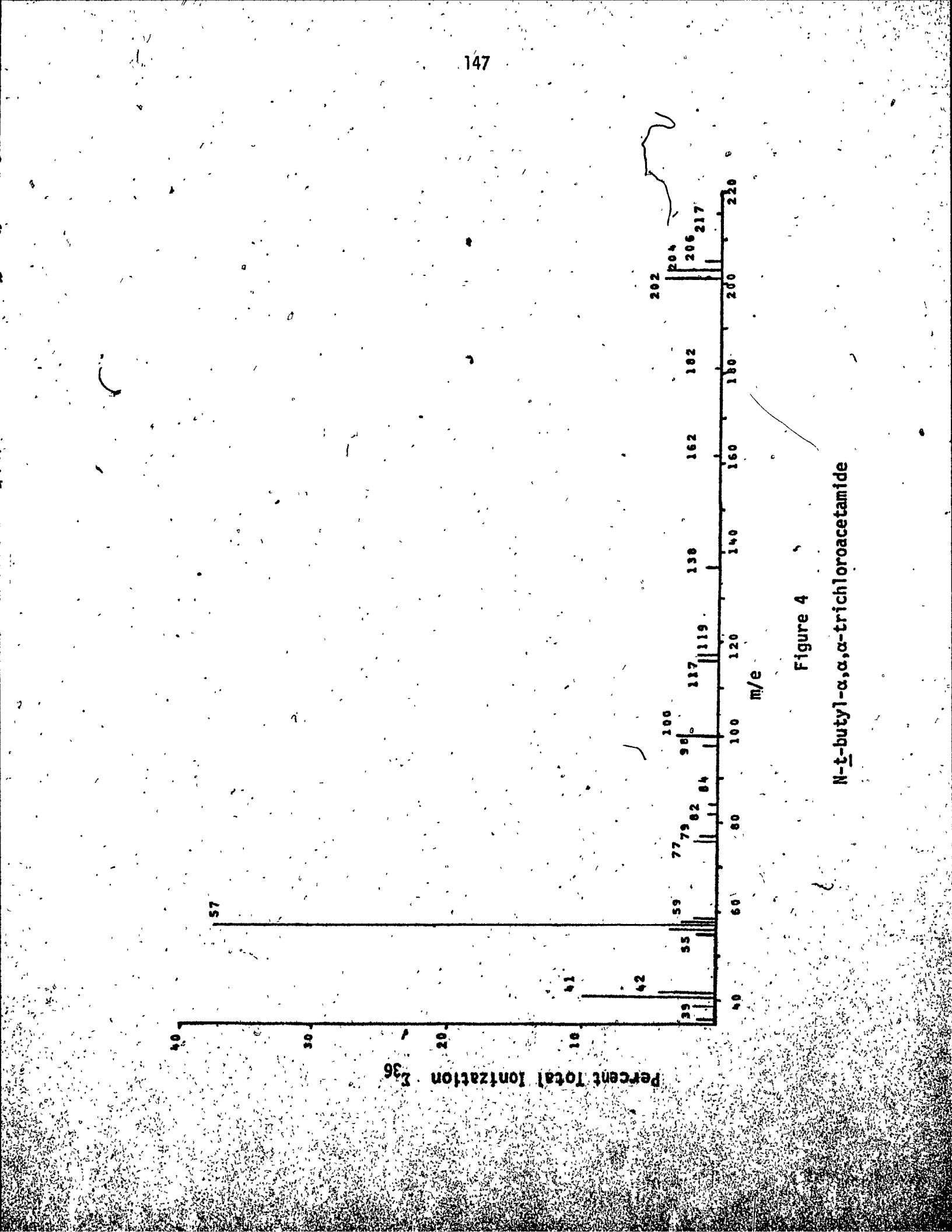

Figure 4

N-t-butyl-α,α,α-trichloroacetamide

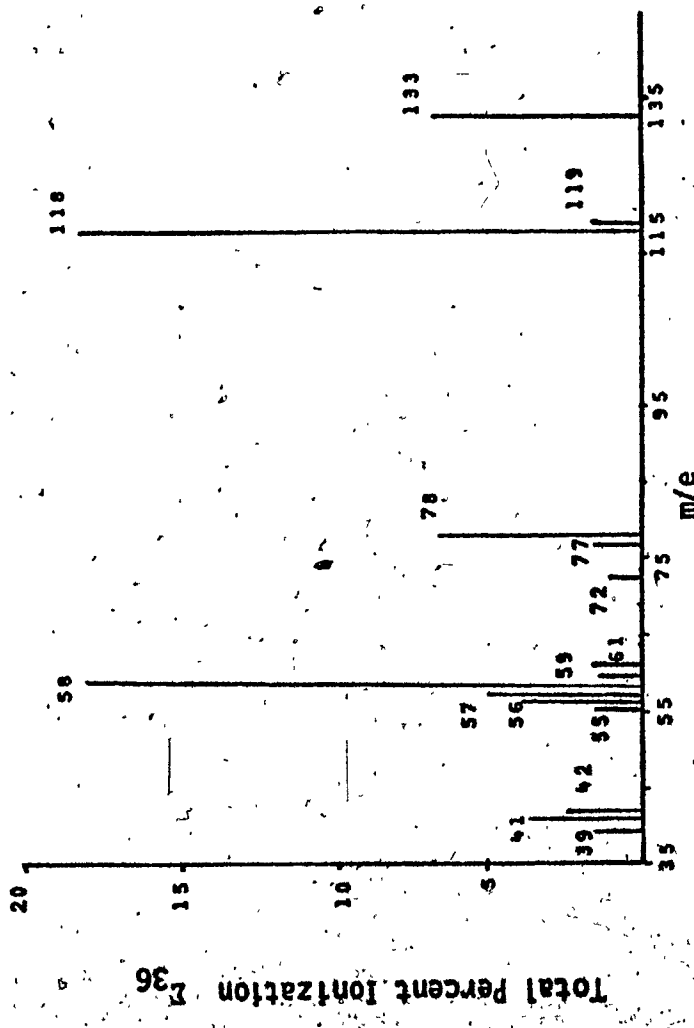

Figure 5

N-t-butyl-α-fluoroacetamide

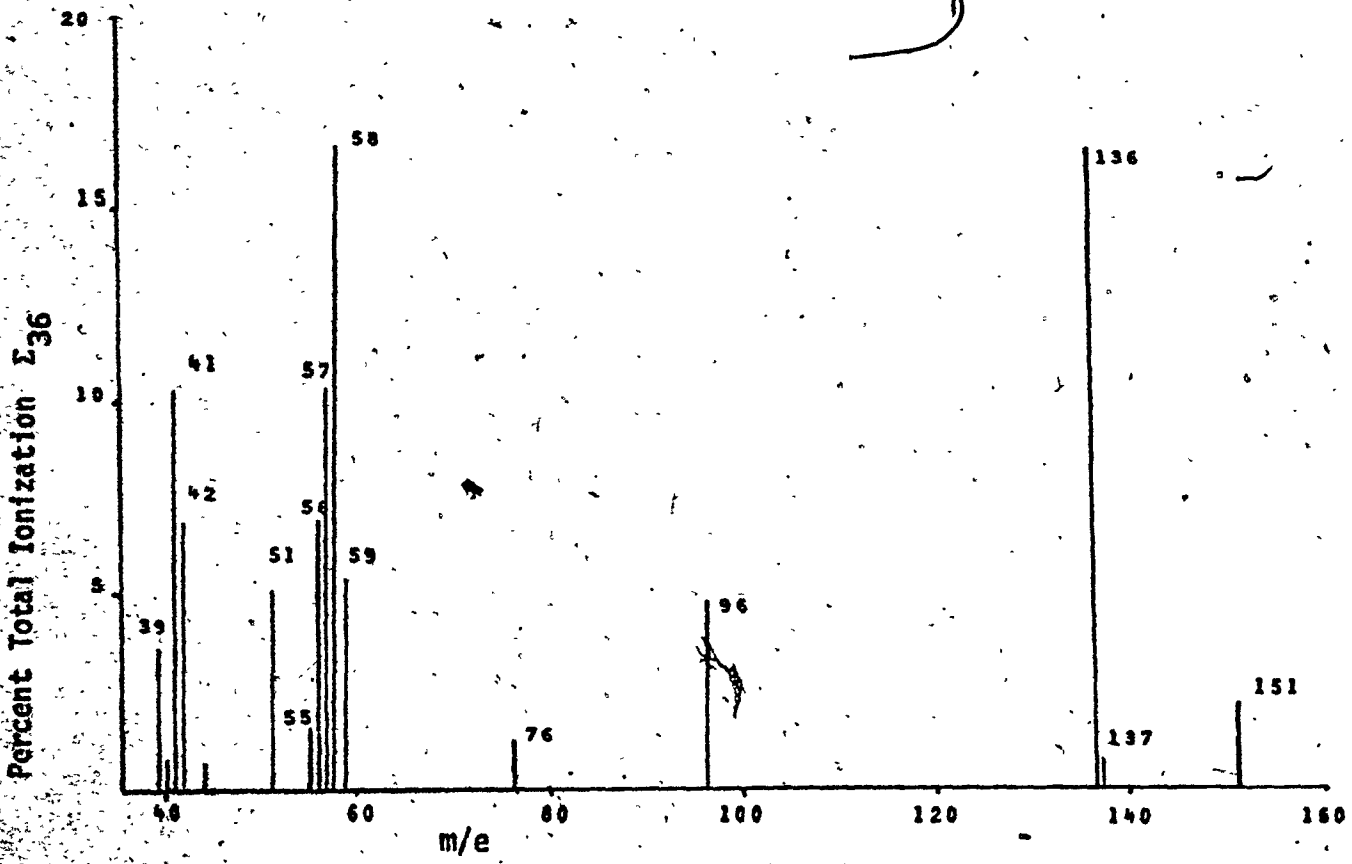

Figure 6

N-t-butyl-α,α-difluoroacetamide

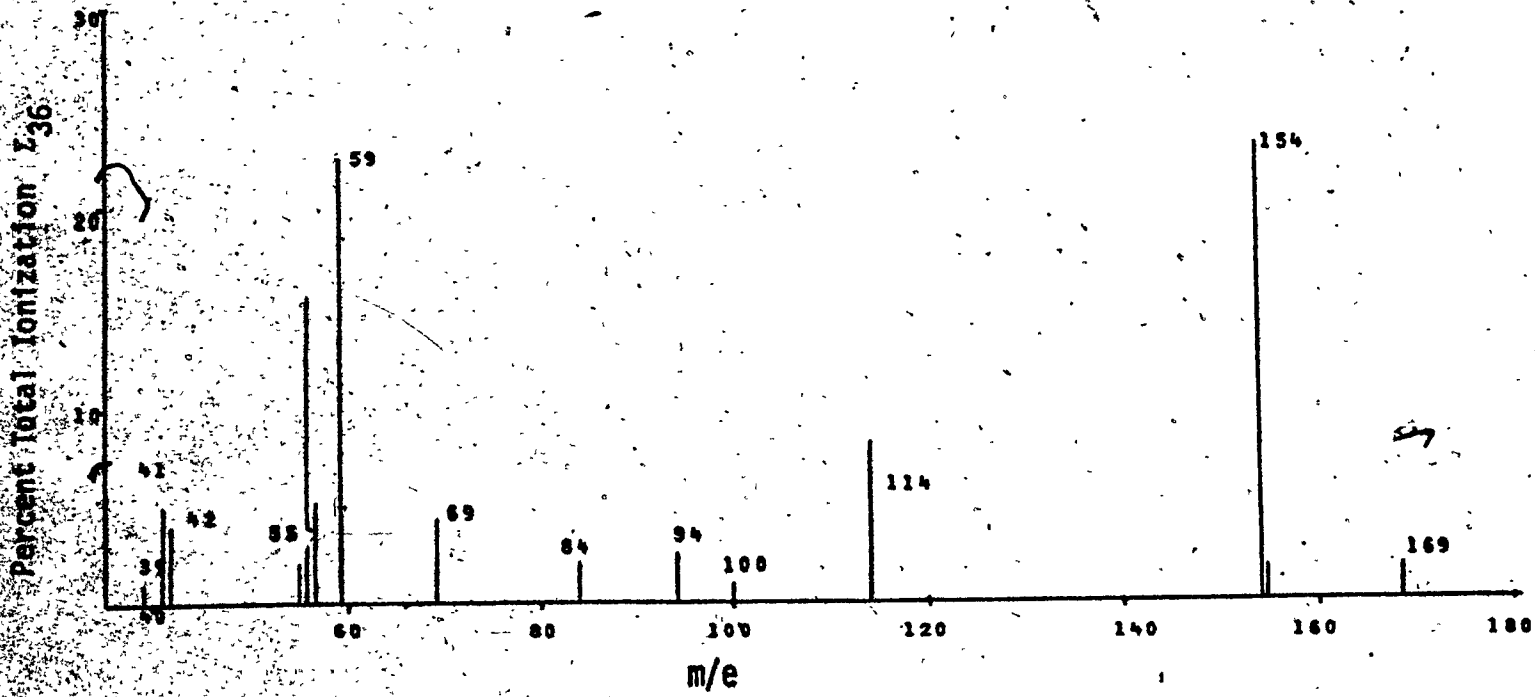

Figure 7

N-t-butyl-α,α,α-trifluoroacetamide

Table 27

N-t-butylacetamide

m/e	$\%\Sigma_{36}$	% base peak
37	0.1	0.3
38	0.2	0.5
39	1.4	3.9
40	0.5	1.5
41	4.1	11.4
42	3.9	10.7
43	8.2	22.6
44	0.5	1.3
50	0.5	1.3
55	1.0	2.7
56	3.7	10.1
57	3.8	10.5
58	36.1	100.0
59	2.1	5.7
60	13.8	38.3
72	0.9	2.5
84	0.1	0.3
100	3.4	9.4
115	12.7	35.3

Table 28

N-t-butyl-α-chloroacetamide

m/e	$\%\Sigma_{36}$	% base peak
36	0.8	3.0
37	0.1	0.5
38	0.2	0.7
39	2.1	7.5
40	0.6	2.1
41	6.8	24.2
42	3.2	11.4
43	0.5	1.6
44	0.4	1.4
47	0.1	0.5
48	0.1	0.5
49	1.8	6.3
51	0.8	2.8
52	0.1	0.5
53	0.2	0.7
54	0.4	1.4
55	1.3	4.4
56	4.4	15.6
57	8.7	31.0
58	28.2	100.0
59	1.3	4.7
68	0.1	0.5
69	0.1	0.5
70	0.1	0.5
71	0.4	1.4
72	0.7	2.3
76	0.3	0.9
77	1.1	4.0
79	0.5	1.6
84	0.5	1.6
94	7.9	28.2
95	0.3	0.9
96	2.5	8.8
97	0.1	0.5
98	0.1	0.5
100	0.4	1.4
114	0.9	3.3
115	0.1	0.2
134	9.7	34.5
135	0.6	2.3
136	3.3	11.7
137	0.3	0.9
149	5.3	18.7

Table 29

N-t-butyl-α,α-dichloroacetamide

m/e	$\%\Sigma_{36}$	% base peak
36	0.9	5.8
37	0.1	0.4
38	0.6	1.9
39	2.7	8.4
40	0.7	2.0
41	9.7	30.1
42	4.8	14.8
43	0.4	1.3
44	0.3	1.0
47	0.2	0.6
48	0.7	2.4
49	0.2	0.6
50	0.2	0.6
51	0.2	0.6
52	0.1	0.4
53	0.2	0.6
54	0.3	0.9
55	1.2	3.6
56	3.7	11.4
57	32.2	100.0
58	17.0	52.9
59	1.3	4.1
64	0.7	2.1
66	0.2	0.6
70	0.2	0.6
72	0.4	1.3
76	0.5	1.7
83	1.7	5.4
84	0.3	1.1
85	0.8	2.4
87	0.2	0.6
92	0.3	0.9
93	0.1	0.4
94	0.1	0.3
98	0.3	0.9
100	4.2	13.0
101	0.3	0.9
104	0.1	0.4
127	0.1	0.4
128	0.9	2.8
129	0.1	0.4
130	0.6	1.8
132	0.1	0.4

m/e	$\%\Sigma_{36}$	% base peak
133	0.1	0.4
148	0.1	0.4
149	0.1	0.4
168	4.1	12.7
169	0.2	0.6
170	2.6	8.1
171	0.1	0.4
172	0.4	1.3
173	0.1	0.4
183	0.5	1.5

Table 30

N-t-butyl-α,α,α-trichloroacetamide

m/e	% Σ_{36}	% base peak
36	1.4	3.6
37	0.1	0.3
38	0.5	1.2
39	1.6	4.4
40	0.5	1.2
41	1.0	26.4
42	4.2	11.1
43	0.3	0.7
44	0.2	0.6
47	0.5	0.3
48	0.1	0.4
49	0.2	0.6
50	0.1	0.3
51	0.1	0.3
52	0.2	0.6
53	0.3	0.7
54	0.3	0.7
55	1.3	3.4
56	3.7	9.7
57	37.7	100.0
58	2.6	7.0
59	1.8	4.8
60	1.1	0.2
61	0.2	0.6
62	0.2	0.6
63	0.2	0.6
64	0.1	0.3
65	0.1	0.3
77	0.7	1.9
79	0.2	0.6
82	0.9	2.4
83	0.5	1.4
84	0.9	2.4
85	0.4	1.0
86	0.1	0.3
92	0.1	0.3
96	0.1	0.3
98	1.0	2.7
100	3.0	8.0
101	0.6	1.7
102	0.1	0.3
104	0.1	0.3
110	0.5	1.4

m/e	% Σ_{36}	% base peak
112	0.4	1.0
117	1.4	3.7
119	1.4	3.6
121	0.5	1.2
126	0.4	1.0
127	0.2	0.5
128	0.3	0.7
129	0.1	0.3
130	0.1	0.3
132	0.4	1.0
134	0.1	0.3
138	1.0	2.7
140	0.6	1.1
154	0.2	0.6
156	0.1	0.3
162	0.7	1.9
164	0.6	1.1
166	0.3	0.7
167	0.2	0.5
168	0.1	0.3
169	0.1	0.3
182	0.4	1.0
184	0.2	0.6
202	4.4	11.6
203	0.3	0.7
204	4.1	10.9
205	0.3	0.7
206	1.3	3.4
207	0.1	0.3
208	0.2	0.6
217	0.2	0.6
219	0.2	0.6

Table 31

N-t-butyl-d_9-acetamide

m/e	% Σ_{36}	% base peak
39	0.3	0.7
40	0.5	1.5
41	0.5	1.5
42	0.5	1.5
43	6.3	18.5
44	0.5	1.5
45	3.5	9.5
46	4.6	12.6
47	0.3	0.7
53	0.3	0.7
54	0.3	0.7
55	0.3	0.7
56	0.5	1.5
57	0.5	1.5
58	0.8	2.2
59	0.3	0.7
60	0.5	1.5
61	0.3	0.7
62	9.7	26.7
63	5.7	15.5
64	36.4	100.0
65	2.4	6.7
66	3.5	9.6
67	0.5	1.5
68	0.3	0.7
72	0.3	0.7
74	0.3	0.7
76	0.3	0.7
77	0.3	0.7
82	1.1	3.0
85	0.8	2.2
104	0.3	0.7
105	0.5	1.5
106	4.3	11.8
122	0.3	0.7
123	1.6	4.4
124	10.2	28.2

Table 32

N-t-butyl-d_9-α-chloroacetamide

m/e	% Σ_{36}	% base peak
36	0.2	0.8
38	0.1	0.5
39	0.1	0.5
40	0.1	0.5
41	0.3	1.0
42	1.7	6.8
43	0.6	2.6
44	0.6	2.6
45	2.8	11.6
46	2.8	11.6
47	0.1	0.5
48	0.1	0.5
49	1.0	4.2
50	0.3	1.0
51	0.3	1.0
56	0.1	0.5
57	0.3	1.0
58	0.9	3.7
59	1.3	5.3
60	0.1	0.5
61	0.3	1.0
62	1.4	5.8
63	4.5	18.4
64	24.6	100.0
65	3.5	14.2
66	8.6	35.0
67	0.8	3.2
72	0.2	0.8
76	0.1	0.5
77	0.9	3.7
78	0.1	0.5
79	0.3	1.0
80	0.4	1.6
81	0.4	1.6
90	0.4	1.6
94	0.1	0.5
95	0.3	1.0
96	6.2	25.3
97	0.3	1.0
98	1.8	7.4
108	0.1	0.5
109	0.6	2.6
110	0.1	0.5

m/e	% Σ_{36}	% base peak
118	0.3	1.0
122	0.1	0.5
123	1.3	5.3
124	0.1	0.5
138	0.1	0.5
139	1.8	7.4
140	10.9	44.2
141	1.2	4.7
142	3.7	15.3
143	0.3	1.0
157	1.2	4.7
158	5.9	24.2

Table 33

N-t-butyl-d_9-α,α-dichloroacetamide

m/e	% Σ_{36}	% base peak
36	0.8	2.9
37	0.2	0.6
38	0.3	1.1
39	0.1	0.3
40	0.2	0.6
41	0.2	0.9
42	1.6	5.8
43	0.4	1.5
44	0.6	2.0
45	3.7	13.0
46	6.2	21.9
47	0.4	1.5
48	1.9	6.7
49	1.2	4.1
50	0.7	2.6
51	0.4	1.5
52	0.2	0.9
57	0.2	0.9
58	0.2	0.9
60	0.1	0.5
61	0.2	0.9
62	0.9	3.2
63	1.9	6.7
64	12.5	44.0
65	5.7	20.3
66	28.4	100.0
67	1.3	4.7
76	0.5	1.7
78	0.2	0.6
79	0.3	1.1
80	0.2	0.6
81	0.2	0.6
82	0.1	0.5
83	1.6	5.5
84	1.2	4.1
85	1.2	4.1
86	0.7	2.6
87	0.3	1.2
88	0.1	0.5
90	0.4	1.3
93	0.2	0.6
95	0.2	0.6
104	0.2	0.6
107	0.2	0.6
108	1.2	4.4
109	6.4	22.4

m/e	% Σ_{36}	% base peak
110	0.4	1.5
128	0.1	0.5
129	0.1	0.5
130	1.0	3.5
131	0.1	0.5
132	0.6	2.2
134	0.1	0.6
139	0.1	0.5
157	0.1	0.5
173	0.7	2.3
174	4.6	16.3
175	8.7	2.3
176	3.0	10.5
177	0.2	0.9
178	0.5	1.7
191	0.2	0.9
192	0.8	2.9

Table 34

N-t-butyl-d_9-α,α,α-trichloroacetamide

m/e	% Σ_{36}	% base peak
36	2.1	6.4
37	0.4	1.2
38	0.7	2.0
40	0.1	0.5
41	0.2	0.6
42	2.2	6.7
43	0.6	1.7
44	1.0	3.2
45	6.8	20.7
46	8.7	26.5
47	1.1	3.5
48	0.2	0.5
49	0.4	1.2
50	0.1	0.5
54	0.1	0.5
57	0.2	0.6
58	0.2	0.6
60	0.1	0.3
61	0.3	0.9
62	1.1	3.5
63	0.8	2.3
64	2.2	6.7
65	7.2	21.9
66	33.0	100.0
67	1.7	5.2
82	2.3	7.0
83	0.5	1.5
84	1.9	5.8
85	0.3	0.9
86	0.2	0.6
89	0.1	0.5
90	0.5	1.5
99	1.1	3.5
100	0.2	0.6
101	0.8	2.3
102	0.1	0.3
107	0.1	0.5
108	0.7	2.0
109	3.0	9.0
110	1.0	2.9

m/e	% Σ_{36}	% base peak
112	0.6	1.7
114	0.1	0.5
117	1.7	5.0
121	0.5	1.5
127	0.4	1.2
129	0.4	1.2
131	0.1	0.5
138	0.4	1.2
140	0.2	0.6
143	0.2	0.6
144	1.1	3.5
145	0.1	0.5
146	0.9	2.6
164	0.2	0.6
165	0.1	0.3
166	0.1	0.3
167	0.1	0.3
173	0.4	1.2
175	0.2	0.6
191	0.4	1.2
193	0.2	0.6
207	0.2	0.6
208	1.9	5.8
209	0.3	0.9
210	1.8	5.5
211	0.1	0.3
212	0.7	2.0

Table 35

N-t-butyl-α-fluoroacetamide

m/e	% Σ_{36}	% base peak
36	0.2	1.3
37	0.5	2.6
38	0.2	1.3
39	1.5	8.2
40	0.5	2.6
41	3.7	20.5
42	2.2	12.2
43	0.6	3.2
44	0.7	3.8
50	0.3	1.9
51	0.6	3.2
52	0.2	1.3
53	0.2	1.3
54	0.3	1.9
55	1.4	7.7
56	3.8	21.2
57	5.0	27.6
58	18.0	99.3
59	1.2	6.4
60	0.3	1.9
61	1.4	8.0
62	0.1	0.5
63	0.2	1.3
64	0.2	1.3
65	0.5	2.6
66	0.2	1.3
67	0.3	1.9
68	0.2	1.3
69	0.5	2.6
70	0.5	2.6
71	0.5	2.6
72	1.0	5.8
73	0.1	0.6
74	0.2	1.3
75	0.2	1.3
76	0.5	2.6
77	1.4	7.7
78	6.5	35.9
79	0.5	2.6
80	0.1	0.6
81	0.5	2.6
82	0.2	1.3
83	0.6	3.2

m/e	% Σ_{36}	% base peak
84	0.6	3.2
85	0.2	1.3
86	0.1	0.6
87	0.1	0.6
88	0.1	0.6
89	0.2	1.3
90	0.2	1.3
91	0.6	3.2
92	0.3	1.9
93	0.5	2.6
94	0.8	4.5
95	0.5	2.6
96	0.2	1.3
97	0.2	1.3
98	0.1	0.6
99	0.1	0.6
100	0.2	1.3
102	0.2	1.3
103	0.2	1.3
104	0.7	3.8
105	0.7	3.8
106	0.2	1.3
107	0.2	1.3
108	0.2	1.3
109	0.3	1.9
110	0.3	1.9
111	0.2	1.3
112	0.2	1.3
113	0.1	0.6
114	0.1	0.6
115	0.9	5.1
116	0.3	1.9
117	0.5	2.5
118	18.1	100.0
119	1.4	7.7
120	0.2	1.3
121	0.2	1.3
122	0.2	1.3
123	0.2	1.3
124	0.2	1.3
125	0.2	1.3
126	0.2	1.3
127	0.3	1.9
128	0.6	3.2
129	0.8	4.5
130	0.2	1.3
131	0.3	1.9
123	0.3	1.9
133	7.0	38.5

Table 36

N-t-butyl-α,α-difluoroacetamide

m/e	% Σ_{36}	% base peak
36	----	----
37	0.1	0.5
38	0.2	1.3
39	3.6	21.4
40	0.8	4.8
41	10.3	62.1
42	6.8	41.1
43	0.4	2.4
44	0.6	3.9
45	0.1	0.5
46	0.1	0.5
48	0.5	3.0
49	0.1	0.5
50	0.2	1.3
51	5.1	30.7
52	0.2	1.1
53	0.3	1.7
54	0.3	1.7
55	1.4	8.7
56	6.9	41.6
57	10.3	61.9
58	16.6	100.0
59	5.5	33.3
60	0.2	1.3
61	0.1	0.9
69	0.1	0.4
70	0.1	0.6
72	0.4	2.2
75	0.1	0.5
76	1.3	8.0
77	0.1	0.5
78	0.1	0.5
79	0.1	0.5
84	0.4	2.6
88	0.2	1.3
89	0.1	0.5
92	0.1	0.4
95	0.1	0.9
96	4.9	29.2
97	0.1	0.5
100	0.2	1.3

m/e	% Σ_{36}	% base peak
135	0.1	0.5
136	16.6	99.6
137	1.0	6.1
138	0.1	0.5
151	2.4	14.3
152	0.3	1.9

Table 37

N-t-butyl-α,α,α-trifluoroacetamide

m/e	% Σ_{36}	% base peak
36	---	---
39	0.9	3.7
40	0.4	1.7
41	4.7	20.4
42	4.0	17.1
43	0.2	1.0
44	0.5	2.1
50	0.1	0.5
51	0.6	2.7
53	0.2	1.0
54	0.3	1.2
55	1.3	5.6
56	15.4	66.2
57	5.3	22.7
58	0.4	1.7
59	20.2	87.1
60	0.8	3.3
61	0.2	0.8
69	3.9	16.7
84	1.7	7.5
85	0.2	0.8
94	2.3	10.0
96	0.4	1.7
98	0.1	0.5
100	0.7	2.9
106	0.2	0.8
110	0.4	1.7
114	7.8	33.7
115	0.2	1.0
154	23.2	100.0
155	1.5	6.5
156	0.2	0.8
169	1.4	6.3

Table 38

N-t-butyl-d_9-α,α-difluoroacetamide

m/e	% Σ_{36}	% base peak
36	0.1	0.8
38	0.2	1.5
39	0.2	1.5
40	0.4	3.8
41	1.1	9.2
42	2.4	21.1
43	1.5	13.1
44	3.2	27.7
45	6.0	51.5
46	5.1	43.8
47	0.3	2.3
48	0.4	3.8
49	0.2	1.9
50	0.2	1.9
51	3.6	31.5
52	0.2	1.5
54	0.1	0.8
56	0.1	0.8
57	0.2	1.9
58	0.4	3.1
59	0.6	5.0
60	1.4	11.9
61	2.8	23.8
62	5.2	44.6
63	8.5	73.8
64	11.6	100.0
65	5.5	47.7
66	5.0	43.1
67	0.2	1.5
76	0.3	2.3
77	0.9	7.7
78	0.2	1.5
79	0.1	0.8
80	0.1	0.8
88	0.1	0.8
89	0.2	1.5
90	0.3	2.3
91	0.2	1.5
92	0.3	2.3
93	0.1	0.8
94	0.1	0.8

m/e	% Σ_{36}	% base peak
95	0.1	0.8
96	0.4	3.4
97	1.2	10.4
98	2.6	22.3
99	0.1	0.8
106	0.1	0.8
107	0.1	0.8
108	0.2	1.5
109	0.3	2.3
110	0.2	1.5
137	0.2	1.5
138	0.5	4.6
139	1.4	12.3
140	3.1	26.9
141	6.1	53.1
142	8.5	73.1
143	0.6	5.0
154	0.1	0.8
155	0.1	0.8
156	0.3	2.3
157	0.5	4.6
158	0.9	8.1
159	1.5	12.7
160	1.6	13.5

Table 39

N-t-butyl-d_9-α,α,α-trifluoroacetamide

m/e	% Σ_{36}	% base peak
36	0.1	0.6
38	0.1	0.6
39	0.1	0.6
40	0.2	1.5
41	0.7	4.6
42	1.5	9.7
43	1.1	7.1
44	2.4	15.3
45	5.0	31.6
46	4.3	27.0
[illegible]	0.2	1.5
50	0.2	1.5
51	0.4	2.5
52	0.3	1.8
53	0.1	0.6
54	0.1	0.6
55	0.1	0.6
56	0.2	1.0
57	0.3	1.8
58	0.3	1.8
59	0.5	3.1
60	1.0	6.1
61	1.9	12.2
62	3.1	19.6
63	4.5	28.6
64	5.6	35.7
65	5.1	32.6
66	2.3	14.8
67	0.1	0.6
69	4.7	30.1
80	0.2	1.0
87	0.2	1.0
88	0.3	2.0
89	0.6	3.6
90	0.6	4.1
91	0.1	0.5
94	0.3	2.0
95	1.3	8.2
96	0.3	2.0
97	0.1	0.6
100	0.1	0.6

m/e	% Σ_{36}	% base peak
107	0.1	0.6
108	0.2	1.0
109	0.2	1.0
111	0.1	0.6
112	0.2	1.0
113	0.3	1.8
114	0.4	2.6
115	2.0	12.8
116	5.0	31.6
117	0.1	0.6
154	0.1	0.5
155	0.4	2.3
156	1.1	6.6
157	2.5	16.1
158	5.7	36.0
159	11.6	73.5
160	15.8	100.0
161	1.0	6.1
173	0.1	0.5
174	0.2	1.0
175	0.2	1.5
176	0.5	3.1
177	0.8	4.8
178	0.8	4.8